Linear and Quadratic Time-Frequency Signal Representations

F. HLAWATSCH and G.F. BOUDREAUX-BARTELS

Time-frequency signal representations characterize signals over a time-frequency plane. They thus combine time-domain and frequency-domain analyses to yield a potentially more revealing picture of the temporal localization of a signal's spectral components. They may also serve as a basis for signal synthesis, coding, and processing.

This paper is a tutorial reviewing both linear and quadratic representations. The linear representations discussed are the short-time Fourier transform and the wavelet transform. The section on quadratic representations concentrates on the Wigner distribution, the ambiguity function, smoothed versions of the Wigner distribution, and various classes of quadratic time-frequency representations.

Time-frequency representations (TFRs) of signals map a one-dimensional signal of time, $x(t)$, into a two-dimensional function of time and frequency, $T_x(t,f)$. Most TFRs are "time-varying spectral representations" which are similar conceptually to a musical score with time running along one axis and frequency along the other axis. The values of the TFR surface above the time-frequency plane give an indication as to which spectral components are present at which times.

TFRs have been applied to analyze, modify, and synthesize non-stationary or time-varying signals. Three-dimensional plots of TFR surfaces have been used as pictorial representations enabling a signal processor to analyze how spectral components of a signal or system vary with time. TFR inversion or synthesis algorithms have been employed to recover a signal from a TFR model, thus allowing a time-frequency implementation of signal design, time-varying filtering, noise suppression, time warping, etc. TFRs have also been used for efficient coding of signals (e.g., subband coding) and as a statistic for signal detection and parameter estimation.

This paper will review several linear and quadratic (bilinear) TFRs, discuss their motivation and properties, and provide examples of their application to typical problems encountered in time-varying signal processing. Other tutorial papers on TFRs are available in [Cla80c, CohL89, Naw88, Rab78, Boa90a, Gab46, Mec87, Boud83, Hla91d, Bast83, FlaP87c,89, Hla92a].

This tutorial is organized into four sections. The first section reviews the time domain and the frequency domain as defined by the Fourier transform. The limitations inherent in separate time-domain and frequency-domain descriptions, including the concepts of instantaneous frequency and group delay, provide a motivation for a joint time-frequency description of signals by means of TFRs.

The next section discusses linear TFRs, concentrating on the *short-time Fourier transform* (STFT) and the time-frequency version of the *wavelet transform* (WT). The STFT is considered in some detail, with emphasis placed on basic properties, running-window and filter interpretations, time resolution versus frequency resolution, STFT-based signal synthesis and processing, and the discrete STFT version with its relation to filterbank methods and the Gabor expansion. Our treatment of the WT is less detailed (since a tutorial review of the WT has appeared in a companion paper [Rio91]) and focuses on the WT's similarities to, and differences from, the STFT.

1053-5888/92/$3.00 © 1992 IEEE

The third section considers quadratic (bilinear) TFRs. We review two motivations for quadratic TFRs, based on energy densities and correlation functions, and comment on the occurrence of quadratic cross terms. The *Wigner distribution* and the *ambiguity function* are presented as two important examples of the "energetic" and "correlative" interpretations, respectively. We next consider two fundamental classes of energetic TFRs, namely, the classical *Cohen class* of shift-invariant TFRs and the recently introduced *affine class*. Motivated by the practical necessity of attenuating quadratic cross terms by means of smoothing, we discuss smoothed versions of the Wigner distribution in each class.

The fourth and final section presents computer simulation results with the aim of comparing various quadratic TFRs and illustrating some of their applications.

TIME DOMAIN AND FREQUENCY DOMAIN

The Fourier transform (FT) and its inverse establish a one-to-one relation between the *time domain* (signal $x(t)$) and the *frequency domain* (spectrum $X(f)$) as depicted in Fig. 1 [Papo77].

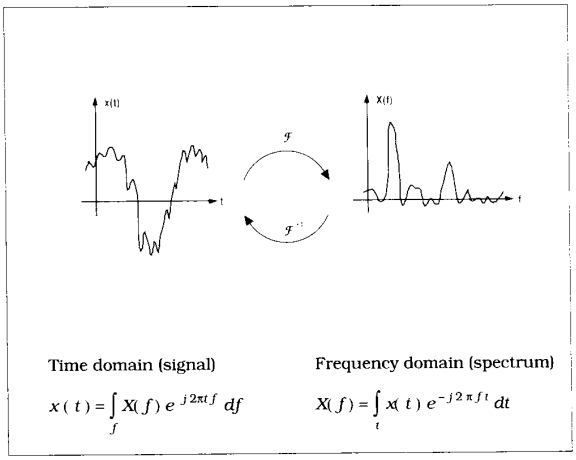

Fig. 1. Time domain and frequency domain: a dualistic approach to signal analysis. The Fourier transform ($\mathcal{F}$) connects the two domains.

Time domain and frequency domain constitute two *alternative* ways of looking at a signal. Although the FT allows a passage from one domain to the other, it does not allow a combination of the two domains. In particular, most time information is not easily accessible in the frequency domain. While the spectrum $X(f)$ shows the overall strength with which any frequency f is contained in the signal $x(t)$, it does not generally provide easy-to-interpret information about the *time localization* of spectral components. (Strictly speaking, this information is contained in the phase spectrum arg $\{X(f)\}$ but often comes in a form that is not easily interpreted, as is discussed in the next section.)

LIST OF ACRONYMS

AF	ambiguity function
AS	ambiguity surface
AM	amplitude modulation
AUD	"active" Unterberger distribution
BED	Bertrand distribution
BJD	Born-Jordan distribution
BUD	Butterworth distribution
CKD	cone-kernel distribution
CND	Cohen's nonnegative distribution
CWD	Choi-Williams distribution (= exponential distribution)
FD	Flandrin-D distribution
FM	frequency modulation
FT	Fourier transform
GD	group delay
GED	generalized exponential distribution
GWD	generalized Wigner distribution
IF	instantaneous frequency
IT	interference term
LD	Levin distribution
PD	Page distribution
PUD	"passive" Unterberger distribution
PWD	pseudo Wigner distribution
RD	Rihaczek distribution
RGD	radially-Gaussian kernel distribution
RGWD	real-valued generalized Wigner distribution
RID	reduced interference distribution
SCAL	scalogram
SPEC	spectrogram
SPWD	smoothed pseudo Wigner distribution
STFT	short-time Fourier transform
TFR	time-frequency representation
WD	Wigner distribution
WT	wavelet transform

Instantaneous Frequency and Group Delay

Clearly, there exist signals which feature a time localization of spectral components. A simple example is the complex-valued frequency-shift-keyed signal shown in Fig. 2. Here, it seems that at any time instant only a *single* frequency is present; this frequency may be obtained as the derivative of the instantaneous phase, $\arg\{x(t)\}$. This concept generalizes to the definition of the *instantaneous frequency* (IF) [Papo77, Vil48]

$$f_x(t) \triangleq \frac{1}{2\pi}\frac{d}{dt}\arg x(t) \qquad (1.1)$$

as the derivative of the instantaneous phase, $\arg\{x(t)\}$, of the complex-valued signal $x(t)$. (In the case of real-valued signals, the signal $x(t)$ has to be replaced by its

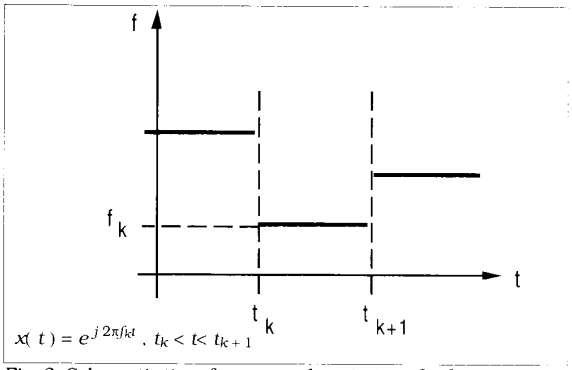

Fig. 2. Schematic time-frequency description of a frequency-shift-keyed signal. In each time interval $[t_k, t_{k+1}]$, only a single frequency f_k is present.

analytic version in (1.1)). A dual quantity is the *group delay* (GD)

$$t_x(f) \triangleq -\frac{1}{2\pi}\frac{d}{df}\arg X(f) \qquad (1.2)$$

where $\arg\{X(f)\}$ is the phase spectrum. The GD is especially meaningful when $x(t)$ is the impulse response of a linear time-invariant system. Under certain conditions, $t_x(f)$ can then be interpreted as the "time delay introduced by the system at frequency f" [Papo77, Prei82].

Unfortunately, the IF and GD are only capable of adequately describing the time localization of spectral components for a very restricted class of signals. The IF represents the frequency as an explicit function of time, $f = f_x(t)$, and thus implicitly assumes that, at each time instant t, there exists only a single frequency component. A simple signal which evidently does not comply with this assumption is the signal $x(t) = e^{j2\pi f_1 t} + e^{j2\pi f_2 t}$ containing *two* frequency components (f_1 and f_2) at all times. A dual restriction applies to the GD; here, the implicit assumption is that a given frequency is concentrated around a single time instant.

Time-Frequency Representations

The restrictions associated with the IF and GD can be removed by describing the time-frequency structure of a signal not by a one-dimensional curve in the time-frequency plane (as in the case of the IF or GD), but by a surface over the time-frequency plane (see Fig. 3). Mathematically, this corresponds to a joint function $T_x(t,f)$ of time t and frequency f. We shall call $T_x(t,f)$ a "time-frequency representation" (TFR) of the signal $x(t)$. Note that the TFR concept resembles a musical score, which indicates which notes (spectral components) are present at which time in a piece of music.

The definitions of all TFRs considered in this paper are summarized in Table I for subsequent reference. Looking at this table, we see that a fundamental property of each TFR, $T_x(t,f)$, corresponds to the manner in which it depends upon the signal $x(t)$. This dependence may be linear, quadratic, or otherwise nonlinear, with

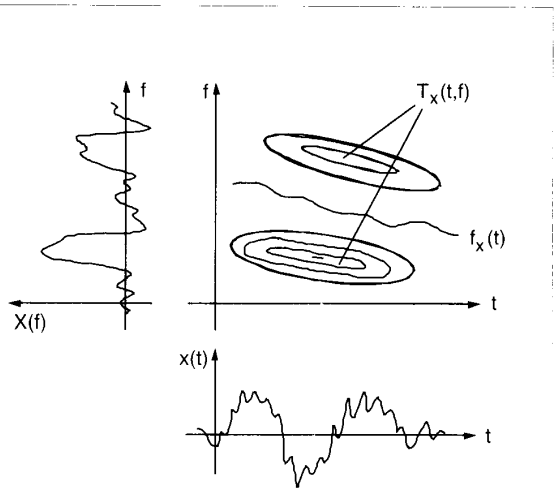

Fig. 3. A time-frequency representation $T_x(t,f)$ displays signals as surfaces over the time-frequency plane. This yields a potentially clear representation of the temporal localization of spectral components even in those cases where one-dimensional representations (curves), such as the instantaneous frequency $f_x(t)$, are no longer meaningful.

the first two cases being by far the most widely used. Therefore, we shall concentrate on linear and quadratic TFRs in the following.

LINEAR TIME-FREQUENCY REPRESENTATIONS

All linear TFRs satisfy the superposition or linearity principle which states that if $x(t)$ is a linear combination of some signal components, then the TFR of $x(t)$ is the same linear combination of the TFRs of each of the signal components:

$$x(t) = c_1 x_1(t) + c_2 x_2(t) \Rightarrow T_x(t,f) = c_1 T_{x_1}(t,f) + c_2 T_{x_2}(t,f)$$

Linearity is a desirable property in any application involving multicomponent signals (e.g., speech). Two linear TFRs of basic importance are the short-time Fourier transform and the wavelet transform; these are discussed in the next two subsections.

The Short-Time Fourier Transform

Definition and Expressions

Although the FT (spectrum) does not explicitly show the time localization of frequency components, such a time localization can be obtained by suitably pre-windowing the signal $x(t)$ as shown in Fig. 4. Accordingly, the *short-time Fourier transform* (STFT) [Naw88, Rab78, All77a,c,d, Port80, Cro83], or short-time spectrum, of a signal $x(t)$ is defined as

$$STFT_x^{(\gamma)}(t,f) = \int_{t'} [x(t')\,\gamma^*(t'-t)]\,e^{-j2\pi f t'}\,dt' \qquad (2.1)$$

TABLE I.

SOME TFRs IN ALPHABETICAL ORDER. The superscript * denotes complex conjugation.

Linear TFRs

Gabor expansion coefficient function $G_x(n,k)$: implicitly defined by

$$x(t) = \sum_n \sum_k G_x(n,k)\, g(t - nT)\, e^{j\,2\pi(kF)t}$$

Short-time Fourier transform (STFT):

$$\mathrm{STFT}_x^{(\gamma)}(t,f) = \int_{t'} x(t')\, \gamma^*(t' - t)\, e^{-j\,2\pi f t'}\, dt' = e^{-j\,2\pi t f} \int_{f'} X(f')\Gamma^*(f' - f)\, e^{j\,2\pi t f'}\, df'$$

Wavelet transform (WT):

$$\mathrm{WT}_x^{(\gamma)}(t,f) = \int_{t'} x(t') \sqrt{|\, f/f_0 \,|}\ \gamma^*\left(\frac{f}{f_0}(t' - t)\right) dt' = \int_{f'} X(f') \sqrt{|\, f_0/f \,|}\ \Gamma^*\left(\frac{f_0}{f} f'\right) e^{j\,2\pi t f'}\, df'$$

Quadratic TFRs

"Active" Unterberger distribution (AUD):

$$\mathrm{AUD}_x(t,f) = f \int_0^\infty X(fu)\, X^*\left(\frac{f}{u}\right)\left(1 + \frac{1}{u^2}\right) e^{j\,2\pi t f(u - 1/u)}\, du$$

Ambiguity function (AF):

$$\mathrm{A}_x(\tau,\nu) = \int_t x\left(t + \frac{\tau}{2}\right) x^*\left(t - \frac{\tau}{2}\right) e^{-j\,2\pi\nu t}\, dt = \int_f X\left(f + \frac{\nu}{2}\right) X^*\left(f - \frac{\nu}{2}\right) e^{j\,2\pi\tau f}\, df$$

Bertrand distribution (BED):

$$\mathrm{BED}_x(t,f) = f \int_u X(f\lambda(u)\, e^{u/2})\, X^*(f\lambda(-u)\, e^{-u/2})\, \lambda(u)\, e^{j\,2\pi t f u}\, du\,, \quad \lambda(u) = \frac{u/2}{\sinh(u/2)}$$

Born-Jordan distribution (BJD):

$$\mathrm{BJD}_x(t,f) = \int_\tau \left[\int_{t'} \varphi(t - t',\tau)\, x\left(t' + \frac{\tau}{2}\right) x^*\left(t' - \frac{\tau}{2}\right) dt' \right] e^{-j\,2\pi f t}\, d\tau, \quad \varphi(t,\tau) = \begin{cases} \dfrac{1}{|\tau|}, & |t/\tau| < 1/2 \\ 0, & |t/\tau| > 1/2 \end{cases}$$

Butterworth distribution (BUD):

$$\mathrm{BUD}_x(t,f) = \int_\tau \int_\nu \Psi(\tau,\nu)\, A_x(\tau,\nu)\, e^{j\,2\pi(t\nu - f\tau)}\, d\tau\, d\nu, \quad \Psi(\tau,\nu) = \frac{1}{1 + \left(\dfrac{\tau}{\tau_0}\right)^{2M}\left(\dfrac{\nu}{\nu_0}\right)^{2N}}$$

Choi-Williams (exponential) distribution (CWD):

$$\mathrm{CWD}_x(t,f) = \int_\tau \int_\nu \Psi(\tau,\nu)\, A_x(\tau,\nu)\, e^{j2\pi(t\nu - f\tau)}\, d\tau\, d\nu, \quad \Psi(\tau,\nu) = \exp\left[- \frac{(2\pi\tau\nu)^2}{\sigma} \right]$$

Cone-kernel distribution (CKD):

$$\mathrm{CKD}_x(t,f) = \int_\tau \left[\int_{t'} \varphi(t - t',\tau)\, x\left(t' + \frac{\tau}{2}\right) x^*\left(t' - \frac{\tau}{2}\right) dt' \right] e^{-j\,2\pi f t}\, d\tau, \quad \varphi(t,\tau) = \begin{cases} g(\tau), & |t/\tau| < 1/2 \\ 0, & |t/\tau| > 1/2 \end{cases}$$

Flandrin D-distribution (FD):

$$\mathrm{FD}_x(t,f) = f \int_u X\left[f\left(1 + \frac{u}{4}\right)^2 \right] X^*\left[f\left(1 - \frac{u}{4}\right)^2 \right] \left[1 - \left(\frac{u}{4}\right)^2 \right] e^{j\,2\pi t f u}\, du$$

Generalized exponential distribution (GED):

$$\mathrm{GED}_x(t,f) = \int_\tau \int_\nu \Psi(\tau,\nu)\, A_x(\tau,\nu)\, e^{j2\pi(t\nu - f\tau)}\, d\tau\, d\nu, \quad \Psi(\tau,\nu) = \exp\left[- \left(\frac{\tau}{\tau_0}\right)^{2M} \left(\frac{\nu}{\nu_0}\right)^{2N} \right]$$

Generalized Wigner distribution (GWD):

$$\mathrm{GWD}_x^{(\alpha)}(t,f) = \int_\tau x\left(t + \left(\frac{1}{2} + \alpha\right)\tau \right) x^*\left(t - \left(\frac{1}{2} - \alpha\right)\tau \right) e^{-j\,2\pi f t}\, d\tau$$

Levin distribution (LD):

$$\mathrm{LD}_x(t,f) = -\frac{d}{dt} \left| \int_t^\infty x(t')\, e^{-j\,2\pi f t'}\, dt' \right|^2 = 2\mathrm{Re}\left\{ x^*(t)\, e^{j\,2\pi t f} \int_t^\infty x(t')\, e^{-j\,2\pi f t'}\, dt' \right\}$$

Page distribution (PD):

$$\mathrm{PD}_x(t,f) = \frac{d}{dt} \left| \int_{-\infty}^t x(t')\, e^{-j\,2\pi f t'}\, dt' \right|^2 = 2\mathrm{Re}\left\{ x^*(t)\, e^{j\,2\pi t f} \int_{-\infty}^t x(t')\, e^{-j\,2\pi f t'}\, dt' \right\}$$

TABLE I. (continued)

"Passive" Unterberger distribution (PUD):

$$\mathrm{PUD}_x(t,f) = f\int_0^{\infty} X(fu)\, X^*(\frac{f}{u})\, \frac{1}{u}\, e^{j\,2\pi t f(u-1/u)}\, du$$

Pseudo Wigner distribution (PWD):

$$\mathrm{PWD}_x^{(\eta)}(t,f) = \int_\tau x(t+\frac{\tau}{2})\, x^*(t-\frac{\tau}{2})\, \eta(\frac{\tau}{2})\, \eta^*(-\frac{\tau}{2})\, e^{-j\,2\pi f\tau}\, d\tau = \int_{f'} H(f-f')\, W_x(t,f')\, df'$$

with $H(f) = \int_\tau \eta(\frac{\tau}{2})\, \eta^*(-\frac{\tau}{2})\, e^{-j\,2\pi f t}\, d\tau$

Real-valued generalized Wigner distribution (RGWD):

$$\mathrm{RGWD}_x^{(\alpha)}(t,f) = \mathrm{Re}\left\{\mathrm{GWD}_x^{(\alpha)}(t,f)\right\}$$

Reduced interference distribution (RID)[1]:

$$\mathrm{RID}_x(t,f) = \int_\tau\int_\nu S(\tau\nu)\, A_x(\tau,\nu)\, e^{j\,2\pi(t\nu - f\tau)}\, d\tau\, d\nu,$$

with $s(\alpha) = 0$ for $|\alpha| > 1/2$, $S(\beta) \in \mathbb{R}$, $S(0) = 1$, $\left.\frac{d}{d\beta} S(\beta)\right|_{\beta=0} = 0$

Rihaczek distribution (RD):

$$\mathrm{RD}_x(t,f) = \int_\tau x(t+\tau)\, x^*(t)\, e^{-j\,2\pi f t}\, d\tau = x^*(t)\, X(f)\, e^{j\,2\pi t f}$$

Scalogram (SCAL):

$$\mathrm{SCAL}_x^{(\gamma)}(t,f) = |WT_x^{(\gamma)}(t,f)|^2 = \left| \int_{t'} x(t') \sqrt{\left|\frac{f}{f_0}\right|}\, \gamma^*\left(\frac{f}{f_0}(t'-t)\right) dt' \right|^2$$

Smoothed pseudo Wigner distribution (SPWD):

$$\mathrm{SPWD}_x^{(g,\,\eta)}(t,f) = \int_\tau \left[\int_{t'} g(t-t')\, x(t'+\frac{\tau}{2})\, x^*(t'-\frac{\tau}{2})\, dt'\right] \eta(\frac{\tau}{2})\, \eta^*(-\frac{\tau}{2})\, e^{-j\,2\pi f t}\, d\tau =$$

$$\int_{t'}\int_{f'} g(t-t')\, H(f-f')\, W_x(t,f')\, dt'\, df' \quad \text{with} \quad H(f) = \int_\tau \eta(\frac{\tau}{2})\, \eta^*(-\frac{\tau}{2})\, e^{-j\,2\pi f t}\, d\tau$$

Spectrogram (SPEC):

$$\mathrm{SPEC}_x^{(\gamma)}(t,f) = |\mathrm{STFT}_x^{(\gamma)}(t,f)|^2 = \left|\int_{t'} x(t')\, \gamma^*(t'-t)\, e^{-j\,2\pi f t'}\, dt'\right|^2$$

Wigner distribution (WD):

$$\mathrm{W}_x(t,f) = \int_\tau x(t+\frac{\tau}{2})\, x^*(t-\frac{\tau}{2})\, e^{-j\,2\pi f\tau}\, d\tau = \int_\nu X(f+\frac{\nu}{2})\, X^*(f-\frac{\nu}{2})\, e^{j\,2\pi t\nu}\, d\nu$$

Nonlinear, nonquadratic TFRs

Signal-adaptive radially-Gaussian kernel distribution (RGD)[2]:

$$\mathrm{RGD}_x(t,f) = \int_\tau\int_\nu \Psi_x(\tau,\nu)\, A_x(\tau,\nu)\, e^{j\,2\pi(t\nu - f\tau)}\, d\tau\, d\nu,$$

with $\Psi_x(\tau,\nu) = \exp\left[-\frac{(\tau/\tau_0)^2 + (\nu/\nu_0)^2}{2\sigma_x^2(\Theta)}\right]$, $\Theta = \arctan\frac{\nu/\nu_0}{\tau/\tau_0}$

Cohen's nonnegative distribution (CND):

$$\mathrm{CND}_x^{(c,\rho)}(t,f) = \frac{|x(t)|^2 |X(f)|^2}{E_x}\left[1 + c\,\rho\left(\xi_x(t),\, \eta_x(f)\right)\right]$$

with $\xi_x(t) = \frac{1}{E_x}\int_{-\infty}^{t} |x(t')|^2\, dt'$, $\eta_x(f) = \frac{1}{E_x}\int_{-\infty}^{f} |X(f')|^2\, df'$, $E_x = \int_t |x(t)|^2\, dt$

[1]Specific members of the RID class are discussed in [Jeo92a]

[2]An algorithm for the signal-adaptive optimization of $\sigma_x^2(\Theta)$ is described in [Bara91]

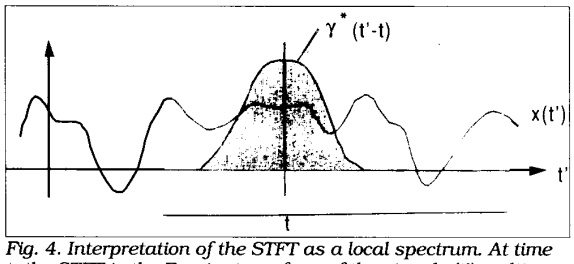

Fig. 4. Interpretation of the STFT as a local spectrum. At time t, the STFT is the Fourier transform of the signal x(t') multiplied by a running analysis window γ(t'-t). Since the window suppresses all signal features outside a local neighborhood around time t, the STFT is simply a "local spectrum."*

The STFT at time t is the FT of the signal $x(t')$ multiplied by a shifted "analysis window" $\gamma^*(t'-t)$ centered around t. (All integrals go from $-\infty$ to ∞. The superscript * denotes complex conjugation.) Because multiplication by the relatively short window $\gamma^*(t'-t)$ effectively suppresses the signal outside a neighborhood around the analysis time point $t' = t$, the STFT is simply a "local spectrum" of the signal $x(t')$ around the "analysis time" t.

The STFT is evidently a linear TFR, and it is complex-valued in general. Note that the STFT result $\mathrm{STFT}_x^{(\gamma)}(t,f)$ for a given signal $x(t')$ is significantly influenced by the choice of the analysis window $\gamma^*(t')$. Other elementary properties describe how the STFT is affected by basic signal transforms. In particular, the STFT preserves frequency shifts in the signal $x(t')$, and it preserves time shifts up to a modulation (phase factor):

$$\tilde{x}(t) = x(t)e^{j2\pi f_0 t} \Rightarrow STFT_{\tilde{x}}^{(\gamma)}(t,f) = STFT_x^{(\gamma)}(t,f-f_0)$$

$$\tilde{x}(t) = x(t-t_0) \Rightarrow STFT_{\tilde{x}}^{(\gamma)}(t,f) = STFT_x^{(\gamma)}(t-t_0,f)e^{-j2\pi t_0 f}$$

The STFT may also be expressed in terms of the signal and window spectra

$$STFT_x^{(\gamma)}(t,f) = e^{-j2\pi tf}\int_{f'} X(f')\,\Gamma^*(f'-f)e^{j2\pi tf'}df'$$

Apart from the phase factor $e^{-j2\pi tf}$, this "frequency-domain expression" is analogous to the time-domain expression (2.1). In fact, it shows that the STFT can also be interpreted as the inverse FT of the "windowed spectrum" $X(f')\Gamma^*(f'-f)$, in which the spectral window $\Gamma(f)$ is simply the FT of the temporal window $\gamma(t)$.

Filter Interpretation

The inverse FT of the windowed spectrum $X(f')\Gamma^*(f'-f)$ can be interpreted as the result of passing the signal $x(t')$ through a filter with frequency response $\Gamma^*(f'-f)$ [Naw88, Rab78, Cro83, Port80]. This filter is a bandpass filter centered around the analysis frequency f, since $\Gamma(f')$ is the FT of a lowpass window function. The resulting implementation of the STFT is illustrated in Fig. 5a. At a given analysis frequency f, the STFT is derived by passing the signal $x(t')$ through an "analysis bandpass filter" with center frequency f and then frequency-shifting the filter's output to frequency 0. Due to the final frequency shift, $\mathrm{STFT}_x^{(\gamma)}(t,f)$ (as a function of t) is a lowpass signal for any fixed f. Note that the impulse response of the bandpass filter is essentially a modulated version of the lowpass window $\gamma^*(t)$. The filter's bandwidth is equal to that of the window, independent of the analysis (center) frequency f.

A "lowpass implementation" of the STFT, which is equivalent to the "bandpass implementation" discussed above, is shown in Fig. 5b. The lowpass filter's impulse response is equal to the time-reversed analysis window $\gamma^*(-t)$.

Time-Frequency Resolution

Because the STFT at time t is the spectrum of the signal $x(t')$ prewindowed by the window $\gamma^*(t'-t)$, all signal features located within the local window interval

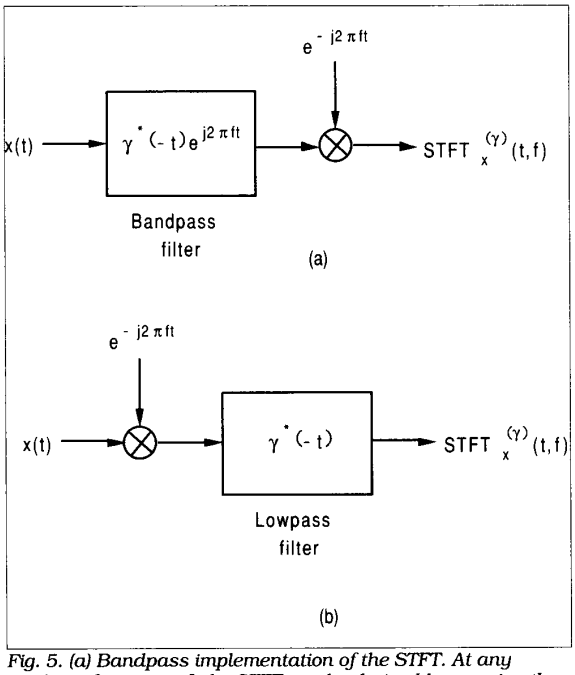

Fig. 5. (a) Bandpass implementation of the STFT. At any analysis frequency f, the STFT can be derived by passing the signal through a bandpass filter with center frequency f, and subsequently demodulating (frequency-shifting) the filter's output to frequency 0. The impulse response of the bandpass filter is $\gamma^*(-t)e^{j2\pi ft}$, where $\gamma^*(t)$ is the STFT analysis window. Note that the filter's bandwidth is independent of the analysis (center) frequency f and equals the bandwidth of the analysis window $\gamma^*(t)$.

(b) Lowpass implementation of the STFT. The STFT at any analysis frequency f can be derived by first frequency-shifting the signal x(t) by -f and then passing the frequency-shifted signal through a lowpass filter. The lowpass filter's impulse response is $\gamma^*(-t)$, i.e., the time-reversed analysis window $\gamma^*(t)$. Again, the filter bandwidth equals that of the window, independently of the analysis frequency f.

around time t show up at time t in the STFT. Thus, it is clear that good time resolution of the STFT requires a short window $\gamma^*(t')$. On the other hand, the STFT at the frequency f is essentially the result of passing the signal $x(t')$ through the bandpass filter $\Gamma^*(f'-f)$. Good frequency resolution of the STFT hence requires a narrowband filter, i.e., a narrowband (and thus long) analysis window $\gamma^*(t')$.

Unfortunately, the uncertainty principle prohibits the existence of windows with arbitrarily small duration *and* arbitrarily small bandwidth [Papo77]. Hence, the joint time-frequency resolution of the STFT is inherently limited. Specifically, there exists a fundamental *resolution tradeoff*: improving the time resolution (by using a short window) results in a loss of frequency resolution, and vice versa.

It is instructive to consider two extreme choices of the analysis window/filter $\gamma(t)$. The first case is that of perfect time resolution, that is, if the analysis window $\gamma(t)$ is an infinitely narrow Dirac impulse,

$$\gamma(t) = \delta(t) \;\Rightarrow\; STFT_x^{(\gamma)}(t,f) = x(t)e^{-j2\pi ft}$$

In this case, the STFT essentially reduces to the signal $x(t)$, preserving all time variations of the signal but not providing any frequency resolution. The second case is that of perfect frequency resolution obtained with the all-constant window $\gamma(t)\equiv 1$,

$$\Gamma(f) = \delta(f) \;\Rightarrow\; STFT_x^{(\gamma)}(t,f) = X(f)$$

Here, the STFT reduces to the FT and does not provide any time resolution.

Time-Frequency Signal Expansion and STFT Synthesis

STFT analysis can be motivated using an alternative approach [Hel66, Mon67]. Consider the representation of a signal $x(t)$ as a superposition (weighted linear combination) of time-frequency-shifted versions of an elementary signal $g(t)$,

$$x(t) = \int_{t'}\int_{f'} T_x(t',f')[g(t-t')\,e^{j2\pi f't}]\,dt'\,df' \qquad (2.2)$$

This may also be viewed as an expansion of the signal $x(t)$ into the "basis signals" $g_{t',f'}(t) = g(t-t')e^{j2\pi f't}$ continuously indexed by t',f'. If $g(t)$ is centered around $t=0$ in the time domain and around $f=0$ in the frequency domain, then $g(t-t')e^{j2\pi f't}$ will be centered around the time-frequency point (t',f'). Hence, the coefficient function $T_x(t',f')$ of the above "time-frequency expansion" will tell us how strongly a neighborhood around the time-frequency point (t',f') contributes to the signal $x(t)$.

It is easily shown that expansion (2.2) exists for any finite-energy signal $x(t)$. Furthermore, the coefficient function $T_x(t,f)$ may be chosen as the STFT,

$$T_x(t,f) = STFT_x^{(\gamma)}(t,f) = \int_{t'} x(t')\gamma^*(t'-t)e^{-j2\pi ft'}\,dt \qquad (2.3)$$

provided the STFT analysis window $\gamma^*(t)$ is selected to satisfy $\int g(t)\gamma^*(t)dt = 1$. This is not a very restrictive condition, and the freedom left in choosing the analysis window $\gamma^*(t)$ shows that the expansion's coefficient function $T_x(t,f)$ is not uniquely defined.

Inserting (2.3) into (2.2) yields the relation

$$x(t) = \int_{t'}\int_{f'} STFT_x^{(\gamma)}(t',f')\,g(t-t')e^{j2\pi f't}\,dt'\,df' \qquad (2.4)$$

which indicates how to recover or "synthesize" the signal $x(t)$ from its STFT [Hel66, Mon67, Port80]. We can in fact view *STFT synthesis* as defined by (2.4) as being the inverse operation of *STFT analysis* (2.3).

Given the analysis window $\gamma^*(t)$, there are infinitely many "synthesis windows" $g(t)$ that satisfy the condition $\int g(t)\gamma^*(t)dt = 1$ and can thus be used in (2.4). A natural choice equates the analysis window and the synthesis window, $g(t) = \gamma(t)$, with appropriate normalization. Two other choices, $g(t) = \delta(t)$ and $g(t)\equiv 1$, are noteworthy since they result in a simplification of the general synthesis relation (2.4) [Port80].

STFT-Based Signal Processing

The inclusion of an *STFT modification* between STFT analysis and STFT synthesis, as shown in Fig. 6a, is an obvious way of implementing time-varying signal processing in a joint time-frequency domain [Cro83, Rab78]. It must be stressed that the overall signal processing system depends not only on the STFT modification performed, but also on the analysis window $\gamma^*(t)$ and synthesis window $g(t)$. The overall system will be linear (but generally time-varying) if the STFT modification itself is linear as, for example, in the case of STFT-based time-varying filtering where the STFT modification is simply a multiplication of the STFT by some signal-independent time-frequency weighting function.

Using a discrete-time/discrete-frequency version of the STFT as considered in the next subsection, the STFT-based time-frequency signal processing scheme discussed above has been applied successfully to a number of problems (cf. the later section entitled "Applications of the STFT").

Discrete STFT Version and Filterbanks

For practical applications of the STFT, it is necessary to discretize the time-frequency plane. We therefore consider samples of the STFT at equidistant time-frequency grid points (nT,kF) where $T > 0$ and $F > 0$ are the sampling periods for the time and frequency variables, respectively, and n and k are integers,

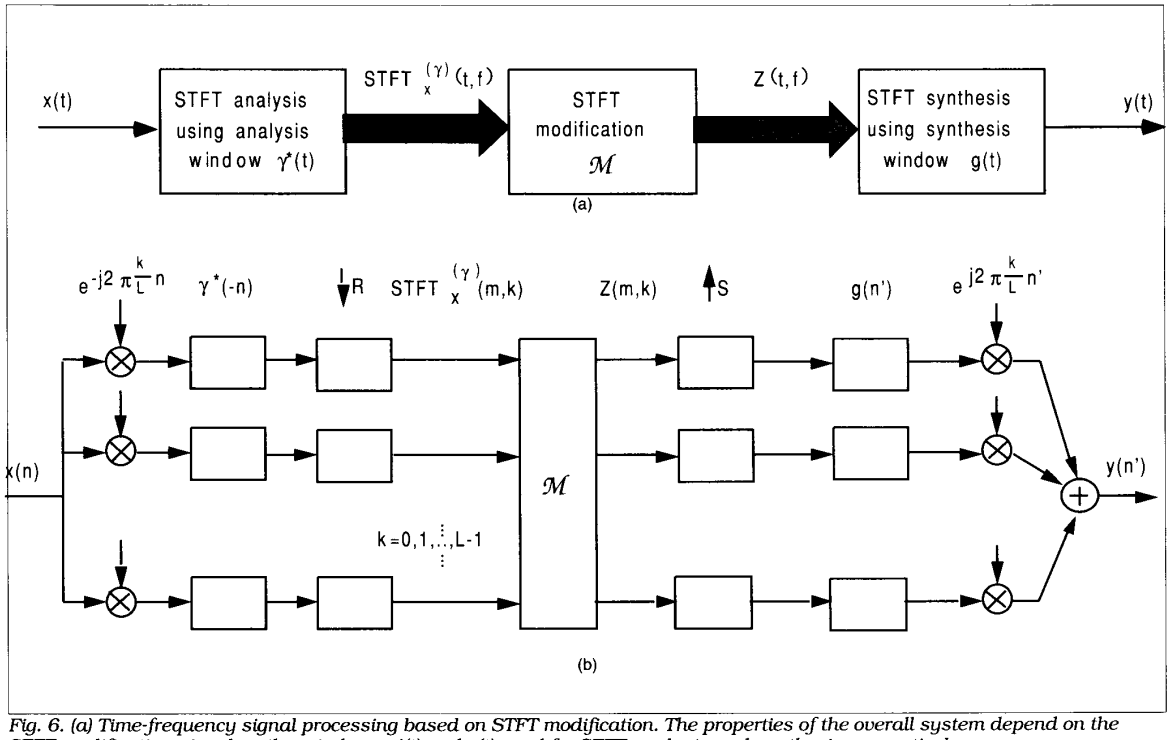

Fig. 6. (a) Time-frequency signal processing based on STFT modification. The properties of the overall system depend on the STFT modification $\mathcal{M}$ and on the windows $\gamma^*(t)$ and $g(t)$ used for STFT analysis and synthesis, respectively.
(b) Filter bank implementation of (discrete) STFT analysis/modification/synthesis. All signals are assumed to be discrete-time. The boxes labeled "↓R" and "↑S" denote sampling-rate down-conversion and up-conversion by the factors R and S, respectively. These factors may be different as part of the overall signal processing scheme. The symbol $\mathcal{M}$ again denotes some modification to the STFT samples. The analysis filter $\gamma^*(-n)$ and the synthesis filter $g(n)$ can be interpreted as a decimation filter and an interpolation filter, respectively.

$$STFT_x^{(\gamma)}(nT,kF) = \int_{t'} x(t')\gamma^*(t'-nT)e^{-j2\pi(kF)t'}dt' \qquad (2.5)$$

The discretized version of the STFT synthesis relation (2.4) is [All77c, Port80]

$$x(t) = \sum_n \sum_k STFT_x^{(\gamma)}(nT,kF)\, g(t-nT)e^{j2\pi(kF)t} \qquad (2.6)$$

This relation is valid provided that the sampling periods T and F, the analysis window $\gamma^*(t)$, and the synthesis window $g(t)$ are chosen such that

$$\frac{1}{F}\sum_n g\left(t + k\frac{1}{F} - nT\right)\gamma^*(t-nT) = \delta[k] \quad \text{for all } t \qquad (2.7)$$

with $\delta[k]$ defined as $\delta[0] = 1$ and $\delta[k] = 0$ for $k \neq 0$. This condition is far more restrictive than the condition $\int g(t)\gamma^*(t)dt = 1$ required in the continuous case [Cro83, Port80].

Both the discrete STFT analysis (2.5) and the discrete STFT synthesis (2.6) can be implemented efficiently by means of overlap FFT techniques [Cro83, All77a,d]. Alternatively, an implementation using filterbanks is possible. In accordance with Fig. 5b, an "analysis filterbank" can be used to calculate the discretized STFT, $STFT_x^{(\gamma)}(nT,kF)$; for each analysis frequency $f_k = kF$, a filter is needed. A "synthesis filter bank" (followed by a summation of all filter outputs) can then be used to recover the signal $x(t)$ from the STFT samples $STFT_x^{(\gamma)}(nT,kF)$ in accordance with the synthesis relation (2.6). The impulse response of the analysis filter equals the time-reversed analysis window $\gamma^*(-t)$; the impulse response of the synthesis filter equals the synthesis window $g(t)$. The construction of $\gamma(t)$ and $g(t)$ such that the "perfect-reconstruction condition" (2.7) is met (or, at least, reasonably well approximated) now becomes a rather nontrivial filter design problem [Cro83, Nay92, Vet86, Vai87,92, SwaK86, Dem87]. A fully discrete-time implementation of the filter bank scheme (including a modification of the discrete STFT) is shown in Fig. 6b. Because the same lowpass filter is used for each channel, the filter bandwidth is the same for each center frequency $f_k = kF$.

Gabor Expansion

The synthesis relation (2.6) can again be interpreted as an expansion of the signal $x(t)$ into time-frequency

shifted versions $g_{nk}(t)$ of an elementary function $g(t)$,

$$x(t) = \sum_n \sum_k G_x(n,k) g_{nk}(t) \quad \text{with} \quad g_{nk}(t) = g(t-nT)\, e^{j 2\pi(kF)t} \tag{2.8}$$

This discrete time-frequency signal expansion is known as the *Gabor expansion* [Gab46, Bast80a, Hel66, Mon67, Nel72, JanA81, Wex90]. The expansion coefficients $G_x(n,k)$ are called *Gabor coefficients*, and the functions $g_{nk}(t)$ are called *Gabor logons*. The logons were originally taken to be time-frequency-shifted Gaussian functions by Gabor because Gaussian signals are maximally concentrated in time and frequency. Although the Gabor coefficients $G_x(n,k)$ may be chosen to be the STFT samples $STFT_x^{(\gamma)}(nT,kF)$ (see Eq. (2.6)), these coefficients are not, in general, uniquely defined for a given signal.

The interest in the Gabor expansion stems from the fact that the basis signals $g_{nk}(t)$ can be constructed such that they are well localized and well concentrated with respect to both time and frequency [Gab46]. Therefore, the expansion coefficient $G_x(n,k)$ may be expected to indicate the signal's time-frequency content around the time-frequency location (nT,kF). Moreover, the logon basis signals $g_{nk}(t)$ can easily be generated since they are all derived from the elementary function $g(t)$ through simple time-frequency shifts.

In the context of the Gabor expansion, important issues are the completeness, linear independence, and orthogonality of the "Gabor basis" $\{g_{nk}(t)\}$ [Bast81a, JanA81, Dau90a,91a]. In particular, completeness of the Gabor basis guarantees that any finite-energy signal can be represented by the linear combination of the Gabor basis functions given in the Gabor expansion (2.8). A *necessary* condition for completeness of the Gabor basis is $TF \leq 1$; this condition is a bound on the density of the "time-frequency sampling grid" employed. In the extreme case of "critical sampling," $TF = 1$, the number of Gabor coefficients equals the number of signal samples (assuming a bandlimited signal sampled with minimum sampling rate); hence, the Gabor coefficients $G_x(n,k)$ do not contain redundancy. Some degree of oversampling ($TF < 1$), which introduces redundancy in the coefficients, is usually recommended for the sake of numerical stability, even though the Gabor basis signals are then not linearly independent (i.e., the Gabor coefficients $G_x(n,k)$ are not uniquely defined). Finally, it has been shown [Dau90a, Bat88] that a Gabor basis with good time-frequency localization may not be orthogonal (see [Dau91a] for an interesting modification of the Gabor expansion resulting in an orthonormal basis).

If completeness of the Gabor basis $g_{nk}(t)$ is assumed, then the *biorthogonality condition* [Bast80a, Aus91a]

$$\int_t g_{nk}(t)\, \gamma^*_{n',k'}(t)\, dt = \delta[n-n']\, \delta[k-k'] \tag{2.9a}$$

or, equivalently,

$$STFT_g^{(\gamma)}(nT,kF) = \int_{t'} g(t')\, \gamma^*(t'-nT)\, e^{-j 2\pi kFt'}\, dt' = \delta[n]\delta[k] \tag{2.9b}$$

is sufficient for the perfect-reconstruction condition (2.7). The construction of a "biorthogonal" analysis window $\gamma^*(t)$ satisfying (2.9b) can be done using the Zak transform [JanA81,88, Aus91a, Orr91]. More generally, the construction of an admissible analysis window $\gamma^*(t)$ may be based on the theory of *frames* [Dau90a].

Applications of the Gabor expansion are discussed in [Davi79, Gla63, Aus90, Fri89, Bast80b, PorM88,89, Zee89, Ein86, PorB91, Nel72, Bil76, Bro90, Boud91a, Pro90].

Applications of the STFT

The STFT (or, in some cases, the STFT's squared magnitude known as the *spectrogram*, see the Section on quadratic TFRs) has been applied to signal processing problems in many different areas. Major applications include time-varying signal analysis [Cro83, All77c, Str87], system identification and spectral estimation [All79, Rab80, Dur85], signal detection and parameter estimation [Wolc83, Alt8O, Aus90, Fin91, Mos86], mode separation and determination of group velocity [Blo68, Dzi69, Levs72, Tri78], speech pitch and formant analysis [All82, Port81a-b, Rab78, Yeg81, FlaJ72, Pot66, McA9O], speaker identification [Bolt69], speech coding [Port76, McA92], estimation of the group delay or the instantaneous frequency of a signal [Kod78, You85], and complex demodulation [Cal76, Web79, Ban73]. Some applications of STFT synthesis techniques [All77a,c, Naw83, Port8O, Gri84] are time-varying filtering [Dau88, Bour88, Cro83, Rab78], nonlinear noise removal [Lim79], correction of helox speech [Ric82], room dereverberation [FlaJ7O, All77b], time-scale modification or warping of speech signals [Port81a, Gri84], and dynamic range and bandwidth compression of acoustical signals [Cro83, Lim79].

The Wavelet Transform

In addition to the STFT discussed so far, another important linear TFR is the time-frequency version of the *wavelet transform* (WT) defined as

$$WT_x^{(\gamma)}(t,f) = \int_{t'} x(t') \sqrt{|f/f_0|}\, \gamma^*\left(\frac{f}{f_0}(t'-t)\right) dt' \tag{2.10}$$

where $\gamma(t)$ (the "analyzing wavelet") is a real or a complex *bandpass* function centered around $t=0$ in the time domain. The parameter f_0 used in (2.10) equals the center frequency of $\gamma(t)$. We note that the WT was originally introduced as a time-*scale* representation [Dau90a,91b, Kro87, Rio91, Mall89a-b, Coi91, Mey89]; this classical formulation of the WT can be re-obtained

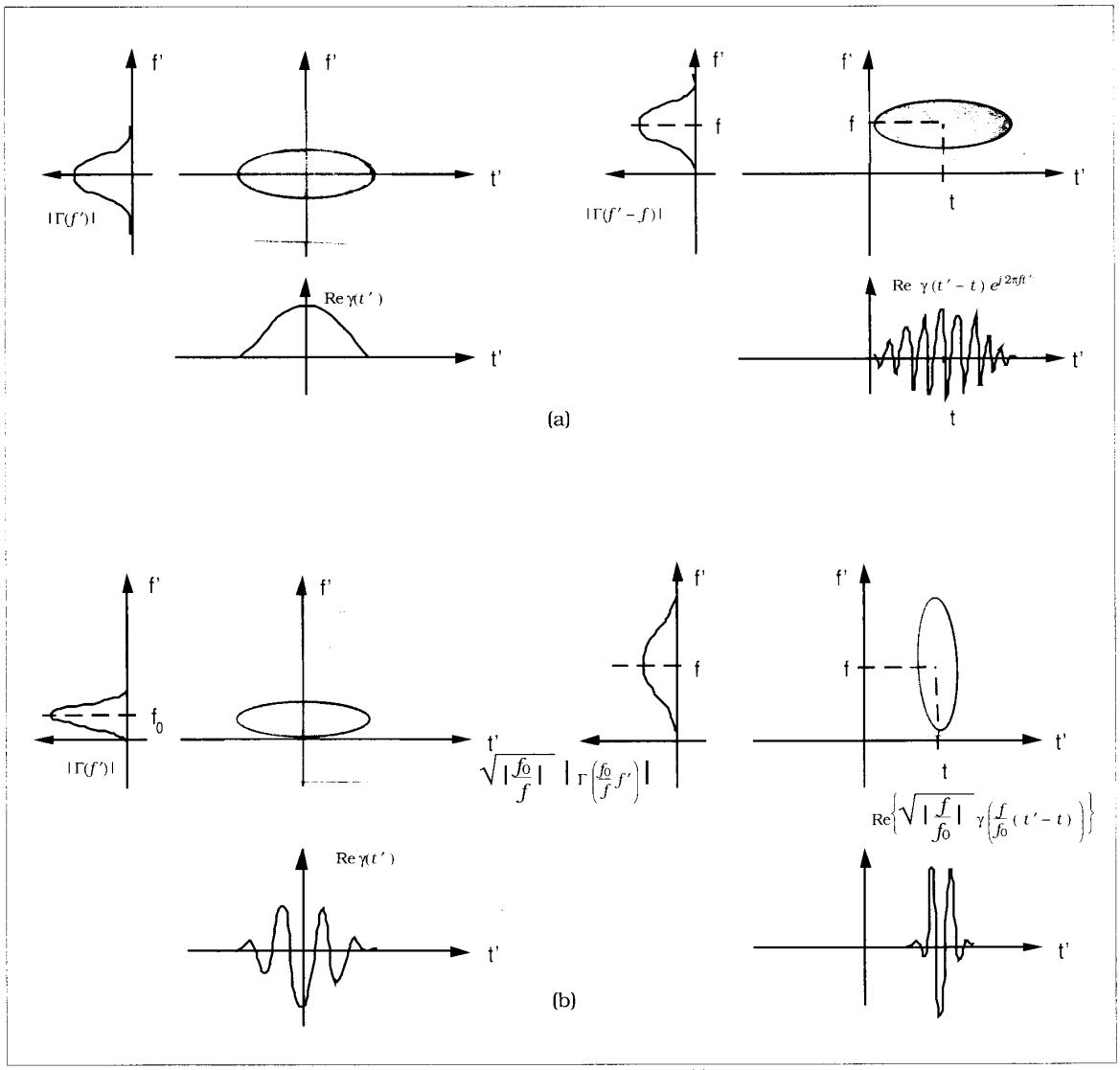

Fig. 7. (a) Effect of the time-shift/frequency-shift operator $\mathbf{S}^{(t,f)}$. *The STFT,* $STFT_x^{(\gamma)}(t,f)$, *is the inner product of the signal x(t') and a time-shifted/frequency-shifted version,* $(\mathbf{S}^{(t,f)}\gamma)(t') = \gamma(t'-t)e^{j2\pi f t'}$, *of the lowpass-type analysis window γ(t). The time-shift/frequency-shift operator* $\mathbf{S}^{(t,f)}$ *causes the analysis window γ(t) to be centered around time t and frequency f. It does not affect the bandwidth or the duration of the window.*

(b) Effect of the time-scaling/time-shift operator $\mathbf{C}^{(t,f)}$. *The WT,* $WT_x^{(\gamma)}(t,f)$, *is the inner product of the signal x(t') and a time-scaled/time-shifted version,* $(\mathbf{C}^{(t,f)}\gamma)(t') = \sqrt{|f/f_0|}\,\gamma\left(\frac{f}{f_0}(t'-t)\right)$, *of the bandpass-type analysis wavelet γ(t). The time-scaling/time-shift operator* $\mathbf{C}^{(t,f)}$ *causes the analysis wavelet γ(t) to be centered around time t and frequency f. Furthermore, the time scaling also affects the wavelet's bandwidth and duration: the bandwidth (duration) is proportional (inversely proportional) to f.*

from the above time-*frequency* formulation by introducing the analysis scale a as $a=f_0/f$ [Rio92, Gram91]. For the time-frequency version (2.10), we have to assume that the FT of $\gamma(t)$ is essentially concentrated around the center frequency f_0. A tutorial discussion of the WT's time-scale version may be found in the October 1991 issue of this magazine [Rio91].

The WT preserves time shifts and time scalings:

$$\tilde{x}(t) = x(t-t_0) \Rightarrow WT_{\tilde{x}}^{(\gamma)}(t,f) = WT_x^{(\gamma)}(t-t_0,f)$$

$$\tilde{x}(t) = \sqrt{|a|}\,x(at) \Rightarrow WT_{\tilde{x}}^{(\gamma)}(t,f) = WT_x^{(\gamma)}(at,\frac{f}{a})$$

It does not, however, preserve frequency shifts.

There exists a strong formal similarity between the STFT and the WT. Indeed, both the STFT and the WT can be written as inner products:

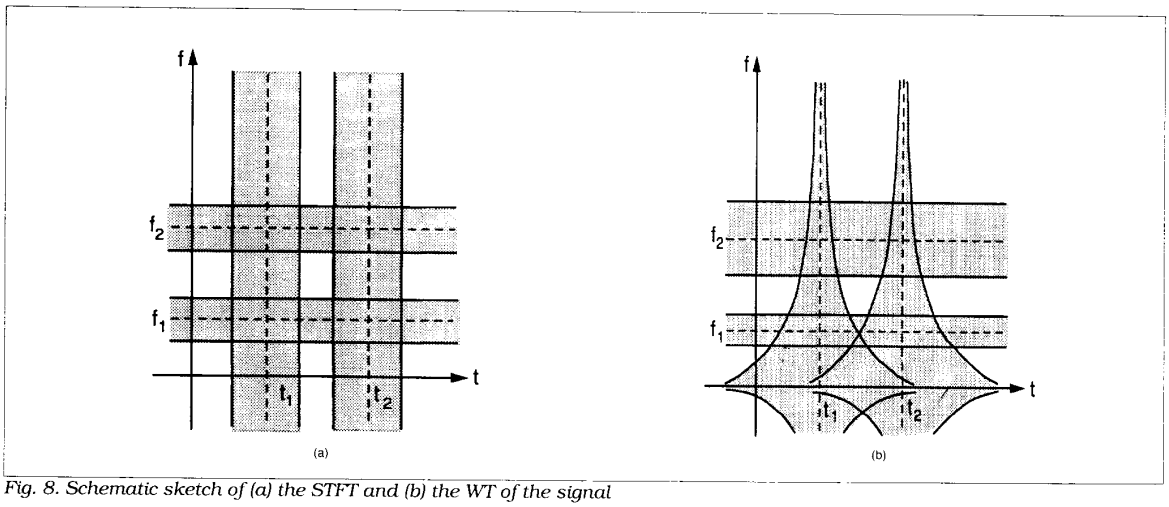

Fig. 8. Schematic sketch of (a) the STFT and (b) the WT of the signal

$$x(t) = \delta(t-t_1) + \delta(t-t_2) + e^{j2\pi f_1 t} + e^{j2\pi f_2 t} \overset{FT}{\leftrightarrow} X(f) = e^{-j2\pi t_1 f} + e^{-j2\pi t_2 f} + \delta(f-f_1) + \delta(f-f_2)$$

The two time-domain Dirac impulses give rise to the vertical support regions around t_1 and t_2 whereas the two complex sinusoids (frequency-domain Dirac impulses) produce the horizontal support regions around f_1 and f_2. It is seen that the time-frequency concentration of the STFT is independent of the analysis frequency f. In contrast, the time concentration (frequency concentration) of the WT becomes better (poorer) as $|f|$ increases.

$$STFT_x^{(\gamma)}(t,f) = (x, \mathbf{S}^{(t,f)}\gamma) \quad \text{with}$$
$$(\mathbf{S}^{(t,f)}\gamma)(t') = \gamma(t'-t)\, e^{j2\pi f t'}$$
$$WT_x^{(\gamma)}(t,f) = (x, \mathbf{C}^{(t,f)}\gamma) \quad \text{with}$$
$$(\mathbf{C}^{(t,f)}\gamma)(t') = \sqrt{|f/f_0|}\ \gamma\left(\frac{f}{f_0}(t'-t)\right)$$

where the inner product is defined as $(x,y) = \int x(t)y^*(t)dt$. It is seen that there are two essential differences between the STFT and the WT. The first difference is the choice of the linear time-shift/frequency-shift operator $\mathbf{S}^{(t,f)}$ or the linear time-scaling/time-shift operator $\mathbf{C}^{(t,f)}$. The second difference is the fact that $\gamma(t)$ is a lowpass signal in the STFT case and a bandpass signal in the WT case.

Figure 7 illustrates the practical consequences of these formal differences by comparing the effects of the linear operators $\mathbf{S}^{(t,f)}$ and $\mathbf{C}^{(t,f)}$. The STFT operator $\mathbf{S}^{(t,f)}$ first time-shifts $\gamma(t')$ by time t and then frequency-shifts the result by frequency f. The WT operator $\mathbf{C}^{(t,f)}$, on the other hand, first time-scales $\gamma(t')$ by a factor f/f_0 and then time-shifts the result by time t. Thus, the frequency shift in the STFT case is replaced by a time scaling in the WT. (Note that a time scaling by a factor a induces a frequency scaling by the inverse factor $1/a$.) *Both* $(\mathbf{S}^{(t,f)}\gamma)(t')$ and $(\mathbf{C}^{(t,f)}\gamma)(t')$ are centered around the time-frequency point (t,f). However, whereas the effective duration and bandwidth of the STFT test signal $(\mathbf{S}^{(t,f)}\gamma)(t')$ are independent of the analysis frequency f, the effective duration of the WT test signal $(\mathbf{C}^{(t,f)}\gamma)(t')$ is inversely proportional to f and the bandwidth is proportional to f.

Like the STFT, the WT can be interpreted (for each analysis frequency f) as the result of filtering the signal $x(t')$ with a bandpass filter with center frequency f. In the STFT case, the bandpass filter's bandwidth is independent of the analysis or center frequency f. In contrast, the bandwidth of the WT bandpass filter is proportional to f or, equivalently, the filter's quality factor Q (= center frequency/bandwidth) is independent of f. In fact, the WT can be viewed as a "constant-Q" analysis [Rio90,91].

In principle, the WT suffers from the same time-frequency resolution limitations as the STFT, i.e., time resolution and frequency resolution of the WT cannot be made arbitrarily good simultaneously. However, the WT is different from the STFT in the following respect: while the STFT's time-frequency resolution is the same for each analysis frequency f, the WT analyzes higher frequencies with better time resolution but poorer frequency resolution. Figure 8 compares the resolution characteristics of the STFT and the WT using a simple signal.

Using a synthesis formula which is analogous to the STFT formulae (2.4) or (2.6), a signal may be reconstructed from its WT [Dau90a, Mall89a,c]. WT analysis and synthesis may be used as a basis for signal and image coding [Mala91, Ant91, Mall89c, Wic89, Bur89, Zet90, Baa90, Uz91, Zhan91], acoustic and seismic signal processing [Gou84, Kro87, Com89, Lar89, Wic89, Yan92, Gin89, Dut88, Morl82], speech analysis [Kad92a, Dave91, Lien87], stochastic signal processing and fractal analysis [Bass89, Chou91, Arn88, Arg89, Gac91, FlaP91a,92a, Wor92a-b, Tew92], system analysis [Arn89], and detection [Fow91, Fri91, Gro87].

TABLE II.
SOME "DESIRABLE" MATHEMATICAL PROPERTIES OF ENERGETIC, QUADRATIC TFRs

P1 – Real-valued: $T_{\tilde{x}}^{*}(t,f) = T_{x}(t,f)$

P2 – Time shift: $T_{\tilde{x}}(t,f) = T_{x}(t - t_0,f)$ for $\tilde{x}(t) = x(t - t_0)$

P3 – Frequency shift: $T_{\tilde{x}}(t,f) = T_{x}(t,f - f_0)$ for $\tilde{x}(t) = x(t)\, e^{j 2\pi f_0 t}$

P4 – Time marginal: $\int_f T_x(t,f)\, df = |x(t)|^2$

P5 – Frequency marginal: $\int_t T_x(t,f)\, dt = |X(f)|^2$

P6 – Time moments: $\int_t \int_f t^n\, T_x(t,f)\, dt\, df = \int_t t^n\, |x(t)|^2\, dt$

P7 – Frequency moments: $\int_t \int_f f^{\,n}\, T_x(t,f)\, dt\, df = \int_f f^{\,n}\, |X(f)|^2\, df$

P8 – Time-frequency scaling: $T_{\tilde{x}}(t,f) = T_x(at, \frac{f}{a})$ for $\tilde{x}(t) = \sqrt{|a|}\; x(at)$ with $a \neq 0$

P9 – Instantaneous frequency: $\dfrac{\int_f f\, T_x(t,f)\, df}{\int_f T_x(t,f)\, df} = f_x(t) = \dfrac{1}{2\pi}\dfrac{d}{dt}\arg|x(t)|$

P10 – Group delay: $\dfrac{\int_t t\, T_x(t,f)\, dt}{\int_t T_x(t,f)\, dt} = t_x(f) = -\dfrac{1}{2\pi}\dfrac{d}{df}\arg|X(f)|$

P11 – Finite time support: $T_x(t,f) = 0$ for t outside $[t_1,t_2]$ if $x(t) = 0$ outside $[t_1,t_2]$

P12 – Finite frequency support: $T_x(t,f) = 0$ for f outside $[f_1,f_2]$ if $X(f) = 0$ outside $[f_1,f_2]$

P13 – Moyal's formula (unitarity): $(T_{x_1,y_1}, T_{x_2,y_2}) = (x_1,x_2)\,(y_1,y_2)^{*}$

P14 – Convolution: $T_{\tilde{x}}(t,f) = \int_{t'} T_h(t - t',f)\, T_x(t',f)\, dt'$ for $\tilde{x}(t) = \int_{t'} h(t - t')\, x(t')\, dt'$

P15 – Multiplication: $T_{\tilde{x}}(t,f) = \int_{f'} T_h(t,f - f')\, T_x(t,f')\, df'$ for $\tilde{x}(t) = h(t)\, x(t)$

P16 – Fourier transform: $T_{\tilde{x}}(t,f) = T_x\left(\dfrac{-f}{c},ct\right)$ for $\tilde{x}(t) = \sqrt{|c|}\, X(ct)$ with $c \neq 0$

P17 – Chirp convolution: $T_{\tilde{x}}(t,f) = T_x(t - \dfrac{f}{c},f)$ for $\tilde{x}(t) = x(t) * \sqrt{|c|}\; e^{j 2\pi \frac{c}{2} t^2}$

P18 – Chirp multiplication: $T_{\tilde{x}}(t,f) = T_x(t,f - ct)$ for $\tilde{x}(t) = x(t)\, e^{j 2\pi \frac{c}{2} t^2}$

TABLE III.

PROPERTIES OF THE WIGNER DISTRIBUTION AND THE AMBIGUITY FUNCTION. The WD properties, denoted P_i, are listed on the left-hand side while the AF properties, denoted P_i', are listed on the right-hand side. The WD properties P_i are numbered according to Table II.

i	P_i	P_i'
1	$W_x^*(t,f) = W_x(t,f)$	$A_x^*(-\tau,-\nu) = A_x(\tau,\nu)$
2	$\tilde{x}(t) = x(t-t_0) \Rightarrow$ $W_{\tilde{x}}(t,f) = W_x(t-t_0,f)$	$\tilde{x}(t) = x(t-t_0) \Rightarrow$ $A_{\tilde{x}}(\tau,\nu) = A_x(\tau,\nu)\, e^{-j2\pi t_0 \nu}$
3	$\tilde{x}(t) = x(t)\, e^{j2\pi f_0 t} \Rightarrow$ $W_{\tilde{x}}(t,f) = W_x(t,f-f_0)$	$\tilde{x}(t) = x(t)\, e^{j2\pi f_0 t} \Rightarrow$ $A_{\tilde{x}}(\tau,\nu) = A_x(\tau,\nu)\, e^{j2\pi f_0 \tau}$
4	$\int_f W_x(t,f)\, df = p_x(t) = \lvert x(t)\rvert^2$	$A_x(0,\nu) = R_x(\nu) = \int_f X(f+\nu)\, X^*(f)\, df$
5	$\int_t W_x(t,f)\, dt = P_x(f) = \lvert X(f)\rvert^2$	$A_x(\tau,0) = r_x(\tau) = \int_t x(t+\tau)\, x^*(t)\, dt$
6	$\int_t \int_f t^n\, W_x(t,f)\, dt\, df = \int_t t^n \lvert x(t)\rvert^2\, dt$	$\left(-\frac{1}{j2\pi}\right)^n \left[\frac{d^n}{d\nu^n} A_x(0,\nu)\right]_{\nu=0} = \int_t t^n \lvert x(t)\rvert^2 dt$
7	$\int_t \int_f f^n\, W_x(t,f)\, dt\, df = \int_f f^n \lvert X(f)\rvert^2\, df$	$\left(\frac{1}{j2\pi}\right)^n \left[\frac{d^n}{d\tau^n} A_x(\tau,0)\right]_{\tau=0} = \int_f f^n \lvert X(f)\rvert^2 df$
8	$\tilde{x}(t) = \sqrt{\lvert a\rvert}\, x(at) \Rightarrow$ $W_{\tilde{x}}(t,f) = W_x\left(at, \frac{f}{a}\right)$	$\tilde{x}(t) = \sqrt{\lvert a\rvert}\, x(at) \Rightarrow$ $A_{\tilde{x}}(\tau,\nu) = A_x\left(a\tau, \frac{\nu}{a}\right)$
9	$\frac{\int_f f\, W_x(t,f)\, df}{\int_f W_x(t,f)\, df} = f_x(t)$	$\frac{1}{j2\pi} \frac{\int_\nu \left[\frac{\partial}{\partial\tau} A_x(\tau,\nu)\right]_{\tau=0} e^{j2\pi t\nu}\, d\nu}{\int_\nu A_x(0,\nu)\, e^{j2\pi t\nu}\, d\nu} = f_x(t)$
10	$\frac{\int_t t\, W_x(t,f)\, dt}{\int_t W_x(t,f)\, dt} = t_x(f)$	$-\frac{1}{j2\pi} \frac{\int_\tau \left[\frac{\partial}{\partial\nu} A_x(\tau,\nu)\right]_{\nu=0} e^{-j2\pi f\tau}\, d\tau}{\int_\tau A_x(\tau,0)\, e^{-j2\pi f\tau}\, d\tau} = t_x(f)$
11	$x(t) = 0$ for t outside $[t_1,t_2] \Rightarrow$ $W_x(t,f) = 0$ for t outside $[t_1,t_2]$	$x(t) = 0$ for t outside $[t_1,t_2] \Rightarrow$ $A_x(\tau,\nu) = 0$ for $\lvert\tau\rvert > t_2 - t_1$
12	$X(f) = 0$ for f outside $[f_1,f_2] \Rightarrow$ $W_x(t,f) = 0$ for f outside $[f_1,f_2]$	$X(f) = 0$ for f outside $[f_1,f_2] \Rightarrow$ $A_x(\tau,\nu) = 0$ for $\lvert\nu\rvert > f_2 - f_1$
13	$(W_{x_1,y_1}, W_{x_2,y_2}) = (x_1,x_2)\, (y_1,y_2)^*$	$(A_{x_1,y_1}, A_{x_2,y_2}) = (x_1,x_2)\, (y_1,y_2)^*$
14	$\tilde{x}(t) = \int_{t'} h(t-t')\, x(t')\, dt' \Rightarrow$ $W_{\tilde{x}}(t,f) = \int_{t'} W_h(t-t',f)\, W_x(t',f)\, dt'$	$\tilde{x}(t) = \int_{t'} h(t-t')\, x(t')\, dt' \Rightarrow$ $A_{\tilde{x}}(\tau,\nu) = \int_{\tau'} A_h(\tau-\tau',\nu)\, A_x(\tau',\nu)\, d\tau'$
15	$\tilde{x}(t) = h(t)\, x(t) \Rightarrow$ $W_{\tilde{x}}(t,f) = \int_{f'} W_h(t,f-f')\, W_x(t,f')\, df'$	$\tilde{x}(t) = h(t)\, x(t) \Rightarrow$ $A_{\tilde{x}}(\tau,\nu) = \int_{\nu'} A_h(\tau,\nu-\nu')\, A_x(\tau,\nu')\, d\nu'$
16	$\tilde{x}(t) = \sqrt{\lvert c\rvert}\, X(ct) \Rightarrow$ $W_{\tilde{x}}(t,f) = W_x\left(-\frac{f}{c}, ct\right)$	$\tilde{x}(t) = \sqrt{\lvert c\rvert}\, X(ct) \Rightarrow$ $A_{\tilde{x}}(\tau,\nu) = A_x\left(-\frac{\nu}{c}, c\tau\right)$
17	$\tilde{x}(t) = x(t) * \sqrt{\lvert c\rvert}\, e^{j2\pi\frac{c}{2}t^2} \Rightarrow$ $W_{\tilde{x}}(t,f) = W_x\left(t-\frac{f}{c}, f\right)$	$\tilde{x}(t) = x(t) * \sqrt{\lvert c\rvert}\, e^{j2\pi\frac{c}{2}t^2} \Rightarrow$ $A_{\tilde{x}}(\tau,\nu) = A_x\left(\tau-\frac{\nu}{c}, \nu\right)$
18	$\tilde{x}(t) = x(t)\, e^{j2\pi\frac{c}{2}t^2} \Rightarrow$ $W_{\tilde{x}}(t,f) = W_x(t,f-ct)$	$\tilde{x}(t) = x(t)\, e^{j2\pi\frac{c}{2}t^2} \Rightarrow$ $A_{\tilde{x}}(\tau,\nu) = A_x(\tau,\nu-c\tau)$

QUADRATIC TIME-FREQUENCY REPRESENTATIONS

Energetic and Correlative Time-Frequency Representations

Although linearity of a TFR is a desirable property, the quadratic structure of a TFR is an intuitively reasonable assumption when we want to interpret a TFR as a time-frequency energy distribution (or "instantaneous power spectrum" [Pag52, Levi67, Rih68b, Ack70, Grac81]), since energy is a quadratic signal representation. An "energetic" TFR $T_x(t,f)$ seeks to combine the concepts of the instantaneous power $p_x(t) = |x(t)|^2$ and the spectral energy density $P_x(f) = |X(f)|^2$ Ideally, this energetic interpretation is expressed by the *marginal properties*

$$\int_f T_x(t,f)df = p_x(t) = |x(t)|^2 \quad , \qquad \int_t T_x(t,f)dt = P_x(f) = |X(f)|^2 \tag{3.1}$$

which state that the one-dimensional energy densities $p_x(t)$ *and* $P_x(f)$ are "marginal densities" of the TRF $T_x(t,f)$ [Wig32-71]. As a consequence, the signal energy $E_x = \int |x(t)|^2 dt = \int |X(f)|^2 df$ can be derived by integrating $T_x(t,f)$ over the entire time-frequency plane. Other desirable mathematical properties of energetic TFRs may be found in Table II.

The marginal properties relate the TFR's frequency and time integrals to the energy densities $|x(t)|^2$ and $|X(f)|^2$, respectively, but they do *not* warrant the interpretation of $T_x(t,f)$ as a "time-frequency energy density" at every point in the time-frequency plane. This concept is *a priori* impossible since the uncertainty principle [Papo77, DeBr67] does not allow the notion of "energy at a specific time and frequency" [Cla84].

Many quadratic TFRs may be loosely interpreted in terms of signal energy even though they do not satisfy the marginal properties. Here, two prominent examples are the *spectrogram* and the *scalogram*, defined as the squared magnitudes of the linear TFRs considered in the previous section:

$$SPEC_x^{(\gamma)}(t,f) \triangleq \left| STFT_x^{(\gamma)}(t,f) \right|^2 \quad , \qquad SCAL_x^{(\gamma)}(t,f) \triangleq \left| WT_x^{(\gamma)}(t,f) \right|^2 \tag{3.2}$$

The spectrogram has been used extensively to analyze speech signals [Koe46, Pot66, Rab78] and other "nonstationary" signals. Similar time-varying spectral representations are the sonagram, rayspan, spectran [Kod78], and FTAN [Levs72]. The scalogram [FlaP90b, Rio91,92] can be considered as a "constant-Q version" of the spectrogram.

Apart from the "energetic" interpretation of quadratic TFRs, there exists another interpretation in terms of correlation functions [CohL86, Hla91c]. A "correlative" TFR $T_x(\tau,\nu)$ seeks to combine the temporal correlation $r_x(\tau)$ and the spectral correlation $R_x(\nu)$ defined below, both of which are again quadratic signal representations. Ideally, this is expressed by the "correlative marginal properties"

$$T_x(\tau,0) = r_x(\tau) = \int_t x(t+\tau)\, x^*(t)\, dt \quad , \qquad T_x(0,\nu) = R_x(\nu) = \int_f X(f+\nu)\, X^*(f)\, df \tag{3.3}$$

Note that the variables τ and ν in the correlative TFR $T_x(\tau,\nu)$ are the *time lag* and *frequency lag*, respectively.

The Quadratic Superposition Principle

The spectrogram of the sum of two signals $x_1(t) + x_2(t)$ is not simply the sum of the individual spectrograms $SPEC_{x_1}^{(\gamma)}(t,f) + SPEC_{x_2}^{(\gamma)}(t,f)$; hence, the linearity structure of the STFT is violated in the quadratic spectrogram. In fact, any quadratic TFR T_x satisfies the "quadratic superposition principle"

$$x(t) = c_1 x_1(t) + c_2 x_2(t) \;\Rightarrow\; T_x(t,f) = |c_1|^2 T_{x_1}(t,f) + |c_2|^2 T_{x_2}(t,f) + c_1 c_2^* T_{x_1,x_2}(t,f) + c_2 c_1^* T_{x_2,x_1}(t,f)$$

where $T_x(t,f)$ is the "auto-TFR" of the signal $x(t)$ and $T_{x_1,x_2}(t,f)$ is the "cross-TFR" of the two signals $x_1(t)$ and $x_2(t)$, with $T_{x,x}(t,f) = T_x(t,f)$. Note that the cross-TFR $T_{x_1,x_2}(t,f)$ is *bilinear* in the signals $x_1(t)$ and $x_2(t)$. Examples of cross TFRs will be given in the next section.

Generalizing the quadratic superposition principle to an N-component signal $x(t) = \sum_{k=1}^{N} c_k x_k(t)$, we obtain the following rule [FlaP84c, Hla92a]:

* To each signal component $c_k x_k(t)$, there corresponds an auto-component ("signal term") $|c_k|^2 T_{x_k}(t,f)$;

* To each *pair* of signal components $c_k x_k(t)$ and $c_l x_l(t)$ (with $k \neq l$), there corresponds a cross component ("interference term") $c_k c_l^* T_{x_k,x_l}(t,f) + c_l c_k^* T_{x_l,x_k}(t,f)$.

Thus, for an N-component signal $x(t)$, the TFR $T_x(t,f)$ will comprise N signal terms and $\binom{N}{2} = N(N-1)/2$ interference terms. Note that the number of interference terms grows quadratically with the number of signal components, a fact that often makes the visual analysis of the TFR of multicomponent signals difficult.

The interference terms of the spectrogram and the scalogram are oscillatory structures which are restricted to those regions of the time-frequency plane where the corresponding auto representations (signal terms) overlap. Hence, if two signal components are sufficiently far apart in the time-frequency plane, then their cross representation (interference term) will be essentially zero [Kad92b, Hla92a, Ril89, Jeo90a,

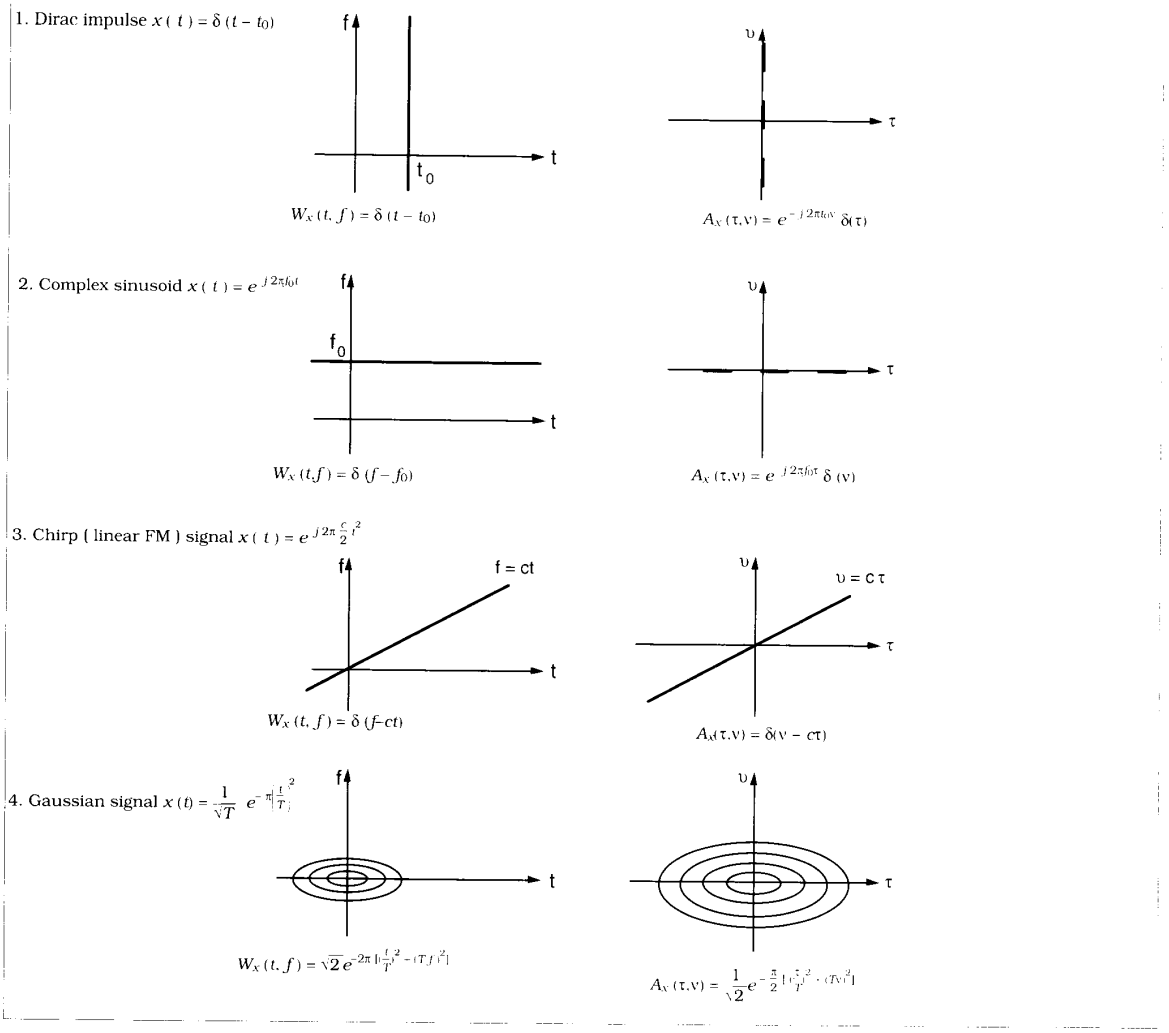

Fig. 9. WD and AF of simple monocomponent signals.

Rio92]. This property is generally deemed desirable. On the other hand, a disadvantage of the spectrogram and the scalogram is their poor time-frequency concentration (or resolution). It will be shown in a later section that there exists a general tradeoff between good time-frequency concentration and small interference terms. The Wigner distribution, to be discussed next, has excellent time-frequency concentration but substantial interference terms.

Wigner Distribution and Ambiguity Function

Definitions and Properties

Among all the quadratic TFRs with energetic interpretation, the *Wigner distribution* (WD) [Wig32-71, Vil48, Cla80a-c, DeBr73, FlaP80]

$$W_{x,y}(t,f) \triangleq \int_{\tau} x(t+\frac{\tau}{2})\, y^*(t-\frac{\tau}{2})\, e^{-j2\pi f\tau} d\tau = \int_{\nu} X(f+\frac{\nu}{2}) Y^*(f-\frac{\nu}{2}) e^{j2\pi t\nu} d\nu \qquad (3.4)$$

satisfies an exceptionally large number of desirable mathematical properties [Wig32, FlaP83a, Cla80a,c, CohL89] as summarized in the left-hand side of Table III. For example, the auto-WD is always real-valued, and the WD preserves time shifts and frequency shifts of the signal. The WD satisfies the marginal properties (3.1), that is, the frequency or time integrals of the WD correspond to the signal's instantaneous power and its spectral energy density, respectively. Hence, the WD can be loosely interpreted as a two-dimensional distribution of signal energy over the time-frequency plane. However, as mentioned earlier, the uncertainty principle prohibits the interpretation as a pointwise

time-frequency energy density [Cla84, Mec87]; this restriction is also reflected by the fact that the WD may locally assume negative values [Esc79, Hud74, JanA85,92, Mou85]. The instantaneous frequency in (1.1) and the group delay in (1.2) can be evaluated using local first-order moments of the WD.

Among the class of correlative TFRs, an equally important role is played by the *ambiguity function* (AF) [Woo53, Papo74, Rih69, Sie58, Sko62, Szu81, Stu64, Van71, Tit66, Aus85]

$$A_{x,y}(\tau,\nu) \triangleq \int_t x(t+\frac{\tau}{2})\, y^*(t-\frac{\tau}{2})\, e^{-j2\pi\nu t}dt = \int_f X(f+\frac{\nu}{2})Y^*(f-\frac{\nu}{2})e^{j2\pi\tau f}df \qquad (3.5)$$

The AF can be interpreted as a joint time-frequency correlation function. Specifically, it satisfies the "correlative marginal properties" in (3.3); when evaluated along its axes, i.e., for $\nu=0$ or $\tau=0$, it simplifies to either the time-domain or the frequency-domain correlation function. In addition, the maximum value of an auto AF occurs at the origin and equals the signal's energy, i.e., $|A_x(\tau,\nu)| \le A_x(0,0) = \int |x(t)|^2 dt$. The right-hand side of Table III lists some mathematical properties of the AF [Van71, Papo77]. We note that the squared magnitude of the AF, $|A_{x,y}(\tau,\nu)|^2$, is commonly called *ambiguity surface* (AS) although some authors use the name "ambiguity function" for $|A_{x,y}(\tau,\nu)|^2$, rather than $A_{x,y}(\tau,\nu)$ [Van71].

The WD and the AF are duals in the sense that they are a Fourier transform pair [Cla80c, Vil48, Szu81],

$$A_{x,y}(\tau,\nu) = \int_t \int_f W_{x,y}(t,f)\, e^{-j2\pi(\nu t - \tau f)}dtdf \qquad (3.6)$$

This duality is reflected by the mathematical properties of the WD and the AF listed in Table III.

Figure 9 depicts the WD and the AF for some simple monocomponent signals [Cla80a]. We see, in particular, that the WD preserves the time or frequency concentration of the signal. This is different from the spectrogram and the scalogram which generally introduce some broadening with respect to time and frequency.

Interference Geometry

Improved time-frequency concentration [Nut88b, JonD92, JanA82, Cla84] and an extensive list of desirable mathematical properties are attractive features of the WD. On the other hand, certain characteristics of the WD's interference terms (ITs) often cause problems in practical applications. Whereas the ITs of the spectrogram or the scalogram will be zero if the corresponding signal terms do not overlap, the ITs of the WD will be nonzero regardless of the time-frequency distance between the two signal terms. The "interference geometries" of the WD and the AF are illustrated in Fig. 10; they need to be taken into account when

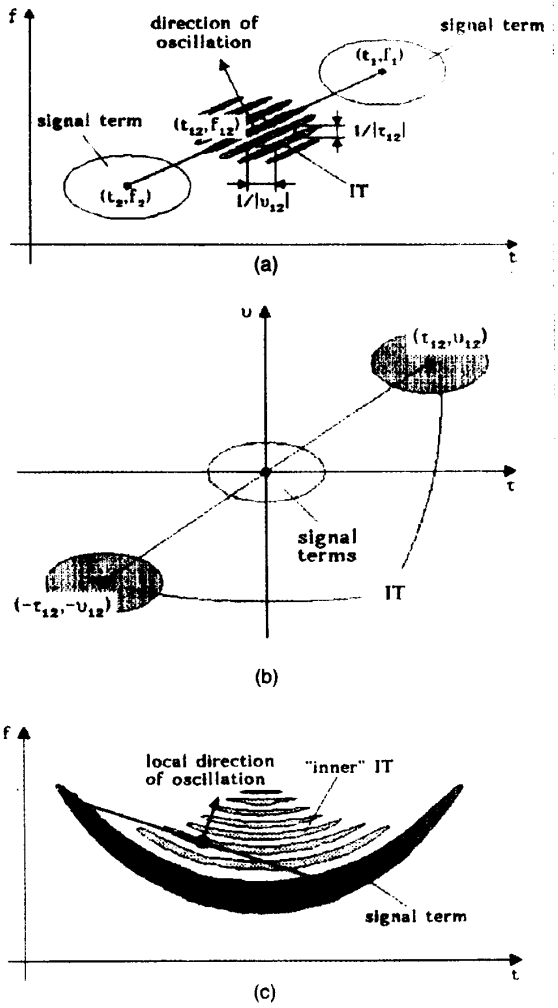

Fig. 10. Interference geometries of the WD and the AF. Two signal components occurring around time-frequency points (t_1, f_1) and (t_2, f_2) give rise to two signal terms and one interference term (IT) in both the WD and the AF. For the following discussion, we define the center point (t_{12}, f_{12}) and the lags τ_{12}, ν_{12} as $t_{12} = (t_1+t_2)/2$, $f_{12} = (f_1+f_2)/2$; $\tau_{12} = t_1-t_2$, $\nu_{12} = f_1-f_2$.
(a) Interference geometry of the WD: The signal terms are located around (t_1, f_1) and (t_2, f_2), respectively. The IT is located around the center point (t_{12}, f_{12}). It oscillates with respect to time with oscillation period $1/|\nu_{12}|$, and with respect to frequency with oscillation period $1/|\tau_{12}|$. The rapidity of oscillation increases with growing distance between the signal points in the time-frequency plane. The direction of oscillation is perpendicular to the line connecting the two signal points.
(b) Interference geometry of the AF: The signal terms are located around the origin of the (τ,ν)-plane. The IT consists of two subterms located around the "lag points" (τ_{12}, ν_{12}) and $(-\tau_{12}, -\nu_{12})$, respectively.
(c) "Inner" interference: In general, ITs occur also in the case of monocomponent signals. The simple geometric laws discussed above are still valid. The figure shows the WD of a complex frequency modulation signal. The signal's energy is concentrated along the curved instantaneous frequency; this also defines the WD's signal term. Oscillatory ITs are seen to exist midway between any two points on the signal term.

interpreting the WD or AF of more complicated signals such as multicomponent signals or signals with nonlinear frequency modulation. In general, the ITs of the WD can be identified by their oscillatory nature, while the ITs of the AF are characterized by their locations away from the origin of the (τ,ν)-plane [FlaP84c, Hla84,92a, JanA82]. The attenuation of WD ITs by means of smoothing will be discussed in later sections.

From a practical viewpoint, ITs are troublesome since they may overlap with auto terms (signal terms) and thus make it difficult to *visually* interpret a WD or AF plot. However, it should be noted that quadratic cross terms naturally occur in the energy densities $p_x(t)$, $P_x(f)$ and the correlations $r_x(\tau), R_x(\nu)$ (see (3.1) and (3.3)). Therefore, if one wants to interpret a quadratic TFR as a two-dimensional time-frequency energy distribution or time-frequency correlation, with the respective marginals equalling the one-dimensional energy densities (cf. (3.1)) or the one-dimensional correlations (cf. (3.3)), then it should be clear that the quadratic TFR *must* contain cross terms as well. Indeed, it can be shown that in many cases oscillatory and partly negative ITs must be present or the marginal properties and instantaneous-frequency/group-delay properties cannot be satisfied [Cla80c, Wig71, Hla92a]. Also, ITs are necessary for a TFR's *unitarity* [Hla92f] or, equivalently, for Moyal's formula [Moy49, Cla80a] (cf. Tables II and V) to hold. Moyal's formula is critical for the time-frequency formulation of optimum detection and estimation methods [Kay85, Kum84a, FlaP88] and for a closed-form solution to the signal synthesis problem [Boud86, Hla92b,e].

Applications of the WD

The WD has served as a useful analysis tool in fields as diverse as quantum mechanics [Wig32-71, Moy49, Ber77, Kru76, Oco83], optics [Bast81b,86,92, Bre82, Jia84, Oje84, Szu86], acoustics [Day88, Boa88a, FlaP90c, MarN86a, JanC83, Pey85, Yen87], bioengineering [Abe89a, Boua84, FlaP86, Kit87, Mart86, Verr89, Morg86], image processing [Sah90, Jac82,88, Cri89], and oceanography [Imb86]. Several researchers have used the WD to analyze time-varying systems [Pei88, Kum87, Hla92c,d], and highly non-stationary signals [Whi87, Kob86, Vel89b]. The WD has been suggested as a method for analyzing the phase distortion encountered in a variety of audio engineering problems [JanC83, Prei82-87, Vers88] and nonlinearities or defects in systems [For89, Ada87, Boa88b, Zhu90]. It has been used to analyze speech [Boa86a, Che83, Gar87, Pres83, Wok87, Ril89, Vel89a], seismic data [Boa86c,90a, Bole87, Boua83, Boud87, Day88], and mechanical vibrations [Chi87]. A coding application in covert optical communication systems has been proposed in [Szu81]. Researchers have applied random signal theory to the WD [FlaP83b,87b, Boa86b, Ham85, Hla91b, JanA79, Mart85a, Whi89,90b] and have used the WD for signal detection [FlaP88, Boa90a,90b,91b, Kay85, Kum84a, Rao91, Mul88], spectrum and instantaneous frequency estimation [CohL91, Har89, Kay85, Whi88,90a, JonG90, Vel90, Nut88a, Ami87, Hea91, Won90, Rao90, Boa89,90a, CohF88, Ram87], and pattern recognition [Boa87a, Boua84, Kum84b, Abe89b, MarN84]. WD synthesis techniques [Boud86,92a, Hla91b,92b,e, Jeo90b,91, Kra88,90,93, McH89, Kum86, Raz90, Sal85, Yu87] have been used to perform time-varying filtering, multi-component signal separation [Boud86,87, Hla89, Koz91, Jeo90b, Koc90] and window and filter design [Boud83,92a].

Discrete-time versions of the WD and implementation issues have been discussed in [Cla80b,83, JanC83, Boud83, Nut89, Pey86, Boa87b, MarN88, FlaP84a, Bre83, Cha82, Jeo92b]. Optical WD implementations are described in [Ath83, Bam83, Bart80, Con85, Gup86, Iwa86, KenO88, Ste82, Sub84, Eas84, Mat86].

Several extensions of the WD definition have been proposed. The expected value of the WD of a nonstationary random process is known as the *Wigner-Ville spectrum* [FlaP83b,87b,92b, Ham85, Hla91d, JanA79, Mart85a,b, Whi90b]. Recently, higher-order versions of the WD have been proposed to generalize the ideas of higher-order cumulants, moments, and spectra to the time-frequency plane [Gerr88, Boa91a, Fon91a,b, SwaA91]. Extensions of the WD to linear signal spaces and linear, time-varying systems have been proposed and applied for analysis and synthesis purposes in [Hla91a,92c,d, Koz91].

Applications of the AF

The AF and its squared magnitude (the ambiguity surface or AS) have been used extensively in the fields of radar, sonar, radio astronomy, communications and optics. In the radar case, the problem is the estimation of the distance and velocity of a moving target, where the distance and velocity correspond to the "range" parameter τ and the "Doppler shift" parameter ν, respectively [Woo53, Sko62, Sie56]. The location of the maximum of the cross-AS of the received signal and the transmitted signal can be interpreted as the maximum-likelihood estimator of the range τ and Doppler shift ν in the case of a nonfluctuating point target [Van71]. Also, the auto-AS of the transmitted signal provides pertinent information about the performance of the maximum-likelihood estimator and is thus a major criterion for designing the transmitted signal. Specifically, the Cramér-Rao bounds on the estimator's variances can be expressed in terms of the second derivatives of the AS with respect to τ and ν, respectively, measured at the origin. Furthermore, the estimator's sensitivity to clutter or reverberation may be related to the values of the AS away from the origin [Van71]. For ideal performance, the AS of the transmitted signal should be a "thumbtack," i.e., a narrow peak at the origin of the (τ,ν)-plane and zero elsewhere [Sie56, Van71]. Unfortunately, the thumbtack shape of a realizable AS is limited by the "radar uncertainty principle" which constrains both the maximum height and the volume of any AS [Rih69, Sko62, Van71, Pri65, Lieb90].

The AF and the AS have been used as analysis tools for the selection of radar waveforms [Ler63, Pri63, Rih69,71, Turi57, Kla6Ob, Miz75, Vak68]. The AF has been applied to design and evaluate the performance of a large variety of radar signals [Rih69, Cos84, Dru91,

MarS90, Bel91, Tit91a-b] including chirp [Kla6Oa] and other FM signals [Rih68a], uniform pulse trains [Ler58, Rih69], Barker codes [Hol67], complementary signals [Tury63, Siv82], phase-reversed codes, staggered pulse trains and polyphase codes [Rih69]. The AF has also been used to analyze the time-varying nature of communication channels [Gers63, Kai63, Gaa68, Gol68, KenR69] and to analyze optical systems [Papo74, Gui78, Szu86]. Efficient algorithms for discrete-time AF computation can be found in [Ste81, Tol85, Aus88,91b, MarN91].

AF and AS synthesis algorithms [Wilc6O, Widn61, Sus62, DeL67, Sed70, Wolf69, Debu70, Jou77] have been used to derive phase-coded signals [Vak67a,76], burst-pulse signals [Bla67], signals that minimize the volume under the AS in certain regions of the (τ,ν)-plane [Pri65, Vak67b] and signals whose cross-AF with a given radar signal minimizes echo clutter given constraints on the target and noise output power [Stu68].

Shift-Invariant Time-Frequency Representations

The Shift-Invariant Class (Cohen Class) and Its Correlative Dual

Beside the WD, there exist many other quadratic TFRs with an energetic interpretation. Most of these TFRs satisfy the basic property of *time-frequency shift invariance* (or "covariance"): if the signal $x(t)$ is delayed in time and/or shifted in frequency, then its TFR will be shifted by the *same* time delay and/or modulation frequency,

$$\tilde{x}(t) = x(t-t_0)\, e^{j2\pi f_0 t} \quad \Rightarrow \quad T_{\tilde{x}}(t,f) = T_x(t-t_0\,,\, f-f_0) \tag{3.7}$$

The class of all time-frequency shift-invariant, quadratic TFRs is known as the *quadratic Cohen class* [CohL66,89, Cla80c, FlaP80, Hla91c]. Prominent members of Cohen's class are the spectrogram (3.2) and the Wigner distribution (3.4).

Every member of Cohen's class may be interpreted as a 2-D filtered WD. In fact, it can be shown that a TFR $T_x(t,f)$ is a member of Cohen's class, denoted C_E, if and only if it can be derived from the WD of the signal $x(t)$ via a time-frequency *convolution* [FlaP87c, Hla91c, Cla80c]:

$$T_x \in C_E \;\Leftrightarrow\; T_x(t,f) = \int\!\!\int_{t'f'} \psi_T(t-t',\, f-f')\, W_x(t',\, f')\, dt'\, df' \tag{3.8}$$

Each member T_x of Cohen's class is associated with a unique, signal-independent kernel function $\psi_T(t,f)$ (or 2-D filter).

Clearly, the convolution in (3.8) will transform into a simple multiplication in the Fourier transform domain. Therefore, to every shift-invariant TFR $T_x(t,f) \in C_E$, we now define a "dual correlative TFR" $T_{dual,x}(\tau,\nu)$ as the two-dimensional FT [FlaP84c, CohL86]

$$T_{dual,x}(\tau,\nu) \triangleq \int\!\!\int_{t\,f} T_x(t,f)\, e^{-j2\pi(\nu t - \tau f)}\, dt\, df \tag{3.9}$$

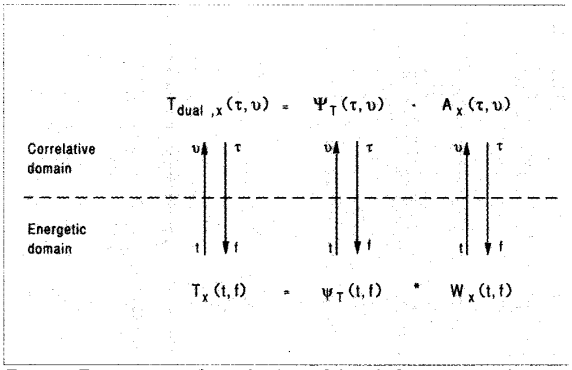

Fig. 11. Fourier transform duality of the shift-invariant classes C_E and C_C. (The arrows denote Fourier transforms mapping time t into frequency lag ν or time lag τ into frequency f.)

A prominent example of a pair of dual TFRs is given by the WD and the AF since they are related by the Fourier transform (3.9) (cf. Eq. (3.6)).

The class of dual correlative TFRs consists of all TFRs satisfying the "correlative shift invariance" [Hla91c]

$$\tilde{x}(t) = x(t-t_0)\, e^{j\,2\pi f_0 t} \;\Rightarrow\; T_{dual,\tilde{x}}(\tau,\nu) = T_{dual,x}(\tau,\nu)\, e^{j\,2\pi(f_0\tau - t_0\nu)}$$

which is motivated by the shift properties

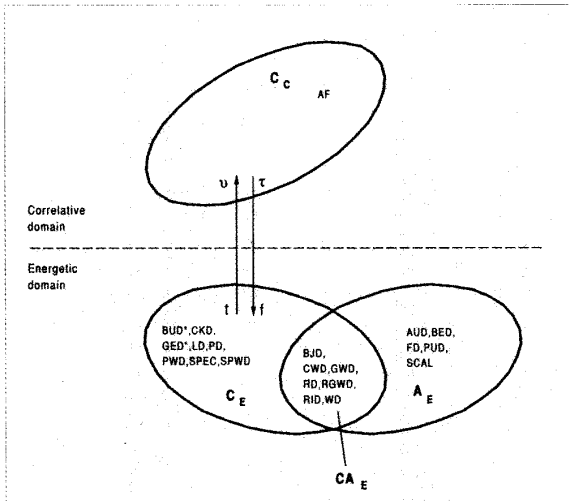

*Fig. 12. Classification of quadratic TFRs (for TFR abbreviations, see Table I). The classes shown are the Cohen class C_E of energetic TFRs which preserve time shifts and frequency shifts; the correlative dual C_C of the Cohen class C_E; the affine class A_E of energetic TFRs which preserve time shifts and time scalings, and the shift-scale invariant class CA_E which forms the intersection of C_E and A_E and comprises all energetic TFRs that preserve time shifts, frequency shifts, and time scalings. *BUD and GED are members of CA_E if N=M.*

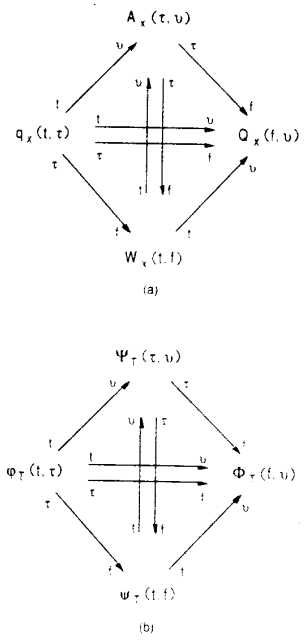

Fig. 13. General expressions for energetic, shift-invariant TFRs (Cohen class C_E). All TFRs of Cohen's class can be written in the following four equivalent ways:

$$T_x(t,f) = \int_\tau \left[\int_{t'} \varphi_T(t-t',\tau)\, q_x(t',\tau)dt'\right] e^{-j2\pi f\tau} d\tau$$

$$= \int_\nu \left[\int_{f'} \Phi_T(f-f',\nu)\, Q_x(f',\nu)df'\right] e^{j2\pi t\nu} d\nu$$

$$= \int\int_{t'f'} \psi_T(t-t', f-f')\, W_x(t',f')\, dt'df'$$

$$= \int\int_{\tau\,\nu} \left[\Psi_T(\tau,\nu)A_x(\tau,\nu)\right] e^{j2\pi(t\nu-f\tau)} d\tau\, d\nu$$

where $q_x(t,\tau) = x(t+\frac{\tau}{2})x^*(t-\frac{\tau}{2})$ *and*

$Q_x(f,\nu) = X(f+\frac{\nu}{2})\,X^*(f-\frac{\nu}{2})$, *and the WD,* $W_x(t,f)$, *and AF,* $A_x(\tau,\nu)$, *have been defined in (3.4) and (3.5), respectively.*

(a) The quadratic signal representations $q_x(t,\tau)$, $Q_x(f,\nu)$, $W_x(t,f)$, *and* $A_x(\tau,\nu)$ *are interrelated by Fourier transforms.*
(b) Identical Fourier-transform relations connect the four kernel functions $\varphi_T(t,\tau), \Phi_T(f,\nu), \psi_T(t,f)$, *and* $\Psi_T(\tau,\nu)$. *A Cohen-class TFR* $T_x(t,f)$ *is uniquely characterized by any of the four kernels.*

$$r_{\tilde{x}}(\tau) = r_x(\tau)\, e^{j2\pi f_0\tau}, \qquad R_{\tilde{x}}(\nu) = R_x(\nu)\, e^{-j2\pi t_0\nu}$$

of the one-dimensional correlations $r_x(\tau)$ and $R_x(\nu)$ (see (3.3)). Note that in the dual correlative domain a time-frequency shift of the signal $x(t)$ affects only the phase and does not lead to an analogous time-frequency shift as in the energetic domain (cf. (3.7)).

Most importantly, any TFR $T_{dual,x}$ which is a member of the correlative class, denoted C_C, can be derived from the AF of the signal $x(t)$ by means of a multiplication [FlaP84c, CohL86]:

$$T_{dual,x} \in C_C \;\Leftrightarrow\; T_{dual,x}(\tau,\nu) = \Psi_T(\tau,\nu)A_x(\tau,\nu) \quad (3.10)$$

The kernel $\Psi_T(\tau,\nu)$ of $T_{dual,x}(\tau,\nu)$ in the above equation and the kernel $\psi_T(t,f)$ of $T_x(t,f)$ in Eq. (3.8) are a Fourier transform pair just as the TFRs $T_{dual,x}(\tau,\nu)$ and $T_x(t,f)$ themselves. The Fourier transform duality between the energetic Cohen class C_E and the dual correlative class C_C is illustrated in Figures 11 and 12.

Even if our only interest is in a TFR of the energetic class C_E, it is often convenient to consider the dual correlative TFR of C_C since the multiplication relation (3.10) is usually simpler than the convolution relation (3.8). Specifically, this approach is fruitful for the study of *smoothed versions of the WD* [FlaP84c, Hla92a], as discussed in the next section.

Figure 13 shows four general expressions for energetic, shift-invariant TFRs. A list of specific members of C_E, together with their kernels and mathematical properties, is given in Table IV. Finally, the middle column of Table V lists constraints on the kernels of Cohen's class corresponding to the TFR properties defined in Table II. A TFR satisfies a given property if the TFR's kernel satisfies the corresponding constraint [Cla80c, JanC83, Hla88].

Shift-Invariant WD Smoothing

Even though the WD is theoretically attractive due to its mathematical properties, practical application of the WD is often restricted by the occurrence of interference terms. Because interference terms are oscillatory, they may be attenuated by means of a smoothing operation (i.e., lowpass filtering) [JanA85, FlaP84c, Hla92a]. The Cohen class C_E of shift-invariant TFRs provides a convenient framework for WD smoothing.

According to (3.8), any shift-invariant TFR T_x can be derived from the WD via a convolution with a kernel $\psi_T(t,f)$. However, it is clear that this convolution will result in a smoothing (or two-dimensional lowpass filtering) of the WD only if the kernel $\psi_T(t,f)$ is a sufficiently *smooth* function. If this is the case, then we shall call the resulting TFR a *smoothed WD* (SWD), and the kernel $\psi_T(t,f)$ will be called a *smoothing function*.

A deeper understanding of SWDs is greatly facilitated by passing into the dual correlative domain. As discussed in the previous section (cf. (3.10)), the dual correlative TFR is derived from the AF by multiplication with a kernel $\Psi_T(\tau,\nu)$ which is the FT of the smoothing function $\psi_T(t,f)$. Since the interference terms in the AF are typically located away from the origin of the (τ,ν)-plane as discussed in Fig. 10b, then the "weighting function" $\Psi_T(\tau,\nu)$ must be concentrated mainly in the "lowpass" region around the origin in order to attenuate the interference terms. Equivalently, $\Psi_T(\tau,\nu)$ must be the transfer function of a two-dimensional lowpass filter, which is consistent with the previous requirement that $\psi_T(t,f)$ be a smooth function [FlaP84c, Hla92a].

Unfortunately, this attenuation of interference terms

TABLE IV.

SOME TFRs OF THE COHEN CLASS (CLASS OF ENERGETIC, SHIFT-INVARIANT, QUADRATIC TFRs) IN ALPHABETICAL ORDER. The TFRs are defined in Table I. The kernels $\varphi_T(t,\tau)$ and $\Psi_T(\tau,\nu)$ are defined in Fig. 13. The properties P_i are defined in Table II. A list of constraints on the kernels is given in Table V.

TFR	$\varphi_T(t,\tau)$	$\Psi_T(\tau,\nu)$	Properties P_i satisfied
Born- Jordan distribution (BJD)	$\begin{cases} \frac{1}{\lvert\tau\rvert}, & \lvert t/\tau\rvert < 1/2 \\ 0, & \lvert t/\tau\rvert > 1/2 \end{cases}$	$\frac{\sin(\pi\tau\nu)}{\pi\tau\nu}$	P_1–P_{12}, P_{16}
Butterworth distribution (BUD)[1]	$\mathcal{F}^{-1}_{\nu\to t}\,\Psi_T(\tau,\nu)$	$\frac{1}{1+\left(\frac{\tau}{\tau_0}\right)^{2M}\left(\frac{\nu}{\nu_0}\right)^{2N}}$	P_1–P_7, P_8 (M=N), P_9 (M>1/2), P_{10} (N>1/2), P_{16} (M=N)
Choi-Williams (exponential) distribution (CWD)	$\sqrt{\frac{\sigma}{4\pi}}\,\frac{1}{\lvert\tau\rvert}\exp\left[-\frac{\sigma}{4}\left(\frac{t}{\tau}\right)^2\right]$	$\exp\left[-\frac{(2\pi\tau\nu)^2}{\sigma}\right]$	P_1–P_{10}, P_{16}
Cone-kernel distribution (CKD)	$\begin{cases} g(\tau), & \lvert t/\tau\rvert < 1/2 \\ 0, & \lvert t/\tau\rvert > 1/2 \end{cases}$	$g(\tau)\,\lvert\tau\rvert\,\frac{\sin(\pi\tau\nu)}{\pi\tau\nu}$	P_1 ($g(\tau)$ even), P_2, P_3, P_{11}
Generalized exponential distribution (GED)[2]	$\mathcal{F}^{-1}_{\nu\to t}\,\Psi_T(\tau,\nu)$	$e^{-\left(\frac{\tau}{\tau_0}\right)^{2M}\left(\frac{\nu}{\nu_0}\right)^{2N}}$	P_1–P_7, P_8 (M=N), P_9 (M>1/2), P_{10} (N>1/2), P_{14} (M=1/2), P_{15} (N=1/2), P_{16} (M=N)
Generalized Wigner distribution (GWD)	$\delta(t+\alpha\tau)$	$e^{j2\pi\alpha\tau\nu}$	P_2–P_8, P_{11}–P_{12} ($\lvert\alpha\rvert\le 1/2$), P_{13}–P_{15}; all other for α=0 (WD)
Levin distribution (LD)	$\delta\left(t+\frac{\lvert\tau\rvert}{2}\right)$	$e^{j\pi\lvert\tau\rvert\,\nu}$	P_1–P_7, P_{11}, P_{13}, P_{15}
Page distribution (PD)	$\delta\left(t-\frac{\lvert\tau\rvert}{2}\right)$	$e^{-j\pi\lvert\tau\rvert\,\nu}$	P_1–P_7, P_{11}, P_{13}, P_{15}
Pseudo Wigner distribution (PWD)	$\delta(t)\,\eta\left(\frac{\tau}{2}\right)\eta^*\left(-\frac{\tau}{2}\right)$	$\eta\left(\frac{\tau}{2}\right)\eta^*\left(-\frac{\tau}{2}\right)$	P_1–P_3 P_4 ($\lvert\eta(0)\rvert=1$), P_6 ($\lvert\eta(0)\rvert=1$) P_9 ($\eta(0)=1$), P_{11}
Real-valued generalized Wigner distribution (RGWD)	$\frac{1}{2}[\delta(t+\alpha\tau)+\delta(t-\alpha\tau)]$	$\cos(2\pi\alpha\tau\nu)$	P_1–P_{10}, P_{11}–P_{12} ($\lvert\alpha\rvert\le 1/2$), P_{16}, all other for α=0 (WD)
Reduced interference distribution (RID)[3]	$\frac{1}{\lvert\tau\rvert}\,s\left(\frac{t}{\tau}\right)$ with constraints[4]	$S(\tau\nu)$ with constraints[4]	P_1–P_{12}, P_{16} (S(β) even)
Rihaczek distribution (RD)	$\delta\left(t-\frac{\tau}{2}\right)$	$e^{j\pi\tau\nu}$	P_2–P_8, P_{11}–P_{15}
Smoothed pseudo Wigner distribution (SPWD)	$g(t)\,\eta\left(\frac{\tau}{2}\right)\eta^*\left(-\frac{\tau}{2}\right)$	$\eta\left(\frac{\tau}{2}\right)\eta^*\left(-\frac{\tau}{2}\right)G(\nu)$	P_1 ($g(t)\in\mathbb{R}$), P_2, P_3
Spectrogram (SPEC)	$\gamma\left(-t-\frac{\tau}{2}\right)\gamma^*\left(-t+\frac{\tau}{2}\right)$	$A_\gamma(-\tau,-\nu)$	P_1–P_3
Wigner distribution (WD)	$\delta(t)$	1	P_1–P_{18}

[1] Closed-form expression for $\varphi_T(t,\tau)$ available for integer N [Papa91]

[2] Closed-form expression for $\varphi_T(t,\tau)$ available for N=1 [Papa91]

[3] Specific members of the RID class are discussed in [Jeo92a]

[4] The functions $s(\alpha) \leftrightarrow S(\beta)$ are constrained as follows:

$$s(\alpha)=0 \text{ for } \lvert\alpha\rvert > 1/2,\ S(\beta)\in\mathbb{R},\ S(0)=1,\ \frac{d}{d\beta}S(\beta)\Big|_{\beta=0}=0$$

TABLE V.
TFR PROPERTIES AND CORRESPONDING KERNEL CONSTRAINTS FOR THE COHEN CLASS C_E AND THE SHIFT-SCALE INVARIANT CLASS CA_E. The properties P_i are defined in Table II. The kernels $\varphi_T(t,\tau)$, $\Phi_T(f,\nu)$ and $\Psi_T(\tau,\nu)$ are defined in Figure 13. The kernels $s_T(\alpha) \leftrightarrow S_T(\beta)$ are defined in the text section "The Shift-Scale Invariant Class."

TFR property (cf. Table II)	Kernel constraint (class C_E)	Kernel constraint (class CA_E)
P_1: Real-valued	$\Psi_T^*(-\tau,-\nu) = \Psi_T(\tau,\nu)$	$S_T(\beta) \in \mathbb{R}$
P_2: Time shift	Always satisfied	Always satisfied
P_3: Frequency shift	Always satisfied	Always satisfied
P_4: Time marginal	$\Psi_T(0,\nu) = 1$	$S_T(0) = 1$
P_5: Frequency marginal	$\Psi_T(\tau,0) = 1$	$S_T(0) = 1$
P_6: Time moments	$\Psi_T(0,\nu) = 1$	$S_T(0) = 1$
P_7: Frequency moments	$\Psi_T(\tau,0) = 1$	$S_T(0) = 1$
P_8: Time-frequency scaling	$\Psi_T\left(a\tau,\frac{\nu}{a}\right) = \Psi_T(\tau,\nu)$ for $a \neq 0$	Always satisfied
P_9: Instantaneous frequency	$\Psi_T(0,\nu) = 1$ and $\frac{\partial}{\partial\tau}\Psi_T(\tau,\nu)\Big\|_{\tau=0} = 0$	$S_T(0) = 1$ and $\frac{d}{d\beta}S_T(\beta)\Big\|_{\beta=0} = 0$
P_{10}: Group delay	$\Psi_T(\tau,0) = 1$ and $\frac{\partial}{\partial\nu}\Psi_T(\tau,\nu)\Big\|_{\nu=0} = 0$	$S_T(0) = 1$ and $\frac{d}{d\beta}S_T(\beta)\Big\|_{\beta=0} = 0$
P_{11}: Finite time support	$\varphi_T(t,\tau) = 0$ for $\lvert t/\tau\rvert > 1/2$	$s_T(\alpha) = 0$ for $\lvert\alpha\rvert > 1/2$
P_{12}: Finite frequency support	$\Phi_T(f,\nu) = 0$ for $\lvert f/\nu\rvert > 1/2$	$s_T(\alpha) = 0$ for $\lvert\alpha\rvert > 1/2$
P_{13}: Moyal's formula (unitarity)	$\lvert\Psi_T(\tau,\nu)\rvert \equiv 1$	$\lvert S_T(\beta)\rvert \equiv 1$
P_{14}: Convolution	$\Psi_T(\tau_1+\tau_2,\nu) = \Psi_T(\tau_1,\nu)\,\Psi_T(\tau_2,\nu)$	$S_T(\beta) = e^{c\beta}$
P_{15}: Multiplication	$\Psi_T(\tau,\nu_1+\nu_2) = \Psi_T(\tau,\nu_1)\,\Psi_T(\tau,\nu_2)$	$S_T(\beta) = e^{c\beta}$
P_{16}: Fourier transform	$\Psi_T\left(-\frac{\nu}{c},c\tau\right) = \Psi_T(\tau,\nu)$ for all $c \neq 0$	$S_T(-\beta) = S_T(\beta)$
P_{17}: Chirp convolution	$\Psi_T\left(\tau-\frac{\nu}{c},\nu\right) = \Psi_T(\tau,\nu)$ for all $c \neq 0$	$S_T(\beta) =$ constant
P_{18}: Chirp multiplication	$\Psi_T(\tau,\nu-c\tau) = \Psi_T(\tau,\nu)$ for all $c \neq 0$	$S_T(\beta) =$ constant

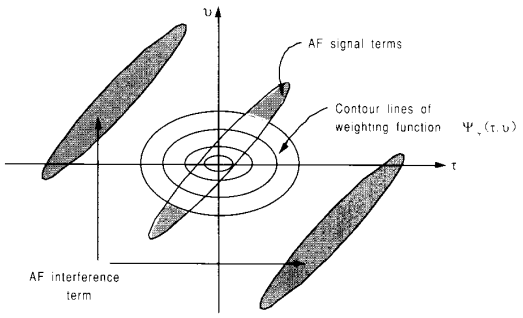

Fig. 14. Weighting operation in the correlative domain. All shaded regions are suppressed by the weighting. In general, the weighting function $\Psi_T(\tau,\nu)$ causes both a (desired) attenuation of the interference terms and an (undesired) truncation of the signal terms. The truncation effect produces a loss of time-frequency concentration in the SWD.

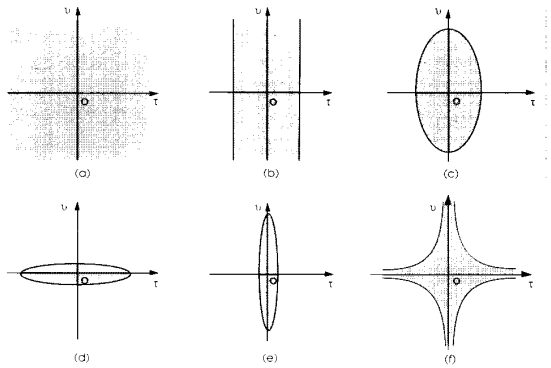

Fig. 15. Effective support of the weighting function $\Psi_T(\tau,\nu)$ for some SWD types: (a) WD, (b) pseudo-WD, (c) smoothed pseudo-WD, (d) spectrogram with long window, (e) spectrogram with short window, and (f) Choi-Williams distribution.

comes at the cost of a loss of time-frequency concentration, since a smoothing generally causes a broadening of the WD's signal terms [JonD92, Hla92a]. In the dual correlative domain, this broadening transforms to a truncation of the AF's signal terms caused by the weighting operation (3.10). Both the interference attenuation effect and the truncation effect are illustrated in Fig. 14 for the simple example of a two-component signal. We note that another disadvantage of smoothing is the potential loss of desirable TFR properties (cf. Tables IV and V).

It is clear that there exists a fundamental tradeoff between good interference attenuation and good time-frequency concentration. A broad WD-domain smoothing function $\psi_T(t,f)$ (corresponding to a narrow lowpass-type AF-domain weighting function $\Psi_T(\tau,\nu)$) yields good interference attenuation but poor time-frequency concentration, whereas a narrow smoothing function $\psi_T(t,f)$ (corresponding to a broad weighting function $\Psi_T(\tau,\nu)$) yields poor interference attenuation but good time-frequency concentration. Figure 15 compares the weighting functions $\Psi_T(\tau,\nu)$ of some specific SWDs.

Spectrogram and Smoothed Pseudo-WD

Two particular shift-invariant SWDs deserve special attention. The classical spectrogram (3.2) can be expressed as [Cla80c]

$$SPEC_x^{(\gamma)}(t,f) = \int\int_{t'f'} W_\gamma(t'-t,f'-f)\,W_x(t',f')\,dt'\,df' \tag{3.11}$$

(Definitions of the STFT which differ slightly in the use of the window $\gamma(t)$ in (2.1) produce a convolution form slightly different from (3.11) [Cla80c]). Due to (3.11), the spectrogram is an SWD with smoothing function $\psi_{SPEC}(t,f) = W_\gamma(-t,-f)$, which is (except for axis reversals) the WD of the spectrogram's analysis window $\gamma(t)$. This, in particular, means that the overall spread of $\psi_{SPEC}(t,f)$ may not be smaller than the minimum spread prescribed by the uncertainty principle. As a consequence, the smoothing in the spectrogram is quite extensive, which results in substantial interference attenuation but also in poor time-frequency concentration [Kad92b, Hla92a, Jeo90a]. The freedom left is essentially a tradeoff between the time spread, Δt, and the frequency spread, Δf, of the smoothing function $\psi_{SPEC}(t,f)$ (cf. the resolution tradeoff of the STFT discussed previously).

This tradeoff is removed by the *smoothed pseudo-WD* (SPWD)

$$SPWD_x^{(g,H)}(t,f) = \int\int_{t'f'} g(t-t')\,H(f-f')\,W_x(t',f')\,dt'\,df'$$

which allows the smoothing spreads, Δt and Δf, to be adjusted freely and independently of each other [FlaP83b,84c, Wok87, Hla92a, Jac83]. The SPWD is defined by a *separable* smoothing kernel $\psi_{SPWD}(t,f) = g(t)H(f)$, in which $g(t)$ and $H(f)$ are two windows whose effective lengths *independently* determine the time smoothing spread Δt and the frequency smoothing spread Δf, respectively. The separable structure of $\psi_{SPWD}(t,f)$ (i.e., $\psi_{SPWD}(t,f)$ is the product of two separate one-dimensional windows) yields significant practical advantages for the SPWD. Specifically, the fact that time smoothing and frequency smoothing are decoupled results in great flexibility in the choice of the time smoothing and frequency smoothing, ease of ap-

plication, and efficient computation. The special case of the SPWD corresponding to the choice $g(t) = \delta(t)$ (i.e., no time smoothing or $\Delta t = 0$) is known as the *pseudo WD* (PWD). The PWD is, in fact, a "short-time WD" using a running analysis window [Cla80a-b, JanC83, FlaP84b]. Figure 16 compares various SWDs in terms of the realizable smoothing spreads Δt and Δf.

In a stochastic framework, both the spectrogram and the SPWD can be used as estimators of the Wigner-Ville spectrum [FlaP83b,87b, Mart85a].

Other Shift-Invariant SWDs

The development of new shift-invariant SWDs is a current research topic. Examples of recently defined SWDs not mentioned previously are the *cone kernel distribution* [Zhao90], the *generalized exponential distribution* [Boud91b, Papa91], and the *Butterworth distribution* [Papa91,92]. Other shift-invariant SWDs correspond to a specific "shift-scale invariant" type of WD smoothing (e.g., the *Choi-Williams distribution*) and will be discussed in a separate section. All of these SWDs feature a WD smoothing which is more sophisticated than the simple smoothing employed in the SPWD; they attempt to attenuate interference terms while simultaneously preserving the signal terms and/or desirable mathematical properties.

Affine Time-Frequency Representations

The Affine Class

An alternative to the energetic shift-invariant class (Cohen class) C_E is provided by the *affine class* A_E (see Fig. 12) comprising all energetic, quadratic TFRs which preserve time scalings (e.g., doubling the time scale of the signal also doubles the time scale of the TFR while halving the TFR's frequency scale) and preserve time shifts [FlaP89,90b,91b, Bert88,91, Rio92]:

$$\tilde{x}(t) = \sqrt{|a|}\, x\big(a(t-t_0)\big) \;\Rightarrow\; T_{\tilde{x}}(t,f) = T_x\Big(a(t-t_0), \frac{f}{a}\Big)$$

Note that a time-frequency scaling naturally occurs when analyzing the Doppler effect in the case of wideband signals [FlaP90a]. Any TFR T_x which is an element of the affine class A_E can be derived from the WD by means of an affine transformation [FlaP90b, Rio92],

$$T_x \in A_E \;\Leftrightarrow\; T_x(t,f) = \int\!\!\int_{t'f'} \chi_T\big(f(t-t'), \frac{f'}{f}\big) W_x(t',f')\,dt'\,df' \qquad (3.12)$$

where $\chi_T(\alpha,\beta)$ is a two-dimensional kernel function depending on the dimensionless variables α and β (but not on the signal $x(t)$).

Members of the affine class A_E which are *not* members of the Cohen class as well (i.e., those which do not preserve frequency shifts) are the scalogram (3.2) and

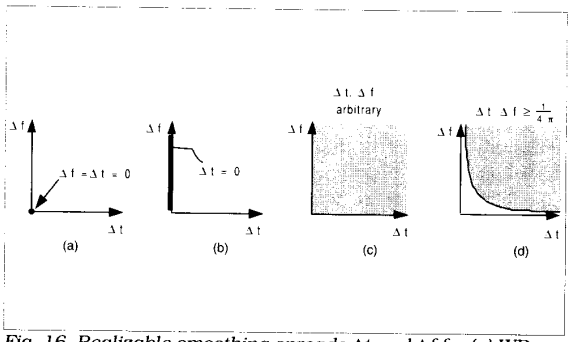

Fig. 16. Realizable smoothing spreads Δt and Δf for (a) WD, (b) pseudo-WD, (c) smoothed pseudo-WD, and (d) spectrogram. The possible choices of Δt and Δf correspond to any point in the shaded regions in the $(\Delta t, \Delta f)$-quadrant. Of the TFRs shown, only the smoothed pseudo-WD allows a free and independent choice of the smoothing spreads Δt and Δf. (TFRs implementing some more sophisticated smoothing, like the Choi-Williams, cone-kernel, generalized exponential and Butterworth distributions, cannot be characterized by simple spreads Δt and Δf and hence are not included in this comparison.)

the TFRs recently defined by Bertrand and Bertrand [Bert88,91], Unterberger [Bert91, FlaP91b], and Flandrin [FlaP91b] (see Table I). Conceptually, these representations are similar to the constant-Q analysis of the wavelet transform but in a quadratic (energetic) framework. They are especially advantageous in the case of hyperbolic FM signals [Bert91] such as those emitted by bats [FlaP86, Alt70]. We note that a quadratic TFR which is similar in the constant-Q spirit but not a member of A_E has recently been proposed in [Alt90] (see also [MarN86b]).

Affine WD Smoothing

If the kernel $\chi_T(\alpha,\beta)$ is a sufficiently smooth function, then the affine transformation (3.12) causes an "affine smoothing" of the WD [FlaP90b, Rio91,92]. Typically, the affine smoothing results in a constant-Q characteristic, i.e., the amount of time smoothing and the amount of frequency smoothing are inversely proportional and proportional, respectively, to the analysis frequency. Such a constant-Q smoothing provides an interesting alternative to the frequency-independent smoothing of shift-invariant SWDs. A prominent example of a constant-Q smoothing is provided by the scalogram (see (3.2)) which can be written as [FlaP90b, Rio91]

$$SCAL_x^{(\gamma)}(t,f) = \int\!\!\int_{t'f'} W_\gamma\Big(\frac{f}{f_0}(t'-t), f_0\frac{f'}{f}\Big) W_x(t',f')\,dt'\,df' \qquad (3.13)$$

Thus, the scalogram's kernel is essentially the WD of the wavelet $\gamma(t)$, $\chi_{SCAL}(\alpha,\beta) = W_\gamma\,(-\frac{\alpha}{f_0}, f_0\beta)$ where f_0 is the center frequency of the bandpass wavelet $\gamma(t)$. Note the analogy of the scalogram expression (3.13) to the spectrogram expression (3.11). Both the spectrogram and the scalogram implement a rather extensive smoothing of the WD.

Shift-Scale Invariant TFRs

The Shift-Scale Invariant Class

Since the axioms defining the Cohen class C_E and the affine class A_E are not mutually exclusive, there exist TFRs which belong to both classes, i.e., which preserve time shifts, frequency shifts, and time scalings. These "shift-scale-invariant" TFRs form the intersection $CA_E = C_E \cap A_E$ of the Cohen class C_E and the affine class A_E (see Fig. 12). They may be derived from the WD by both the convolution (3.8) and the affine convolution (3.12). However, although the shift-scale invariant TFRs are members of the affine class, they do not feature a constant-Q behavior since they are frequency-shift invariant.

A characteristic feature of shift-scale-invariant TFRs is that $\Psi_T(\tau,\nu)$ takes on the form of a "product kernel," i.e., $\Psi_T(\tau,\nu)$ only depends on the *product* of τ and ν.

$$T_x \in CA_E \quad \Leftrightarrow \quad \Psi_T(\tau,\nu) = S_T(\tau\nu) \tag{3.14}$$

The *one-dimensional* function $S_T(\beta)$ fully characterizes the TFR T_x. This implies that the time/time-lag kernel $\varphi_T(t,\tau)$ (cf. Fig. 13) assumes the form

$$\varphi_T(t,\tau) = \frac{1}{|\tau|} s_T\left(\frac{t}{\tau}\right)$$

where $s_T(\alpha)$ is the inverse FT of $S_T(\beta)$ [FlaP87c, Hla88,91c]. A theoretically interesting member of the shift-scale-invariant class CA_E is the family of *generalized WD* (GWD, see Table I) [Cla80c, JanA82, FlaP87a, Hla92a] which encompasses the WD and the Rihaczek distribution [Rih68b,69, Cla80c] as special cases. A list of constraints on the kernels $s_T(\alpha)$ or $S_T(\beta)$ corresponding to the properties of Table II is given in the right-hand column of Table V [Hla88, Jeo92a].

Shift-Scale Invariant WD Smoothing

While the GWD is interesting mainly from a formal viewpoint, other shift-scale invariant TFRs are of more practical importance since they may be interpreted as smoothed WDs (SWDs) and thus feature an overall reduction of interference terms as compared to the WD. A theoretical disadvantage of many SWDs such as the spectrogram, SPWD, and scalogram is the loss of most of the attractive mathematical properties of the WD (cf. Table IV). In contrast, *shift-scale invariant* SWDs are capable of retaining many of the properties satisfied by the WD [Jeo92a, Will91, Hla92a]. For example, the simple condition $S_T(0) = 1$ implies that the resulting product kernel in (3.14) satisfies $\Psi_T(\tau,0) = \Psi_T(0,\nu) \equiv 1$ which guarantees validity of the marginal properties (cf. Table V).

A shift-scale invariant TFR T_x will be an SWD only if the function $S_T(\beta)$ is concentrated around β=0 and thus tends to zero for large $|\beta|$, since only then is the ambiguity-domain weighting function $\Psi_T(\tau,\nu) = S_T(\tau\nu)$ concentrated mainly around the origin of the (τ,ν)-plane. A prominent example of a shift-scale invariant SWD is the *Choi-Williams distribution* or *exponential distribution* [Choi89] for which $S_T(\beta)$ is Gaussian, $S_{CWD}(\beta) = e^{-(2\pi\beta)^2/\sigma}$. Furthermore, the *"reduced-interference" distributions* have been defined in [Jeo92a, Will91] as a family of shift-scale invariant SWDs satisfying a large number of desirable mathematical properties (see Table IV).

While shift-scale invariant smoothing is compatible with nice mathematical properties of the resulting SWD, the product form $\Psi_T(\tau,\nu) = S_T(\tau\nu)$ of the weighting function $\Psi_T(\tau,\nu)$ results in certain limitations of interference attenuation. The essential support of the weighting function $\Psi_T(\tau,\nu) = S_T(\tau\nu)$ necessarily is a cross-shaped region of the (τ,ν)-plane with hyperbolic boundaries (i.e., ν = constant / τ) as shown in Fig. 15f; specifically, $\Psi_T(\tau,\nu)$ is constant along the τ-axis and the ν-axis. This means that the attenuation of interference terms corresponding to signal terms occurring either at the same time or at the same frequency (i.e., zero time or frequency lag) will be somewhat limited, since here the corresponding interference term of the AF intersects the ν-axis (τ=0) or the τ-axis (ν=0), respectively [Hla92a, Papa91, Urb90]. The resulting behavior will be illustrated in a later section (cf. Figs. 19 and 20).

Signal-Adaptive SWDs and TFRs with Higher-Order Nonlinearity

A significant performance gain may often be obtained by adapting the smoothing characteristics of an SWD to the signal $x(t)$ to be analyzed [JonD90, And87, Kad89, Bara91]. Of course, the resulting signal-adaptive TFR is then no longer quadratic. For example, the optimum choice of a Gaussian smoothing in the case of FM signals with known instantaneous frequency is discussed in [And87]. Another example is the use of a radially-Gaussian weighting function $\Psi_T(\tau,\nu)$ where the Gaussian spread in each radial direction in the (τ,ν)-plane is optimally adapted to the signal [Bara91] (see the radially-Gaussian kernel distribution in Table I). This scheme is particularly suited for multicomponent signals consisting of linear FM (chirp) components.

Higher-order versions of the WD have been proposed in [Gerr88, Boa91a, Fon91a,b, SwaA91]. A highly nonlinear TFR (listed in Table I under the acronym CND) which satisfies the marginal properties while being always nonnegative has been considered in [CohL85,89]; an important shortcoming of this TFR is debated in [JanA87].

SIMULATIONS AND APPLICATIONS

No one TFR is perfect for all signal processing applications. Therefore, in this section, we give examples which apply various quadratic TFRs (specifically, smoothed WD versions) to synthetic and real data in order to illustrate the relative performance of these TFRs in some specific situations and applications. We emphasize, however, that the limited results presented in this section should not be used as the only basis for

adopting a particular TFR for a specific signal analysis task. Depending on the type of WD smoothing featured by the TFR, any TFR will perform well for some classes of signals or applications and poorly for others. Moreover, the results obtained also depend heavily on the extent of smoothing which usually can be adjusted via one or more parameters. Finally, much depends also on the way the resulting TFR surface is displayed graphically. A thorough discussion of all these issues would go far beyond the scope of this paper.

Interference Terms of the Spectrogram, Scalogram, and WD

In applications, the interference terms (ITs) of quadratic TFRs are often a problem. The ITs of the *spectrogram* and the *scalogram* occur only in those regions of the time-frequency plane where the auto-TFRs of the signal components overlap; hence, if these auto-TFRs do not overlap, the ITs are zero [Kad92b, Hla92a, Ril89, Jeo90a]. In contrast, the ITs of the *WD* always occur midway between each pair of signal components, whether the auto-WDs overlap or not.

We will illustrate this point using the two-component signal $x(t) = x_1(t) + x_2(t)$ consisting of the complex sinusoidal bursts

$$x_1(t) = \begin{cases} e^{j 2\pi f_1 t}, & 0 < t < t_1, \\ 0, & \textit{otherwise} \end{cases} \quad \text{and} \quad x_2(t) = \begin{cases} e^{j 2\pi f_2 t}, & t_2 < t < t_3 \\ 0, & \textit{otherwise} \end{cases}$$

Figure 17a shows the signal $x(t)$ for the parameters t_1 = 16 ms, t_2 = 48 ms, t_3 = 64 ms, f_1 = 800 Hz and f_2 = 1800 Hz. The signal's spectrogram, scalogram, and WD are

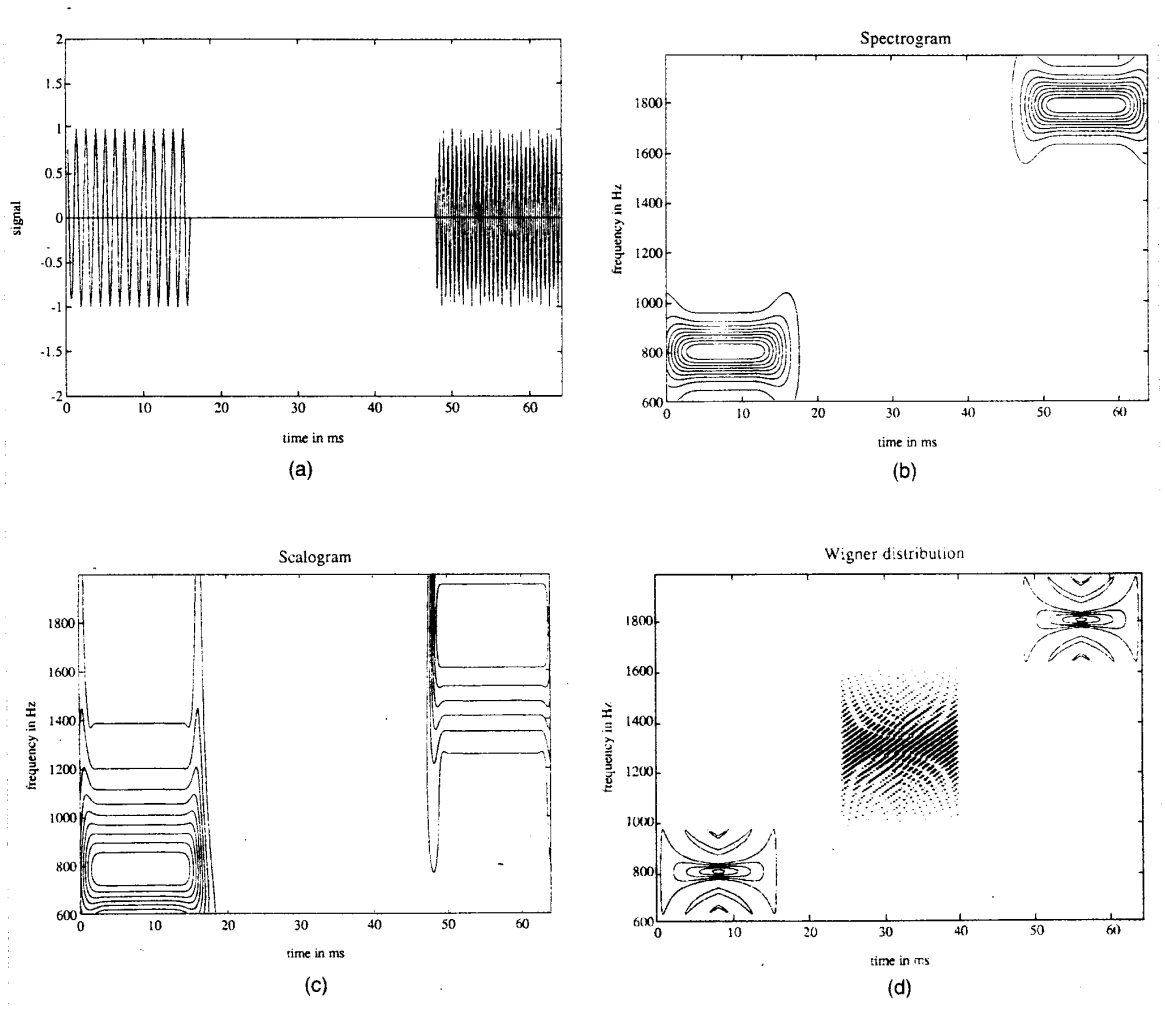

Fig. 17. Time-frequency analysis of a two-component signal consisting of finite-length complex sinusoids whose spectrogram and scalogram signal terms are non-overlapping. (a) Real part of signal. (b) spectrogram. (c) scalogram. and (d) WD.

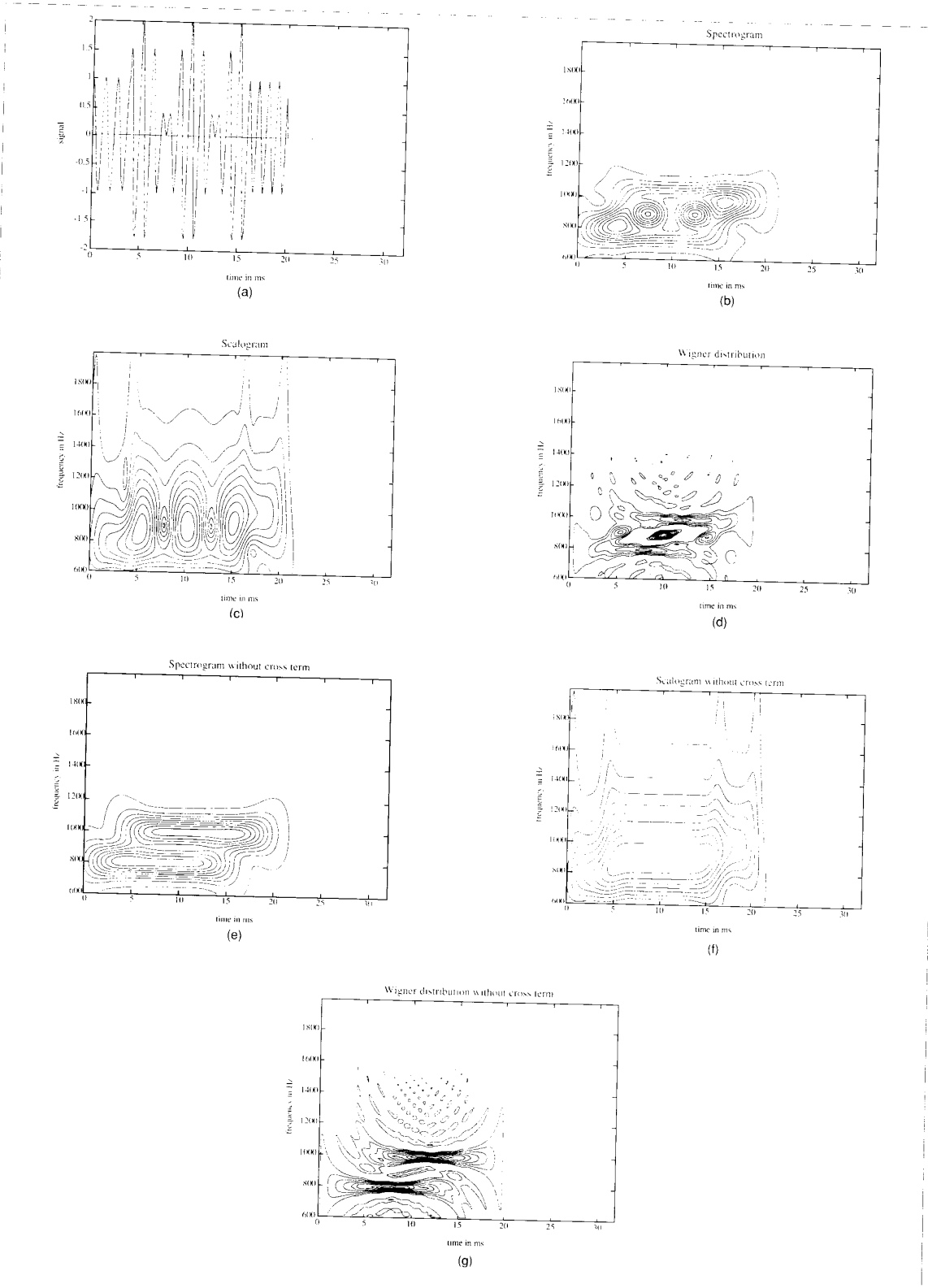

Fig. 18. Time-frequency analysis of a two-component signal consisting of finite-length complex sinusoids whose spectrogram and scalogram signal terms are overlapping. (a) Real part of signal. (b) spectrogram. (c) scalogram, and (d) WD: (e)-(g) signal terms (without IT) of the spectrogram, scalogram, and WD, respectively.

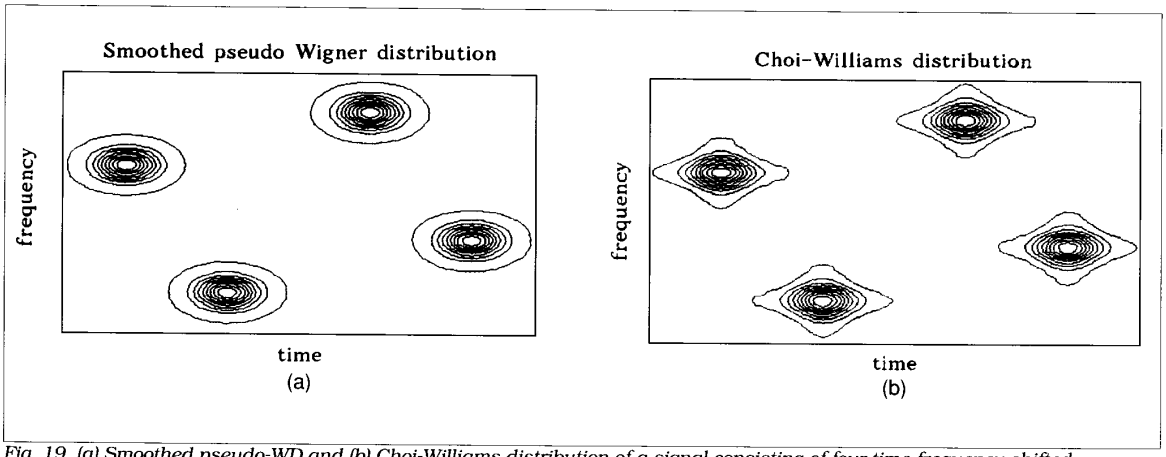

Fig. 19. (a) Smoothed pseudo-WD and (b) Choi-Williams distribution of a signal consisting of four time-frequency shifted Gaussian signal components located at different times and frequencies.

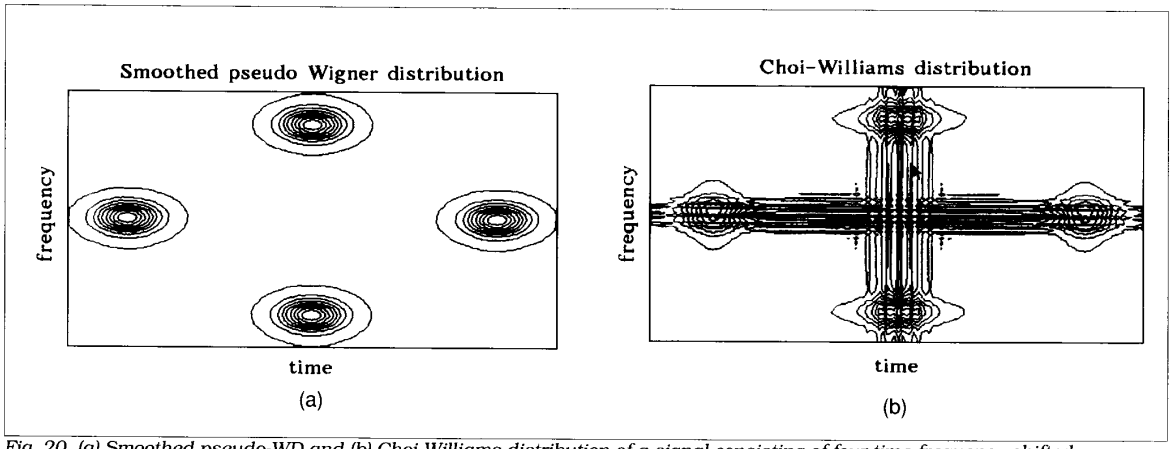

Fig. 20. (a) Smoothed pseudo-WD and (b) Choi-Williams distribution of a signal consisting of four time-frequency shifted Gaussian signal components, where two components occur at the same time and the other two components occur at the same frequency.

plotted in Figs. 17b-d, respectively. Since for this choice of parameters the signal components' auto-spectrograms and auto-scalograms do not overlap, there is no IT in the spectrogram and the scalogram. In the WD, on the other hand, a rapidly oscillatory IT is clearly visible midway between the auto-WDs.

Figures 18a-d show the signal $x(t)$ and its spectrogram, scalogram, and WD, respectively, for the parameters t_1 = 16 ms, t_2 = 4 ms, t_3 = 20 ms, f_1 = 800 Hz and f_2 = 1000 Hz. Now the signal terms of the spectrogram and scalogram overlap, leading to a non-zero, oscillatory IT. To illustrate the effect of the IT, Figs. 18e-g show only the signal terms (without IT) of each TFR, that is,

$$SPEC_{x_1}(t,f) + SPEC_{x_2}(t,f),$$
$$SCAL_{x_1}(t,f) + SCAL_{x_2}(t,f),$$

and $W_{x_1}(t,f) + W_{x_2}(t,f)$. We also note from Figs. 18b and 18c that neither the spectrogram nor the scalogram shows two distinct spectral peaks at the frequencies f_1 and f_2.

Interference Attenuation in Shift-Scale Invariant SWDs

As discussed in the section on shift-scale invariant WD smoothing, the IT attenuation in a shift-scale invariant SWD will be limited whenever the interfering signal components are located around the same time or the same frequency. Figures 19 and 20 compare the smoothed pseudo WD (SPWD), which is not shift-scale invariant, with the shift-scale invariant Choi-Williams distribution (CWD) [Choi89] for two slightly different signals. Each of the two signals consists of four time-frequency-shifted Gaussian signal components [Urb90]. In the first signal, all of the Gaussian signals occur at different times and frequencies; it is here seen that both the SPWD (Fig. 19a) and the CWD (Fig. 19b) feature good IT attenuation. However, in the second signal, two of the Gaussian signals occur at the same time and the other two Gaussian signals occur at the same frequency. While the IT attenuation in the SPWD (Fig. 20a) is unchanged, the CWD (Fig. 20b) now shows significant ITs with large spreads in the time and frequency directions.

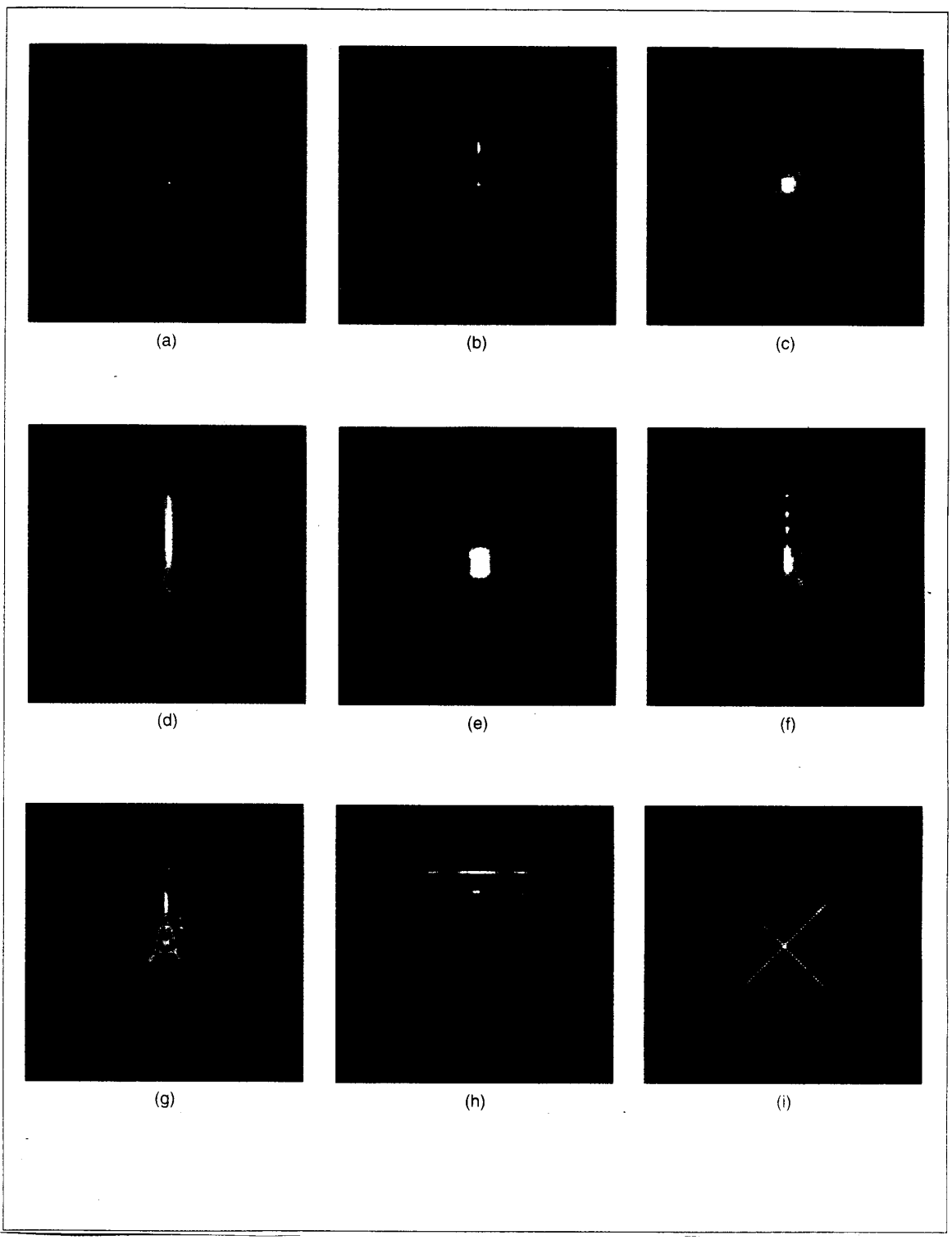

Fig. 21. Comparison of smoothed WD versions. The signal analyzed consists of two complex linear-FM chirp components and one time-frequency shifted Gaussian component. (a) WD, (b) pseudo-WD, (c) smoothed pseudo WD, (d) spectrogram with "short" window, (e) spectrogram with "medium-length" window, (f) Choi-Williams distribution, (g) generalized exponential distribution, (h) cone-kernel distribution, and (i) radially-Gaussian kernel distribution (signal-adaptive). Time and frequency are plotted in the horizontal and vertical directions, respectively. The signal length is 128 samples, and the (normalized) frequency interval shown is 0 to 1/2. These plots were created by R. Baraniuk, W. Kozek, T. Manickam, G. Niedrist, and B. Wistawel.

Comparison of Smoothed WD Versions

In Fig. 21, we evaluate the performance of various smoothed WD versions for the case of a three-component complex-valued signal consisting of two "crossed" chirp signals (linear FM signals) and one time-frequency shifted Gaussian signal. The goal is to attenuate the oscillatory ITs while trying to preserve the time-frequency concentration of the three signal terms. This particular signal contains closely spaced and intersecting linear-FM chirps which give rise to ITs occurring near the origin of the ambiguity-function plane ((τ,ν)-plane, cf. Fig. 10b and Fig. 14). Hence, it is a difficult test case for any quadratic TFR's ability to suppress ITs without severely broadening the desired signal terms.

As a point of reference, the *WD* (i.e., the limiting case of *no smoothing*) is shown in Fig. 21a. The signal terms corresponding to the chirp signal components are clearly visible and highly concentrated, but the WD signal term corresponding to the Gaussian signal component is covered by the oscillatory IT caused by the two chirps.

The remaining figures show the results for various types of WD smoothing. In the *pseudo WD* plot of Fig. 21b, the ITs oscillating in the frequency direction are attenuated, revealing the Gaussian signal term. No smoothing occurs in the time direction. The *smoothed pseudo WD* (SPWD) is shown in Fig. 21c; it features an additional time smoothing which attenuates the ITs oscillating in the time direction. Most ITs are now reasonably well attenuated but the time-frequency concentration of the signal terms has been impaired by the smoothing. Figs. 21d,e show the *spectrogram* for two different lengths of the analysis window. The "short" window (Fig. 21d) produces extensive frequency smoothing but little time smoothing, which results in the Gaussian not being properly resolved. A "long" window, on the other hand, would produce extensive time smoothing but little frequency smoothing. The result obtained with a compromise "medium-length" window is shown in Fig. 21e. Compared to the SPWD result (Fig.21c), the overall smoothing is unnecessarily large in both spectrograms.

Figures 21f-h show the results of TFRs implementing a more sophisticated type of smoothing. The *Choi-Williams distribution* (CWD) [Choi89] and the *generalized exponential distribution* (GED) [Boud91b, Papa91] are plotted in Fig. 21f and Fig. 21g, respectively. Like any shift-scale invariant SWD, the CWD does not allow independent choices of the amounts of time smoothing and frequency smoothing. Indeed, in the CWD the amounts of smoothing in the two directions are simultaneously controlled by a single parameter σ (cf. the expression for the CWD weighting function $\Psi_T(\tau,\nu)$ given in Table IV). In this example, a comparatively large σ is needed to retain good concentration of the chirp's CWD signal terms; unfortunately, the resulting smoothing is then not strong enough to sufficiently attenuate the IT covering the Gaussian signal term. (A smaller σ will uncover the Gaussian signal term but only at the cost of poorer time-frequency concentration of all signal terms.) In contrast, the GED (Fig. 21g) allows different choices of time smoothing and frequency smoothing since it has several independent design parameters (cf. the GED weighting function in Table IV). This additional flexibility was utilized to choose the frequency smoothing to be stronger than the time smoothing, which results in an uncovering of the Gaussian signal term with less loss of time-frequency concentration.

The result of the *cone-kernel distribution* (CKD) [Zhao90] is shown in Fig. 21h. The specific form of the CKD weighting function (in particular, $\Psi_T(0,\nu) \equiv 0$ in Table IV) causes the CKD to feature good attenuation of ITs oscillating in the time direction but potentially poor attenuation of ITs oscillating in the frequency direction. In this example, this property of the CKD results in an inability of the CKD to uncover the Gaussian signal term. Note, however, that the CKD preserves the signal's finite time support.

Finally, Fig. 21i shows the result of the signal-adaptive *radially-Gaussian kernel distribution* [Bara91]. It is seen that the signal adaptivity indeed leads to a clearly improved performance regarding IT attenuation and auto-term preservation as compared to the non-adaptive TFRs considered previously.

Bat Sonar Signals

TFRs have been used by Flandrin et al. to analyze the active sonar echolocation systems used by bats [FlaP86]. The bat emits different AM-FM-type signals for hunting, navigation, and prey identification. The SPWDs of signals emitted by a bat during the "hunting," "approach," "pursuit," and "capture" phases are plotted in Figs. 22a-d, respectively. During the hunting phase, before a potential prey has been identified, the bat emits relatively long signals (Fig. 22a). The first part of the hunting signal is an FM signal with rapidly decreasing instantaneous frequency (IF), allowing the bat to estimate its position. The second part has semi-constant frequency, allowing the bat to estimate its speed. After a prey has been located, the bat emits a succession of "approach" signals, one of which is plotted in Fig. 22b. Successive approach signals are characterized by a gradual decrease in signal duration obtained by shortening the semi-constant frequency component of the hunt signal. Finally, in the "pursuit" and "capture" phases (Figs. 22c and 22d, respectively), the bat emits harmonic signals in order to realize broadband signals in a relatively short period of time.

The use of TFRs for IF estimation is considered next. In Fig. 23a, Flandrin has plotted a slightly time-smoothed PWD of a "hunting" signal. Figure 23b shows an IF estimate (obtained from the SPWD's local first-order frequency moments, see property P_9 in Table II) for the "hunting" signal; here, the IF estimate is meaningful since the signal is monocomponent. In contrast, Fig. 24 shows the SPWD and resulting IF estimate for a chirp-like bat signal superimposed with corrupting echoes. Since the echoes overlap in time with the bat signal, the IF of the overall signal significantly deviates from the IF of the bat signal. In Fig. 25b, Flandrin isolates the SPWD signal term corresponding to the desired bat signal by multiplying the overall SPWD with

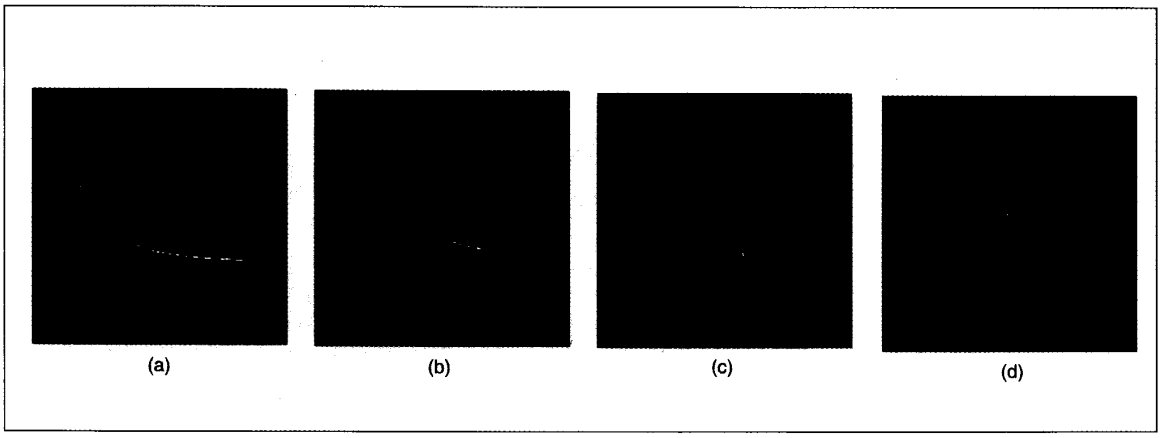

Fig. 22. Smoothed pseudo-WDs of bat sonar signals. (a) "Hunting" signal, (b) "approach" signal, (c) "pursuit" signal, and (d) "capture" signal. Time (0 to 5.5 ms) is plotted horizontally and frequency (0 to 110 kHz) vertically. These plots and those contained in Figs. 23-26 were provided by P. Flandrin [FlaP86]; they were part of a study performed at Institut Chimie et Physique Industrielles (ICPI) at Lyon, France with the support of the National Center for Scientific Research (CNRS) in France.

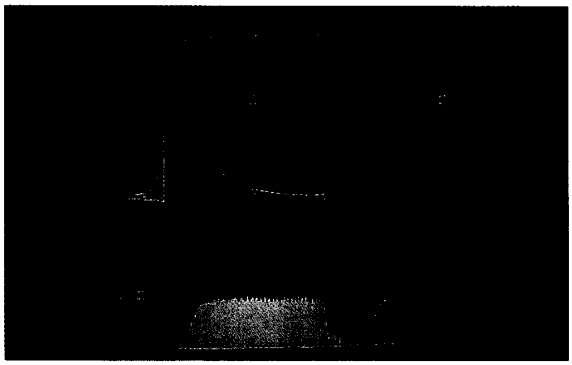

Fig. 23. (a) Smoothed pseudo-WD (SPWD) of a bat sonar signal emitted during a hunting phase, with the signal magnitude and the signal's Fourier transform magnitude plotted along the horizontal time axis and the vertical frequency axis, respectively, for comparison. (b) Estimate of the instantaneous frequency.

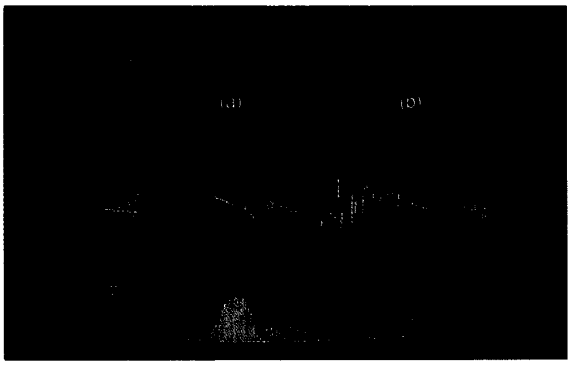

Fig. 24. (a) SPWD and (b) instantaneous frequency estimate of a bat signal corrupted by echoes.

Fig. 25. (a) The SPWD of Fig. 24 and (b) a time-frequency masking function (outlined in red) designed to zero out the time-frequency region corresponding to the corrupting echoes.

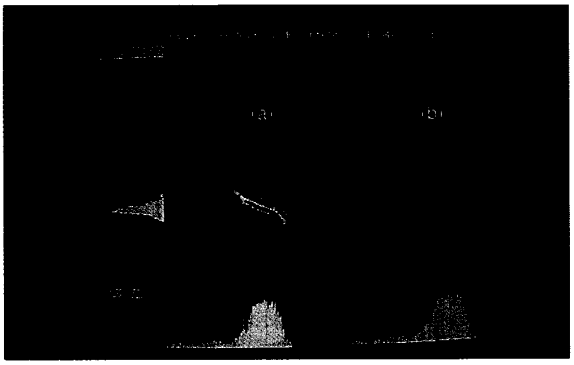

Fig. 26. (a) The masked SPWD and (b) the instantaneous frequency estimate obtained from the masked SPWD.

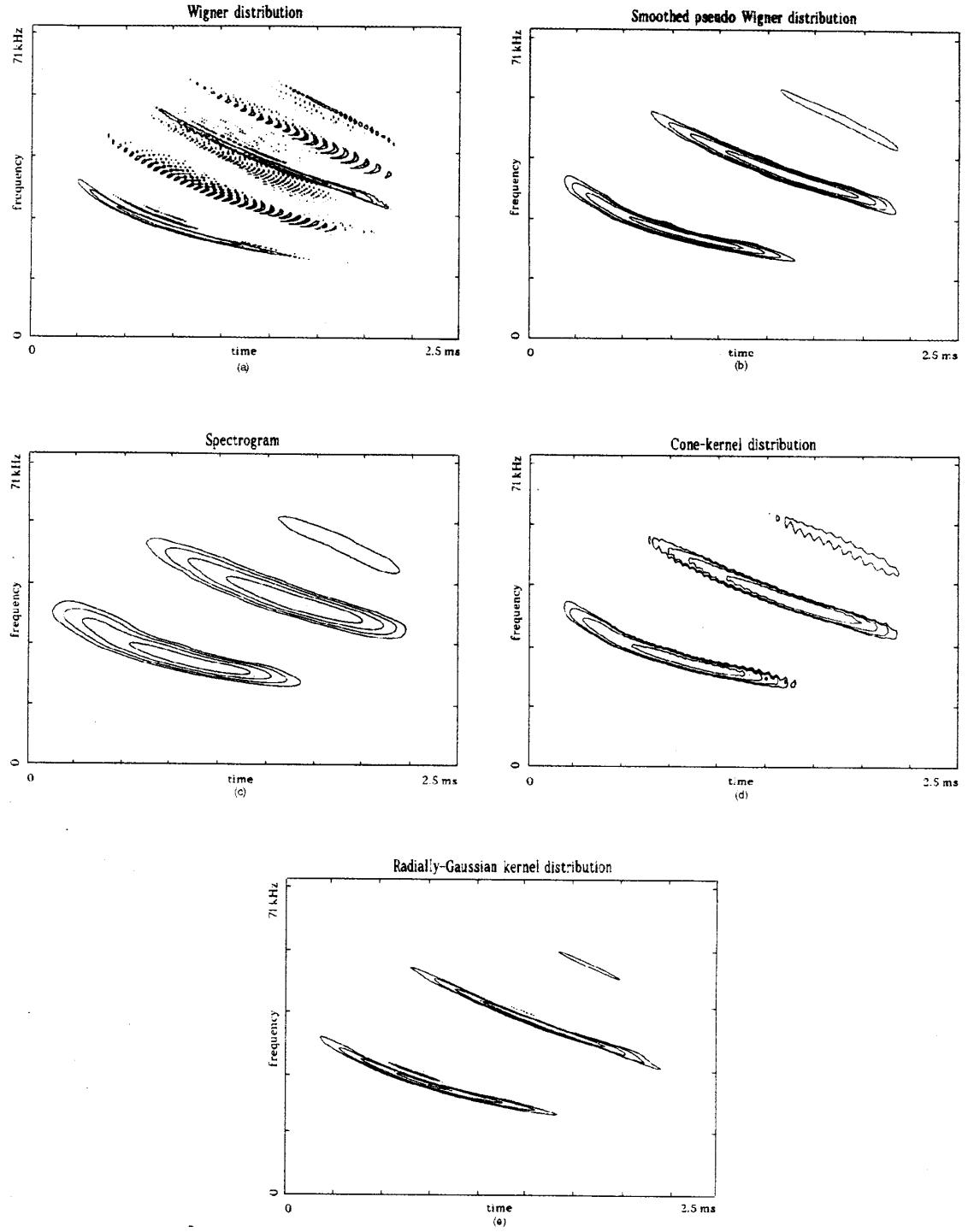

Fig. 27. Time-frequency analysis of a bat sonar signal consisting of three nonlinear FM components. (a) WD. (b) smoothed pseudo-WD. (c) spectrogram. (d) cone-kernel distribution, and (e) signal-adaptive radially-Gaussian kernel distribution. These plots were created by R. Baraniuk and D. Jones from data provided by C. Condon, K. White, and Prof. A. Feng.

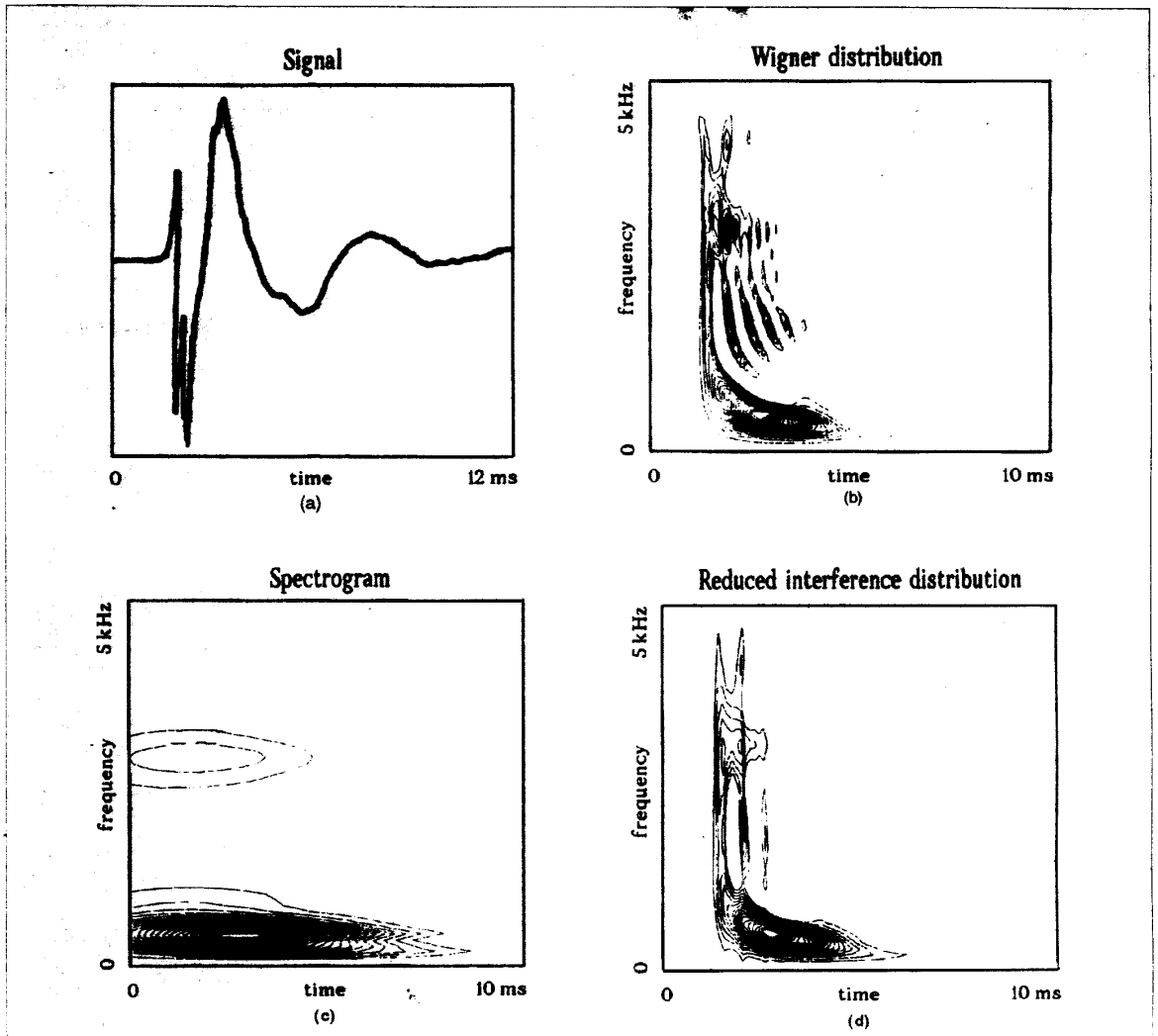

Fig. 28. Time-frequency analysis of a temporo mandibular joint clicking sound. (a) Signal, (b) WD, (c) spectrogram, and (d) reduced interference distribution. The TFRs were applied to the signal's analytic (complex) version. These plots were provided by W. Williams et al. [Widm92, Zhe89].

a time-frequency mask whose region of support is outlined in red. Since in the time-frequency plane the echoes do not overlap significantly with the bat signal, the mask is capable of suppressing the corrupting echoes, as demonstrated in Fig. 26a. A satisfactory IF estimate (shown in Fig. 26b) is then obtained from the *masked* SPWD in Fig. 26a via local first-order frequency moments.

In the next example, Baraniuk and Jones have compared the results of the WD and various smoothed WD versions obtained for bat sonar signals consisting of three nonlinear FM signal components. In the *WD* (Fig. 27a), oscillatory ITs are seen to exist midway between all pairs of signal terms. These ITs are suppressed in the *smoothed pseudo WD* (Fig. 27b) with only a moderate loss of time-frequency concentration. In contrast, the *spectrogram*'s extensive smoothing produces a significant concentration impairment (Fig. 27c). The concentration loss in the *cone-kernel distribution* (Fig. 27d) is between that of the smoothed pseudo WD and that of the spectrogram. Finally, the signal-adaptive *radially-Gaussian kernel distribution* (Fig. 27e) is seen to produce good IT attenuation with very little broadening of the signal terms.

Bio-Acoustical Sounds

Williams et al. [Widm92, Zhe89] have used the "reduced interference" distribution (RID) to analyze abnormalities in the temporo mandibular joint (TMJ). The signal corresponding to an abnormal TMJ clicking sound is plotted in Fig. 28a. Figures 28b-d show the signal's WD, spectrogram, and RID, respectively. The

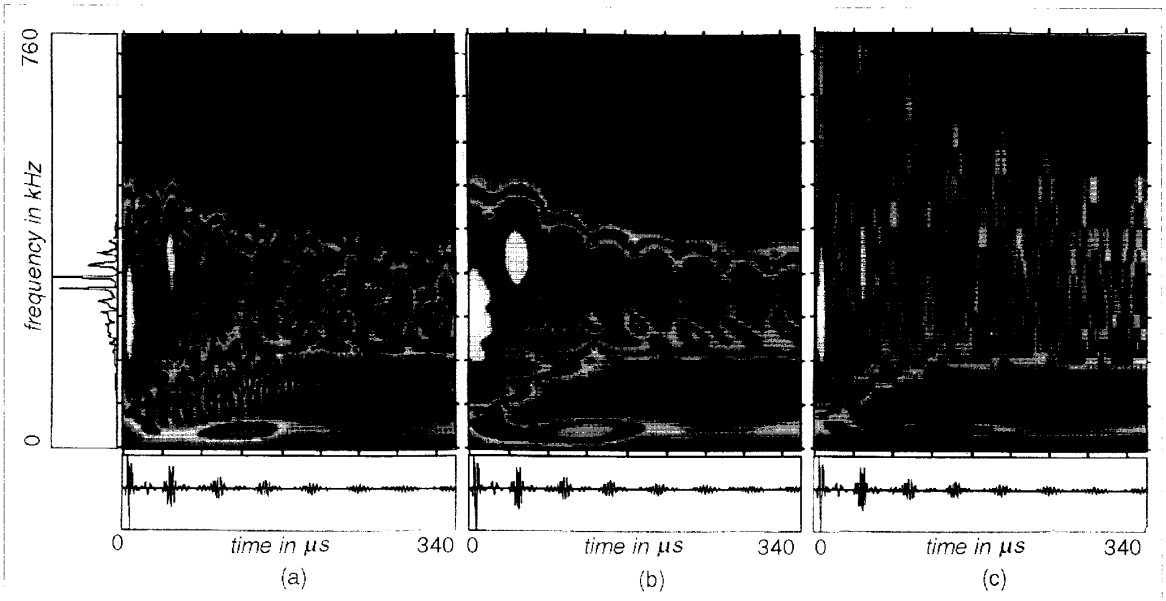

Fig. 29. Time-frequency analysis of the acoustical response of a thin spherical shell immersed in water: (a) smoothed pseudo-WD, (b) spectrogram, and (c) scalogram of an analytic version of the acoustical response. The time-domain signal and its spectral magnitude are plotted along the horizontal time axis and the vertical frequency axis, respectively. The plots in Figs. 29 and 30 were created by P. Flandrin et al. [FlaP90c, Ses89] in a study performed at Institut Chimie et Physique Industrielles (ICPI) at Lyon, France, and at Laboratoire de Mécanique et Acoustique (LMA) at Marseille, France with the support of a grant from Directoire des Recherches et Etudes Techniques (DRET), Department of Defense, France.

WD (Fig. 28b) is seen to contain many oscillatory ITs. The extensive smoothing inherent in the *spectrogram* (Fig. 28c) has suppressed all ITs present in the WD but has also caused excessive spreading in the time direction, such that the initial broad-band burst is no longer visible and the low-frequency component has been broadened considerably. Compared to the WD and the spectrogram, the *RID* (Fig. 28d) is a good compromise; while it does not remove all of the oscillatory ITs, it essentially preserves the time-frequency concentration of the signal terms.

Acoustical Field Surrounding a Submerged Spherical Shell

In various radar, sonar, seismic, and echo location situations, "active" target identification is performed by comparing a known emitted signal to the signal reflected from an unknown target or obstruction. Flandrin et al. [FlaP90c, Ses89] have used the SPWD to analyze the scattered acoustical field induced by a thin spherical shell immersed in water. The waves returned by the shell depend upon the shell's physical properties and geometry. In addition to the initial (specular) echo, there are also "creeping" waves, i.e., acoustical waves which travel around the surface of the sphere one or more times before they are reflected. These waves are dispersive (i.e., different frequency components travel with different propagation velocities), and their average time separation or period results in a quasi-periodic signal with harmonically spaced spectral peaks.

Classical methods of echo characterization estimate the size, thickness or composition of a target using one-dimensional time-domain or frequency-domain techniques. Temporal techniques [Ses89] are used to analyze the arrival times of the initial specular echo and the creeping waves. Unfortunately, the attenuation of higher frequencies and the dispersive nature of the waves causes the individual echoes to change shape and to overlap; this makes the estimation of the echoes' arrival times difficult. Spectral techniques may be used to analyze target-induced resonance frequencies, but cannot take into account the echoes' dispersive nature.

Since the signal consists of a large number of individual signal components which overlap in both the time and the frequency domain, it is difficult to analyze using conventional one-dimensional techniques. However, the individual signal components are fairly disjoint (non-overlapping) in the time-frequency plane and may thus be analyzed separately using TFRs. In addition to giving all the information that can ideally be found using conventional one-dimensional techniques (e.g., arrival time information, target-dependent resonance frequencies, high-frequency propagation attenuation), a TFR analysis also shows such time-varying characteristics as velocity dispersion [FlaP90c, Ses89].

The SPWD of the acoustical response of a thin spherical shell is shown in Fig. 29a along with the signal and its spectrum. The time-domain signal shows the successive echoes generated by creeping waves, and the spectrum shows the target-induced resonance frequencies. However, the echoes' dispersive character is manifested only in the SPWD; it is visible from the gradually increasing inclination of the SPWD signal terms corresponding to successive echoes, indicating

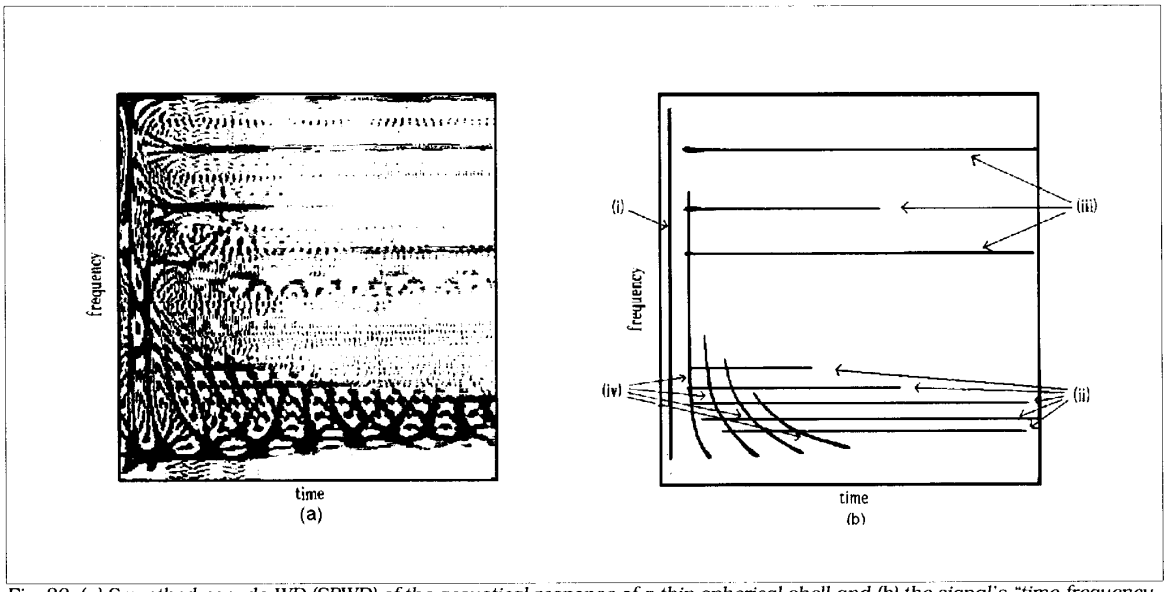

Fig. 30. (a) Smoothed pseudo-WD (SPWD) of the acoustical response of a thin spherical shell and (b) the signal's "time-frequency signature" derived from the SPWD result. This time-frequency signature shows the specular echo (i), resonance frequencies with strong damping factors (ii), or weak damping factors (iii), and dispersive creeping waves echoes (iv) with gradually increasing inclination.

that higher frequencies are travelling faster than lower frequencies. Frequency-dispersion measurements can be obtained very easily from the disjoint SPWD signal terms corresponding to a small number of creeping-wave echoes. For comparison purposes, the signal's spectrogram and scalogram are plotted in Figs. 29b and 29c, respectively.

Based upon a barely time-smoothed PWD of the signal, plotted in Fig. 30a, Flandrin et al. constructed a "time-frequency signature" shown in Fig. 30b. This time-frequency signature clearly indicates the arrival time of the specular echo, the dispersive nature of the creeping-wave echoes, and various resonance frequencies, all of which provide useful information for target identification and characterization.

Speech Analysis

For the past five decades, the spectrogram has been one of the classical TFRs for the analysis of speech signals. However, other TFRs incorporating a WD smoothing which is less extensive than that of the spectrogram may be advantageous whenever the "fine structure" of a speech signal is of interest. Figure 31 compares various smoothed WD versions (including the spectrogram) for a short speech segment consisting of two pitch periods of a voiced speech sound. The speech signal, shown in Fig. 31a, may be interpreted as the response of the vocal tract to a quasi-periodic excitation by the glottal pulse train. The resonance frequencies of the vocal tract (formants) are dependent on the specific sound spoken [Rab78].

Figures 31b-i show the signal's WD, pseudo-WD, smoothed pseudo-WD, spectrogram, Choi-Williams distribution, generalized exponential distribution, cone-kernel distribution, and radially-Gaussian kernel distribution, respectively. The WD (Fig. 31b) features excellent time and frequency concentration, resulting in a sharp display of both temporal features (the glottal excitation) and spectral features (the formants), but it contains a substantial amount of oscillatory interference terms (ITs). These ITs are essentially suppressed in the spectrogram (Fig. 31e) at the cost of significantly impaired time-frequency concentration. The SPWD result (Fig. 31d) shows that a judicious smoothing which is less extensive than that of the spectrogram is capable of sufficiently attenuating ITs without a dramatic loss of time-frequency concentration. Both the Choi-Williams distribution (Fig. 31f) and the generalized exponential distribution (Fig. 31g) are seen to feature good concentration but significant residual ITs between signal components occurring around the same time or frequency. The cone-kernel distribution (Fig. 31h) is seen to contain significant residual interference between signal terms occurring around the same frequency. Finally, the signal-adaptive radially-Gaussian kernel distribution is shown in Fig. 31i.

Time-Varying Filtering and Signal Separation

WD-based signal synthesis techniques permit the calculation of a signal whose WD is closest to a given time-frequency "model function" [Boud86,92a, Hla92b]. The application of these techniques to time-varying filtering is considered in Figures 32 and 33.

A windowed, complex, linear-FM chirp signal (plotted in Fig. 32c) was contaminated with complex, white Gaussian noise with signal-to-noise ratio 0 dB. The WDs of the original chirp and the noisy chirp are plotted

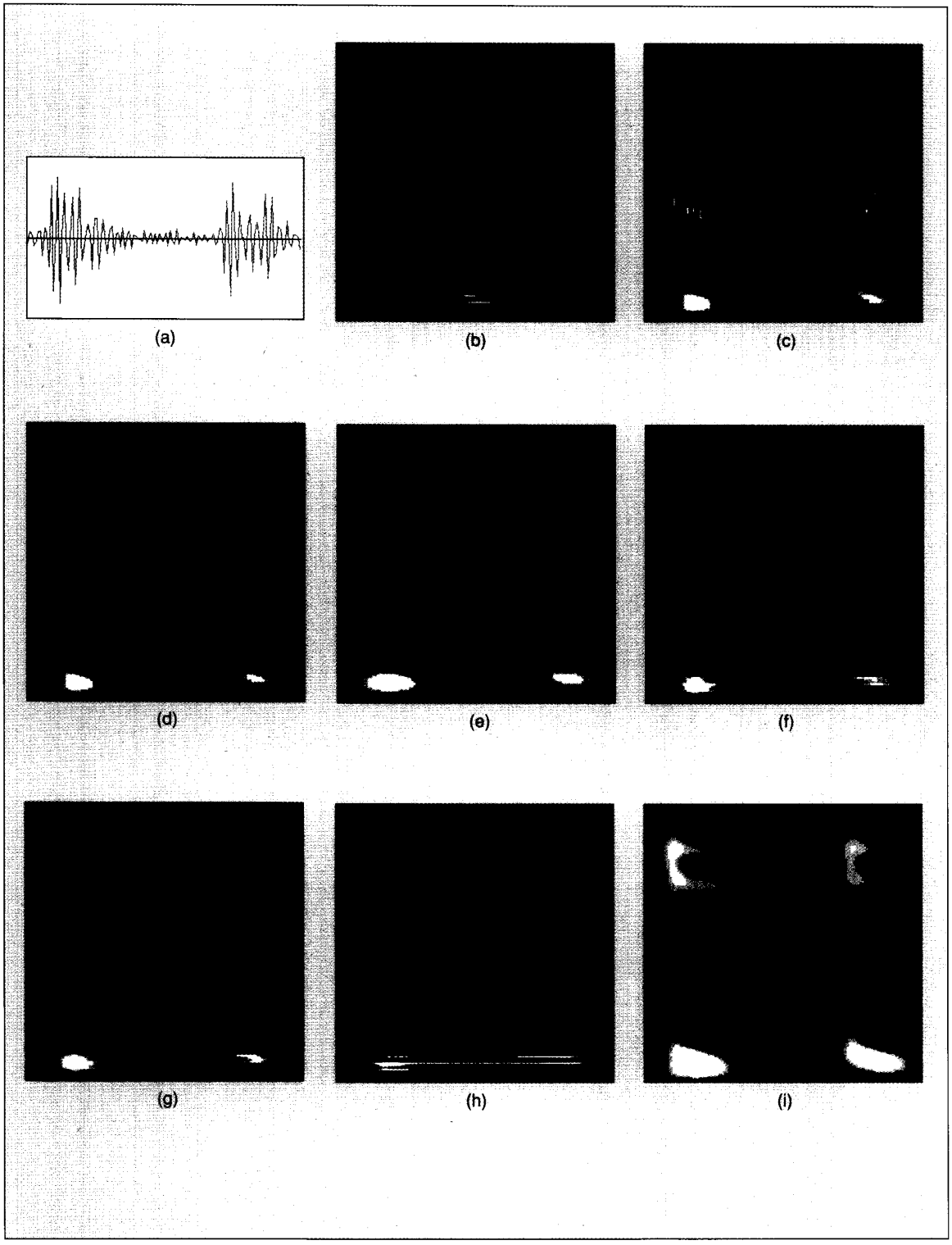

Fig. 31. Time-frequency analysis of a voiced speech sound. (a) Two pitch periods of the vowel [a] spoken by a male German speaker; (b) WD, (c) pseudo-WD, (d) smoothed pseudo-WD, (e) spectrogram, (f) Choi-Williams distribution, (g) generalized exponential distribution, (h) cone-kernel distribution, and (i) radially-Gaussian kernel distribution of an analytic version of the speech signal. Higher formants have been amplified by pre-filtering the speech signal. Time (0 to 16 ms) is plotted horizontally and frequency (0 to 4 kHz) vertically.

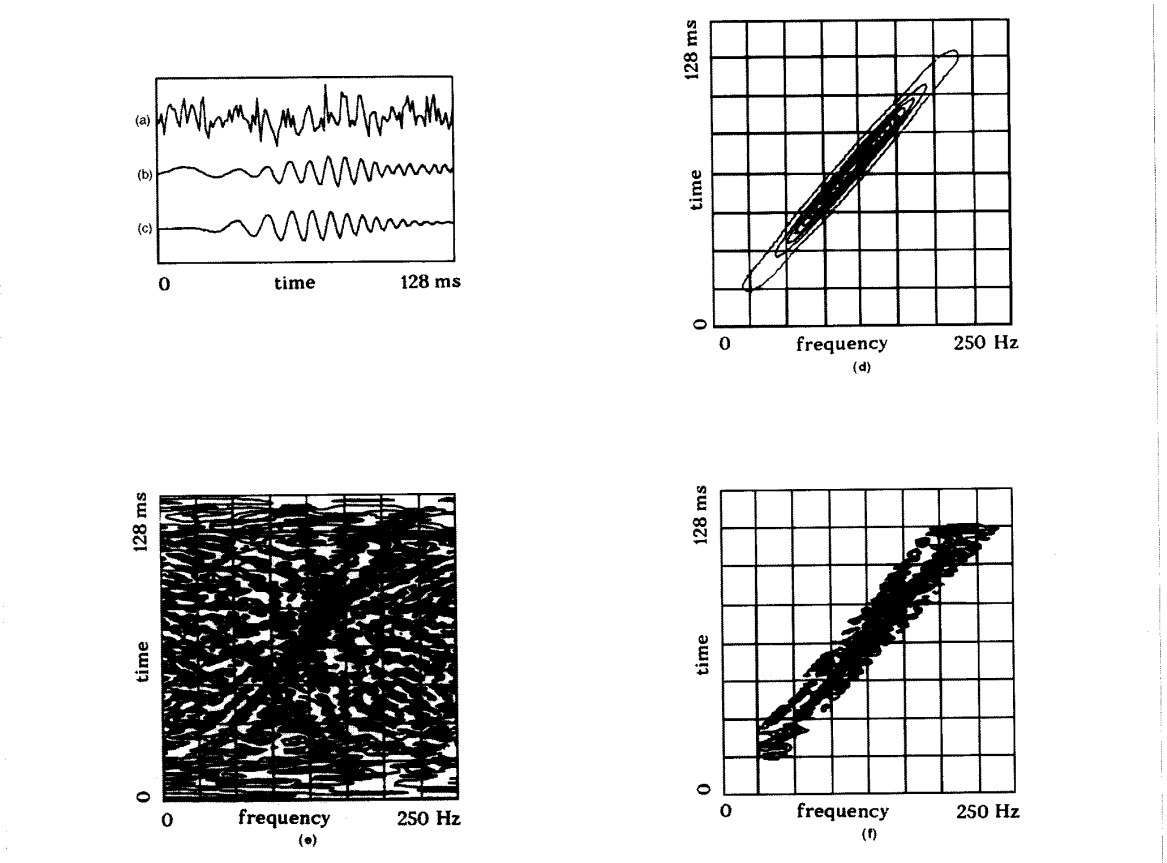

Fig. 32. Noise suppression by means of WD masking and WD based signal synthesis. (a) Real part of a windowed, complex chirp signal corrupted by white noise (SNR=0 dB); (b) real part of the signal estimate obtained by WD masking and signal synthesis; (c) real part of the original (noise-free) chirp signal; (d) WD of the noise-free chirp signal; (e) WD of the noisy chirp signal; and (f) masked WD of the noisy chirp signal.

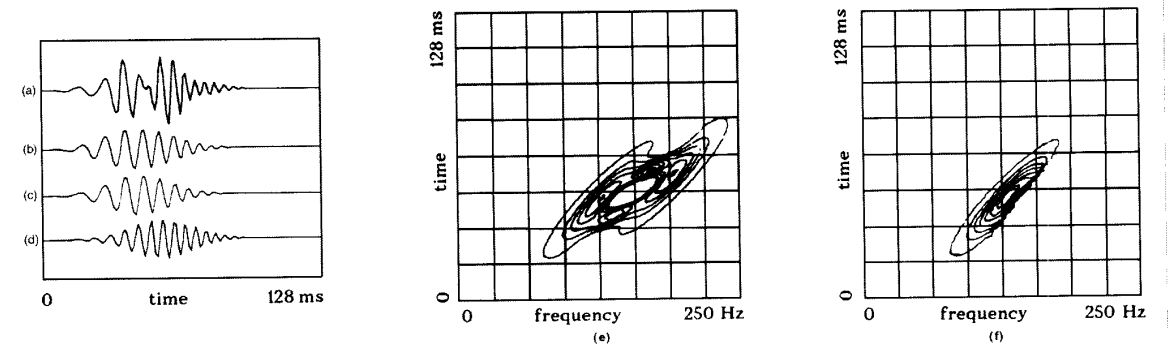

Fig. 33. Signal separation by means of WD masking and WD-based signal synthesis. (a) Real part of a two-component signal consisting of two windowed, complex chirp components; (b) real part of the estimate of the lower-frequency chirp component obtained by WD masking and signal synthesis; (c) real part of the original lower-frequency chirp component; (d) real part of the higher-frequency chirp component; (e) WD of the two-component signal plotted in Fig. 33a; and (f) masked WD of the two-component signal.

in Figs. 32d and 32e, respectively. While the WD of the chirp signal is concentrated along the chirp's instantaneous-frequency (IF) line, the noise is scattered all over the time-frequency plane. Hence, a nonlinear, time-varying filtering resulting in noise reduction can be achieved by i) multiplying the WD of the noisy chirp with a suitable mask and ii) applying signal synthesis techniques to the masked WD. Figure 32f shows the masked WD. (We note that the mask can be designed automatically based on a maximum-likelihood estimate of the chirp's IF obtained from the noisy signal [Kay85, CohF88, Won90].) The result of the signal synthesis algorithm (using the masked WD as time-frequency model function) is shown in Fig. 32b to be very close to the original chirp signal plotted in Fig. 32c. Note that, since the chirp signal and the noise overlap significantly in both the time domain and the frequency domain, neither a time-domain windowing nor a conventional time-invariant filtering could be used for noise suppression.

WD-based signal synthesis techniques can also be used for isolating a desired component of a multicomponent signal, provided that the WD signal term corresponding to the desired signal component does not overlap significantly with other signal terms or ITs. Figure 33e shows the WD of the sum of two windowed complex chirp signals. The two-component signal is plotted in Fig.33a, and the two chirp components are shown individually in Figs. 33c and 33d. While the two chirp components overlap significantly in both the time domain and the frequency domain, their WDs are fairly disjoint in the time-frequency plane. A mask was applied to the WD of the two-component signal, resulting in the masked WD plotted in Fig. 33f. Figure 33b shows a good approximation to the low-frequency chirp component, which was obtained by applying the WD signal synthesis algorithm to the masked WD of Fig. 33f.

CONCLUSION

Time-frequency representations (TFRs) are powerful tools for the analysis and processing of "nonstationary" signals for which separate time-domain and frequency-domain analyses are not adequate. In this tutorial, we have outlined the motivations, interpretations, mathematical fundamentals, properties, and applications of various linear and quadratic TFRs.

Although we have attempted to provide a coherent framework of TFRs, a truly unified framework is difficult to obtain because the large variety of existing methods and approaches causes the field of time-frequency analysis to be somewhat disparate. Also, possible applications of TFRs are as varied as, for example, time-frequency filtering, speech analysis, efficient signal coding, parameter estimation in radar and sonar, or visual inspection of TFR plots by a human analyst. It is thus clear that the choice of a TFR must depend on the specific application.

A question which has led to some controversy in the past few years is the choice of a quadratic TFR for the *visual* analysis of nonstationary signals. The numerous TFRs which have been proposed to this end may be interpreted as smoothed versions of the WD, with the type of smoothing determining the amount of attenuation of interference terms, loss of time-frequency concentration, and mathematical properties. Here again, the choice of the "best" TFR depends on the nature of the signals to be analyzed and on additional issues such as the mathematical properties required, limitations in computation and storage, etc. Once a specific TFR has been selected, the user often has to select certain TFR parameters (e.g., window lengths which determine the amount of smoothing). Finally, the analysis result will also depend upon the graphical representation of the TFR surface (e.g., 3D plots versus contour-line plots, number and spacing of contour lines, etc.). Accordingly, a successful application of TFRs (as is the case for many other signal analysis methods) presupposes some degree of expertise on the part of the user. It is seldom possible to view time-frequency analysis as a "black box" where the signal is input and some clear and meaningful result is automatically obtained as the output: some prior knowledge about the signal must generally be available in order to select the most suitable TFR and to adapt the TFR's parameters to the signal.

If the application at hand is an automated signal analysis (rather than the purely visual one considered above), then the existence of cross or interference terms is not necessarily a problem; in fact, in some situations (e.g., optimum detection methods) cross terms are necessary for a meaningful result.

TFRs continue to be a field of research. Interesting recent developments include the wavelet transform, the affine class and "wideband versions" of quadratic TFRs, higher-order WD versions, the design of new kernels of smoothed WD versions, signal-adaptive WD smoothing, and the extension of WD analysis to linear signal spaces and linear, time-varying systems.

Acknowledgments

The authors would like to acknowledge the valuable suggestions and contributions of the following reviewers: Drs. J. Deller, P. Flandrin, D. Jones, L. Marple, W.F.G. Mecklenbräuker, O. Rioul, and W. Williams. Some of the data and simulations in the last section of this paper were provided by Drs. R. Baraniuk, C. Condon, A. Feng, P. Flandrin, D. Jones, S. Kadambe, K. White, W. Williams, and W. Wokurek. The authors would also like to thank B. Jones, W. Kozek, T. Manickam, G. Niedrist, A. Papandreou, and B. Wistawel for help in generating simulations and figures. Support from the Fonds zur Förderung der wissenschaftlichen Forschung and from the Office of Naval Research is gratefully acknowledged.

Franz Hlawatsch (S'85, M'88) received the Diplom-Ingenieur and Dr. Techn. degrees in electrical engineering from the Vienna University of Technology, Austria, in 1983 and 1988, respectively.

Since 1983 he has been a Research and Teaching Assistant at the Department of Communications and Radio-Frequency Engineering, Vienna University of Technology. In 1991, he spent a sabbatical leave at the Department of Electrical Engineering, University of Rhode Island, RI. His research interests are in signal theory and signal processing with emphasis on time-frequency methods.

G. Faye Boudreaux-Bartels (S'78, M'84) was born in Lafayette, LA on March 18, 1953. She received the B.S. Degree (summa cum laude) in computer science from the University of Southwestern Louisiana in 1974 and the M.S. and Ph.D. degrees in electrical engineering from Rice University in 1980 and 1983, respectively. She was a Research Mathematician for Shell Development Company, Houston, TX from 1974-1977 and a Fulbright Scholar at Ecole Nationale Superieure des Telecommunications, Paris, France, from 1981-1982. Since 1984, Dr. Boudreaux-Bartels has been teaching at the University of Rhode Island where she is currently an Associate Professor of Electrical Engineering. Her research and teaching interests are in the areas of digital signal processing, communications, numerical methods, and computer engineering. She has published over 40 papers, one of which won the "1988 Senior Paper Award" given by the IEEE Signal Processing Society (SPS). She has also received two URI Faculty Excellence Awards and has served as an associate editor of the *IEEE Transactions on Signal Processing*, Vice-Chair of the Digital Signal Processing Technical Committee, and an elected member of the IEEE SPS Advisory Committee.

REFERENCES

Short-Time Fourier Transform and Spectrogram References (see also [Ack70, Aus88, Aus90, Bast81a, Boud83, Boud92b, Cla80c, FlaP84c, FlaP87b, FlaP87c, Fri91, Hel66, Hla91d, JonD92, Kad92b, McA90, McA92, Mec87, Mon67, Nut88a, PorB91, Ril89, Rio91])

[All77a] Allen, J.B., "Short-term Spectral Analysis, Synthesis, and Modification by Discrete Fourier Transform," *IEEE Trans. Acoust., Speech, Sig. Proc.*, vol. ASSP-25, pp. 235-238, June 1977.

[All77b] Allen, J.B., Berkley, D.A., and Blauert, J., "Multimicrophone Signal Processing Techniques to Remove Room Reverberation from Speech Signals, *J. Acoust. Soc. Amer.*, vol. 62, pp. 912-915, Oct. 1977.

[All77c] Allen, J.B. and Rabiner, L.R., "A Unified Approach to STFT Analysis and Synthesis," *Proc. IEEE*, vol. 65, pp. 1558-1564, Nov. 1977.

[All77d] Allen, J.B., "Corrections to 'Short Term Spectral Analysis, Synthesis, and Modification by Discrete Fourier Transform'," *IEEE Trans. Acoust., Speech, Sig. Proc.*, vol. ASSP-25, p. 589, Dec. 1977.

[All79] Allen, J.B. and Rabiner, L.R., "Unbiased Spectral Estimation and System Identification Using Short-Time Spectral Analysis Methods," *Bell Syst. Tech. J.*, vol. 58, pp. 1743-1763, Oct. 1979.

[All82] Allen, J.B., "Application of Short-Time Fourier Transform to Speech Processing and Spectral Analysis," *IEEE Int. Conf. Acoust., Speech, Sig. Proc.*, pp. 1012-1015, Paris, France, May 1982.

[Alt80] Altes, R.A., "Detection, Estimation, and Classification with Spectrograms," *J. Acoust. Soc. Am.*, vol. 67, no. 4, pp. 1232-1246, Apr. 1980.

[Ban73] Banks, R.J., "Data Processing and Interpretation in Geomagnetic Deep Sounding," *Phys. Earth Planet Inter., U.K.*, vol. 7, p. 339, 1973.

[Blo68] Bloch, S. and Hales, A.L., "New Technique for Determination of Surface Waves Phase Velocities," *Bul. Seism. Soc. Am.*, vol. 58, 1968.

[Bolt69] Bolt, R.H. et al., "Speaker Identification by Speech Spectrograms," *Science*, vol. 166, pp. 338-343, 1969.

[Bour88] Bourdier, R., Allard, J.F., and Trumpf, K., "Effective Frequency Response and Signal Replicas Generation for Filtering Algorithms using Multiplicative Modification of the STFT," *Signal Proc.*, vol. 15, no. 2, 1988.

[Cal76] Callahan, M.J., "Acoustic Signal Processing Based on the Short-Time Spectrum," Univ. Utah Rep. CSC-76-209, Mar. 1976.

[Cro83] Crochiere, R.E. and Rabiner, L.R., Multi-Rate Digital Signal Processing, Prentice-Hall, Inc., Englewood Cliffs, NJ, 1983.

[Dau88] Daubechies, I., "Time-Frequency Localization Operators: A Geometric Phase Space Approach," *IEEE Trans. on Info. Th.*, vol. 34, no. 4, pp. 605-612, July 1988.

[Dem87] Dembo, A. and Malah, D., "The Design of Optimal Uniform Filter Banks with Specified Composite Response," *IEEE Trans. Acoust., Speech, Sig. Proc.*, vol. 35, pp. 807-817, June 1987.

[Dur85] Durand, L.G., Genest, J., Jr., and Guardo, R., "Modeling of the Transfer Function of the Head-thorax Acoustic Systems in Dogs," *IEEE Trans. Biomed. Eng.*, vol. 32, pp. 592-601, Aug. 1985.

[Dzi69] Dziewonski, A., Bloch, S., and Landisman, M., "A Technique for the Analysis of Transient Seismic Signals," *Bul. Seism. Soc. Am.*, vol. 59, 1969.

[Fin91] Fineberg, A. and Mammone, R.J., "Detection and Classification of Multi-Component Signals," *Asilomar Conf. on Sig., Syst., Comp.*, pp. 1093-1097, Pacific Grove, CA, Nov. 1991.

[FlaJ70] Flanagan, J.L. and Lummis, R.C., "Signal Processing to Reduce Distortion in Small Rooms," *J. Acoust. Soc. Amer.*, vol. 47, pp. 1465-1481, June 1970.

[FlaJ72] Flanagan, J., Speech Analysis Synthesis and Perception, New York, Springer, 1972.

[Gri84] Griffin, D.W. and Lim, J.S., "Signal Estimation from Modified Short-Time Fourier Transform," *IEEE Trans. Acoust., Speech, Sig. Proc.*, vol. ASSP-32, no. 2, pp. 236-243, April 1984.

[Jeo90a] Jeong, J. and Williams, W.J., "On the Cross-Terms in Spectrograms," *Proc. IEEE Int. Symp. Ckts and Syst.*, pp. 1565-1568, 1990.

[Kod78] Kodera, K., Gendrin, R., and DeVilledary, C., "Analysis of Time-Varying Signals with Small BT Values," *IEEE Trans. Acoust., Speech, Sig. Proc.*, vol. ASSP-26, pp. 64-76, Feb. 1978.

[Koe46] Koenig, R., Dunn, H.K., and Lacy, L.Y., "The Sound Spectrograph," *J. Acoust. Soc. Amer.*, vol. 18, pp. 19-49, 1946.

[Levs72] Levshin, A., Pisarenko, V.F., and Pogrebinsky, G.A., "On a Frequency-Time Analysis of Oscillations," *Ann. Geophys.*, vol. 28, pp. 211-218, 1972.

[Lim79] Lim, J.S., "Enhancement and Bandwidth Compression of Noisy Speech," *Proc. IEEE*, vol. 67, pp. 1586-1604, Dec. 1979.

[Mos86] Moser, J.M. and Aunon, J.I., "Classification and Detection of Single Evoked Brain Potentials Using Time-Frequency Amplitude Features," *IEEE Trans. Biomed. Eng.*, vol. 33, pp. 1096-1106, Dec. 1986.

[Naw83] Nawab, S.H., Quatieri, T., and Lim, J.S., "Algorithms for Signal Reconstruction from Short-Time Fourier Transform

Magnitude," *IEEE Int. Conf. on Acoust., Speech, Sig. Proc.*, pp. 800-803, Boston, MA, Apr. 1983.

[Naw88] Nawab, S.N. and Quatieri, T.F., "Short-Time Fourier Transform," chapter in Advanced Topics in Signal Processing, J.S. Lim and A.V. Oppenheim, eds., Prentice Hall, Englewood Cliffs, NJ, 1988.

[Nay92] Nayebi, K., Barnwell, T.P., and Smith, M.J.T., "Time Domain Filter Bank Analysis: A New Design Theory," *IEEE Trans. Sig. Proc.*, June 1992.

[Port76] Portnoff, M.R., "Implementation of the Digital Phase Vocoder Using the Fast Fourier Transform," *IEEE Trans. Acoust., Speech, Sig. Proc.*, vol. 24, pp. 243-246, June 1976.

[Port80] Portnoff, M.R., "Time-Frequency Representations of Digital Signals and Systems based on Short-Time Fourier Analysis," *IEEE Trans. Acoust., Speech, Sig. Proc.*, vol. 28, pp. 55-69, Feb. 1980.

[Port81a] Portnoff, M.R., "Time-Scale Modification of Speech Based on Short-Time Fourier Transform," *IEEE Trans. Acoust., Speech, Sig. Proc.*, vol. 29, pp. 374-390, June 1981.

[Port81b] Portnoff, M.R., "Short-time Fourier Analysis of Sampled Speech," *IEEE Trans. Acoust., Speech, Sig. Proc.*, vol. 29, pp. 364-373, June 1981.

[Pot66] Potter, R.K., Kopp, G.A., and Green, H.C., Visible Speech, D. Van Nostrand Co., New York, 1947. Republished by Dover Publications, Inc., 1966.

[Rab78] Rabiner, L.R. and Schafer, R.W., Digital Processing of Speech Signals, Prentice-Hall, Inc., Englewood Cliffs, NJ, 1978.

[Rab80] Rabiner, L.R. and Allen, J.B., "On the Implementation of a Short-time Spectral Analysis Method for System Identification," *IEEE Trans. Acoust., Speech, Sig. Proc.*, vol. 28, pp. 69-79, Feb. 1980.

[Ric82] Richards, M.A., "Helium Speech Enhancement Using the Short-Time Fourier Transform," *IEEE Trans. Acoust., Speech, Sig. Proc.*, vol. 30, pp. 841-853, Dec. 1982.

[Str87] Strawn, J., "Analysis and Synthesis of Musical Transitions Using the Discrete Short-Time Fourier Transform," *J. Aud. Eng. Soc.*, vol. 35, pp. 3-13, Jan.-Feb. 1987.

[SwaK86] Swaminathan, K. and Vaidyanathan, P.P., "Theory and Design of Uniform DFT, Parallel FIR Quadrature Mirror Filter Banks," *IEEE Trans. Ckts. and Sys.*, vol. 33, pp. 1170-1191, December 1986.

[Tri78] Tribolet, J.M., "Application of Short-time Homomorphic Signal Analysis to Seismic Wavelet Estimation," *IEEE Trans. Acoust., Speech, Sig. Proc.*, vol. 26, pp. 343-353, Aug. 1978.

[Vai87] Vaidyanathan, P.P., "Theory and Design of M Channel Maximally Decimated Quadrature Mirror Filters with Arbitrary M, Having the Perfect Reconstruction Property," *IEEE Trans. Acoustics, Speech, Sig. Proc.*, vol. 35, no. 4, pp. 476-492, Apr. 1987.

[Vai92] Vaidyanathan, P.P., Multirate Systems and Signal Processing, book manuscript preprint, Prentice Hall, Englewood Cliffs, NJ, to appear.

[Vet86] Vetterli, M., "Filter Banks Allowing Perfect Reconstruction," *Sig. Proc.*, vol. 10, no. 3, pp. 219-244, Apr. 1986.

[Web79] Webb, D.C., "The Analysis of Non Stationary Data Using Complex Demodulation," *Ann. Telecomm.*, vol. 34, pp. 131-137, 1979.

[Wolc83] Wolcin, J.J., "Maximum Likelihood Detection of Transient Signals Using Sequenced Short-time Power Spectra," Naval Underwater Systems Center, New London, Conn., Tech. Mem. # 831138, Aug. 26, 1983.

[Yeg81] Yegnanarayana, B., "Speech Analysis by Pole-Zero Decomposition of Short-Time Spectra," *Signal Proc.*, vol. 3, Jan. 1981.

[You85] Youn, D.H., "Short Time Fourier Transform Using a Bank of Low-Pass Filters," *IEEE Trans. Acoust., Speech, Sig. Proc.*, vol. 33, pp. 182-185, Feb. 1985.

Gabor Expansion References (see also [Boud83, Boud92b, Dau90a, Raz90])

[Aus90] Auslander, L., Buffalano, C., Orr, R., and Tolimieri, R., "A Comparison of the Gabor and Short-Time Fourier Transforms for Signal Detection and Feature Extraction in Noisy Environments," *Proc. SPIE Conf.*, vol. 1348, pp. 230-247, Nov. 1990.

[Aus91a] Auslander, L. and Gertner, I., "The Discrete Zak Transform Application to Time-Frequency Analysis and Synthesis of Nonstationary Signals," *IEEE Trans. Sig. Proc.*, vol. 39, no. 4, Apr. 1991.

[Bast80a] Bastiaans, M.J., "Gabor's Expansion of a Signal into Gaussian Elementary Signals," *Proc. IEEE*, vol. 68, no. 4, pp. 538-539, 1980.

[Bast80b] Bastiaans, M.J., "The Expansion of an Optical Signal into a Discrete Set of Gaussian Beams," *Optik*, vol. 57, no. 1, pp. 95-102, 1980.

[Bast81a] Bastiaans, M.J., "A Sampling Theorem for the Complex Spectrogram and Gabor's Expansion of a Signal in Gaussian Elementary Signals," *Optical Eng.*, vol. 20, no. 4, pp. 594-598, July/Aug. 1981.

[Bat88] Battle, G., "Heisenberg Proof of the Balian-Low Theorem," *Lett. Math. Phys.*, vol. 15, pp. 175-177, 1988.

[Bil76] Billings, A.R. and Scolaro, A.B., "The Gabor Compression-Expansion System using Non-Gaussian Windows and its Application to Television Coding and Decoding," *IEEE Trans. Info. Th.*, vol. IT-22, pp. 174-190, 1976.

[Boud91a] Boudreaux-Bartels, G.F., Tufts, D.W., and Umesh, S., "On Improving the Detection of Gabor Components of Transient Signals," *Third Biennial Acoust., Speech, Sig. Proc. Mini-Conf.*, pp. S17.1-2, Boston, MA, Apr.19-20, 1991.

[Bro90] Broder, B. and Schwartz, S., "Transient Detection Using the Gabor Representation: Potentials and Problems," *Second Acoustical Transient Workshop*, Naval Research Laboratory, Nov. 1-2, 1990.

[Dau91a] Daubechies, I., Jaffard, S., and Journé, J.-L., "A Simple Wilson Orthonormal Basis with Exponential Decay," *SIAM J. Math. Anal.*, pp. 554-573, Mar. 91, erratum, pp. 878, May 1991.

[Davi79] Davis, M.J. and Heller, E.J., "Semiclassical Gaussian Basis Set Method for Molecular Vibrational Wave Functions," *J. Chem. Phys.*, vol. 71, no. 8, pp. 3383-3395, 1979.

[Ein86] Einziger, P.D., Raz, S., and Shapira, M., "Gabor Representation and Aperture Theory," *J. Opt. Soc. Amer. A*, vol. 3, pp. 508-522, Apr. 1986.

[Fri89] Friedlander, B.and Porat, B., "Detection of Transient Signals by the Gabor Representation," *IEEE Trans. Acoust., Speech, Sig. Proc.*, vol. 37, No. 2, pp. 169-180, Feb. 1989.

[Gab46] Gabor, D., "Theory of Communication," *J. IEE (London)*, vol. 93(III), pp. 429-457, Nov. 1946.

[Gla63] Glauber, R.J., "Coherent and Incoherent States of the Radiation Field," *Phys. Rev.*, vol. 131, pp. 2766-2788, Sept. 1963.

[Hel66] Helstrom, C.W., "An Expansion of a Signal in Gaussian Elementary Signals," *IEEE Trans. Info. Th.*, vol. IT-12, pp. 81-82, Jan. 1966.

[JanA81] Janssen, A.J.E.M., "Gabor Representation of Generalized Functions," *J. Math. Anal. Appl.*, vol. 83, pp. 377-394, 1981.

[JanA88] Janssen, A.J.E.M., "The Zak Transform: A Signal Transform for Sampled Time-Continuous Signals," *Philips J. Res.*, vol. 43, pp. 23-69, 1988.

[Mon67] Montgomery, L.K. and Reed, I.S., "A Generalization of the Gabor-Helstrom Transform," *IEEE Trans. Info. Th.*, vol. IT-13, pp. 344-345, Apr. 1967.

[Nel72] Nelson, G.A., "Signal Analysis in Time and Frequency Using Gaussian Wavefunctions," in *NATO Advanced Studies Institute on Network and Signal Theory*, J. O. Scanlan, ed., pp. 454-460, 1972.

[Orr91] Orr, R.S., "Computational Assessment of Gabor Representations," *Int. Conf. Acoust., Speech, Sig. Proc.*, pp. 2217-2220, Toronto, Canada, May 1991.

[PorM88] Porat, M. and Zeevi, Y. Y., "The Generalized Gabor Scheme of Image Representation in Biological and Machine Vision," *IEEE Trans. Patt. Anal. Mach. Intell.*, vol. 10, no. 4, pp. 452-467, July 1988.

[PorM89] Porat, M. and Zeevi, Y.Y., "Localized Texture Processing in Vision: Analysis and Synthesis in the Gaborian Space," *IEEE Trans. Biomed. Engg.*, vol. 36, no. 1, pp. 115-129, Jan. 1989.

[PorB91] Porat, B. and Friendlander, B., "Performance Analysis of a Class of Transient Detection Algorithms - A Unified Framework," pre-print, Dec. 11, 1991.

[Pro90] Probasco, J. and Boudreaux-Bartels, G.F., "Detection of Transient Signals Using Arbitrary Elementary Signals," *IEEE 1990 Dig. Sig. Proc. Workshop*, New Paltz, NY, Sept. 1990.

[Wex90] Wexler, J. and Raz, S., "Discrete Gabor Expansions," *Sig. Proc.*, vol. 21, pp. 207-220, 1990.

[Zee89] Zeevi, Y.Y., Porat, M. and Geri, G.A., "Image Generation for Flight Simulators: the Gabor Approach," *J. Visual Comput.*, to be published.

Wavelet Transform References(see also [Boud92b, FlaP89, FlaP90b, FlaP91b, Vai92])

[Ant91] Antonini, M., Barlaud, M., and Mathieu, P., "Image Coding Using Lattice Vector Quantization of Wavelet Coefficients," *Int. Conf. Acoust., Speech, Sig. Proc.*, pp. 2273-2276, Toronto, Canada, May 1991.

[Arg89] Argoul, F., Arnéodo, A., Elezgaray, J., Grasseau, G., and Murenzi, R., "Wavelet Transform of Fractal Aggregates," *Phys. Lett. A*, vol. 135, p. 327, 1989.

[Arn88] Arnéodo, A., Grasseau, G., and Holschneider, M., "Wavelet Transform of Multifractals," *Phys. Rev. Lett.*, vol. 61, no. 20, pp. 2281-2284, 1988.

[Arn89] Arnéodo, A., Grasseau, G., Holschneider, M., "Wavelet Transform Analysis of Invariant Measures of Some Dynamical Systems," in [Com89], pp. 182-196, 1989.

[Baa90] Baazit, N. and Labit, C., "Laplacian Pyramid Versus Wavelet Decomposition for Image Sequence Coding," *IEEE Int. Conf. Acoust., Speech, Sig. Proc.*, Albuquerque, NM, Apr. 3-6, 1990.

[Bass89] Basseville, M. and Benveniste, A., "Multiscale Statistical Signal Processing," *IEEE Int. Conf. Acoust., Speech, Sig. Proc.*, Glasgow, Scotland, pp. 2065-2068, May 23-26, 1989.

[Bur89] Burt, P., "Multiresolution Techniques for Image Representation, Analysis and 'Smart' Transmission," *SPIE Conf. Visual Commun. and Image Proc. IV*, vol. 1199, Nov. 1989.

[Chou91] Chou, K.C., Golden, S., and Willsky, A.S., "Modeling and Estimation of Multiscale Stochastic Processes," *IEEE Int. Conf. Acoust., Speech, Sig. Proc.*, Toronto, Canada, pp. 1709-1712, May 14-17, 1991.

[Coi91] Coifman, R.R., Meyer, Y., and Wickerhauser, V., Wavelet Analysis and Signal Processing, Yale University, 1991.

[Com89] Combes, J.M., Grossman, A. and Tchamitchian, P., eds. Wavelets, Time-Frequency Methods and Phase-Space, Proc. of Int. Conf. on Wavelets, Time-Frequency Methods and Phase Space: Inverse Problems and Theoretical Imaging, Marseille, France, Dec. 14-18, 1987, Springer-Verlag, Berlin, 1989.

[Dau90a] Daubechies, I., "The Wavelet Transform, Time-Frequency Localization and Signal Analysis," *IEEE Trans. Info. Th.*, vol. 36, no. 5, pp. 961-1005, Sept. 1990.

[Dau91b] Daubechies, I., "The Wavelet Transform: A Method for Time-Frequency Localization," Chapter 8 of Advances in Spectrum Analysis and Array Processing: Vol. 1, S. Haykin, ed., pp. 366-417, Prentice Hall, Englewood Cliffs, NJ, 1991.

[Dave91] Davenport, M.R. and Garudadri, H., "A Neural Net Acoustic Phonetic Feature Extractor Based on Wavelets," *Proc. IEEE Pacific Rim Conf.*, Victoria, B.C., May 1991.

[Dut88] Dutilleux, P., Grossman, A., and Kronland-Martinet, R., "Application of the Wavelet Transform to the Analysis, Transformation and Synthesis of Musical Sounds," *Proc. 25th AES Convention*, nr. 2727, section A-2, 1988.

[FlaP90a] Flandrin, P., Magand, F., and Zakharia, M., "Generalized Target Description and Wavelet Decomposition," *IEEE Trans. Acoust., Speech, Sig. Proc.*, vol. 38, no. 2, pp. 350-352, Feb. 1990.

[FlaP91a] Flandrin, P., "Fractional Brownian Motion and Wavelets," in Wavelets, Fractals, and Fourier Transforms - New Developments and New Applications, M. Farge, J.C.R. Hunt and J.C. Vassilicos, eds., Oxford Univ. Press, 1991.

[FlaP92a] Flandrin, P., "Wavelet Analysis and Synthesis of Fractional Brownian Motion," *IEEE Trans. Info. Th.*, Mar. 1992.

[Fow91] Fowler, M.L. and Sibul, L.H., "A Unified Formulation for Detection Using Time-Frequency and Time-Scale Methods," *Asilomar Conf. on Sig., Syst., and Comp.*, pp. 637-642, Pacific Grove, CA, Nov. 1991.

[Fri91] Friedlander, B. and Porat, B., "Performance Analysis of Transient Detectors Based on Linear Data Transforms," preprint, Feb. 28, 1991.

[Gac91] Gache, N., Flandrin, P., Garreau, D., "Fractal Dimension Estimators for Fractional Brownian Motions," *IEEE Int. Conf. Acoust., Speech, Sig. Proc.*, pp. 3557-3560, Toronto, Canada, May 1991.

[Gin89] Ginette, S., Grossmann, A., and Tchamitchian, Ph., "Use of Wavelet Transforms in the Study of Propagation of Transient Acoustic Signals Across a Plane Interface Between Two Homogeneous Media," in [Com89], pp. 139-146.

[Gou84] Goupillaud, P., Grossman, A., and Morlet, J., "Cycle-Octave and Related Transforms in Seismic Signal Analysis," *Geoexploration*, vol. 23, pp. 85-102, 1984.

[Gram91] Gram-Hansen, K., "A Bandwidth Concept for CPB Time-Frequency Analysis," *IEEE Int. Conf. Acoust., Speech, Sig. Proc.*, pp. 2033-2036, Toronto, Canada, May 1991.

[Kad92a] Kadambe, S. and Boudreaux-Bartels, G.F., "Application of the Wavelet Transform for Pitch Detection of Speech Signals," *IEEE Trans. Info. Th.*, Mar. 1992.

[Kad92b] Kadambe, S. and Boudreaux-Bartels, G.F., "A Comparison of the Existence of 'Cross Terms' in the Wigner Distribution and the Squared Magnitude of the Wavelet Transform and the Short Time Fourier Transform," *IEEE Trans. Sig. Proc.*, Oct. 1992.

[Kro87] Kronland-Martinet, R., Morlet, J., and Grossman, A., "Analysis of Sound Patterns Through Wavelet Transforms," *Int. J. Pattern Recog. and Art. Intell.*, vol. 1, pp. 273-301, 1987.

[Lar89] Larsonneur, J.L. and Morlet, J., "Wavelets and Seismic Interpretation," in [Com89], pp. 126-131, 1989.

[Lien87] Lienard, J.S. and d'Allessandro, C., "Wavelets and Granular Analysis of Speech," *Proc. Int. Conf. on Wavelets, Time-Frequency Methods and Phase Space*, Marseille, France, pp. 158-163, Dec. 14-18, 1987, also in [Com89].

[Mala91] Malassenet, F.J. and Mersereau, R.M., "Wavelet Representations and Coding of Self-affine Signals," *IEEE Int. Conf. Acoust. Speech, Sig. Proc.*, Toronto, Canada, May 1991.

[Mall89a] Mallat, S., "A Theory for Multiresolution Signal Decomposition: The Wavelet Representation," *IEEE Trans. Pat. Anal., Machine Intell.*, vol. 11, no.7, pp. 674-693, July 1989.

[Mall89b] Mallat, S., "Multifrequency Channel Decompositions of Images and Wavelet Models," *IEEE Trans. Acoust., Speech, Sig. Proc.*, vol. 37, no. 12, pp. 2091-2110, Dec. 1989.

[Mall89c] Mallat, S. and Zhong, S., "Complete Signal Representation with Multiscale Edges," Courant Inst. of Math. Sci., Technical Report 483, Dec. 1989, also submitted to *IEEE Trans. Pat. Anal., Machine Intell.*, 1989.

[Mey89] Meyer, Y., "Orthonormal Wavelets," in [Com89], pp. 21-37, 1989.

[Morl82] Morlet, J., Arens, G., Fourgeau, E. and Giard, D., "Wave Propagation and Sampling Theory - Part II: Sampling Theory and Complex Waves," *Geophysics*, vol. 47, no.2, pp.

222-236, Feb. 1982.

[Rio90] Rioul, O., "A Discrete Time Multiresolution Theory Unifying Octave-Band Filter Banks, Pyramid and Wavelet Transforms," submitted to *IEEE Trans. Sig. Proc.*, 1990.

[Rio91] Rioul, O. and Vetterli, M., "Wavelets and Signal Processing," *IEEE Sig. Proc. Magazine*, pp. 14-38, Oct. 1991.

[Rio92] Rioul, O. and Flandrin, P., "Time-Scale Energy Distributions: A General Class Extending Wavelet Transforms," to appear in *IEEE Trans. Sig. Proc.*, July 1992.

[Tew92] Tewfik, A.H. and Kim, M., "Correlation Structure of the Discrete Wavelet Coefficients of Fractional Brownian Motions," *IEEE Trans. Info. Th.*, vol. IT-38, no. 2, Mar. 1992.

[Uz91] Uz, K., Vetterli, M., and LeGall, D., "Interpolative Multiresolution Coding of Advanced Television and Compatible Subchannels," *IEEE Trans. Ckt and Syst. for Video Tech.*, vol. 1, no. 1, Mar. 1991.

[Wic89] Wickerhauser, M.V., "Acoustic Signal Compression with Wave Packets," preprint, Yale University, 1989.

[Wor92a] Wornell, G.W. and Oppenheim, A.V., "Wavelet-Based Representations for a Class of Self-Similar Signals with Application to Fractal Modulation," *IEEE Trans. Info. Th.*, Mar. 1992.

[Wor92b] Wornell, G.W. and Oppenheim, A.V., "Estimation of Fractal Signals from Noisy Measurements Using Wavelets," to appear in *IEEE Trans. Sig. Proc.*, 1992.

[Yan92] Yang, X., Wang, K., and Shamma, S.A., "Auditory Representation of Acoustic Signals," *IEEE Trans. Info. Th.*, March 1992.

[Zet90] Zettler, W., Huffmann, J., and Linden, D., "Applications of Compactly Supported Wavelets to Image Compression," *SPIE Conf. Image Proc. Alg. and Tech.*, vol. 1244, p. 150-160, Santa Clara, CA, Feb. 13-15, 1990.

[Zhan91] Zhang, Y. and Zafar, S., "Motion-Compensated Wavelet Transform Coding for Color Video Compression," *SPIE Conf. Visual Comm. and Image Proc.*, pp. 301-316, Boston, MA, Nov. 10-15, 1991.

Wigner Distribution References (see also [Boud92b, Cla84, CohL66, CohL89, Esc79, FlaP84c, FlaP87c, FlaP89, Hla88, Hla91c, Hla91d, Hla92e, JanA85, JanA92, JonD92, Kad92b, Lieb90, Mec87, Ril89])

[Abe89a] Abeysekera, R.M.S.S. and Boashash, B., "Time-Frequency Domain Features of ECG Signals: Their Application in P Wave Detection Using the Cross Wigner-Ville Distribution," *IEEE Int. Conf. Acoust., Speech, Sig. Proc.*, Glasgow, Scotland, 1989.

[Abe89b] Abeysekera, R.M.S.S., "Time-Frequency Domain Features of ECG Signals: An Interpretation and Their Application in Computer Aided Diagnosis," PhD Dissertation, University of Queensland, Australia, 1989.

[Ada87] Adampopoulos, P.G. and Hammond, J.K., "The Use of the Wigner-Ville Spectrum as a Method of Identifying/Characterising Non-Linearities in Systems," *IEEE Int. Conf. Acoust., Speech, Sig. Proc.*, pp. 1541-1544, 1987.

[Alt90] Altes, R.A., "Wide-Band, Proportional Bandwidth Wigner-Ville Analysis," *IEEE Trans. Acoust., Speech, Sig. Proc.*, vol. 38, no. 6, pp. 1005-1012, June 1990.

[Ami87] Amin, M., "Time and Lag Window Selection in the Wigner-Ville Distribution," *IEEE Int. Conf. Acoust., Speech, Sig. Proc.*, pp. 1529-1532, Dallas, TX, 1987.

[And87] Andrieux, J.C., Feix, M.R., Mourgues, G., Bertrand, P., Izrar, B., and Nguyen, V.T., "Optimum Smoothing of the Wigner-Ville Distribution," *IEEE Trans. Acoust., Speech, Sig. Proc.*, vol. 35, no. 6, pp. 764-769, June 1987.

[Ath83] Athale, R.A., Lee, J.N., Robinson, E.L., and Szu, H.H., "Acousto-optic Processors for Real-time Generation of Time-frequency Representations," *Opt. Lett.*, vol. 8, pp. 166-168, 1983.

[Bam83] Bamler, R. and Glunder, H., "The Wigner Distribution Function of Two-Dimensional Signals. Coherent-optical Generation and Display," *Opt. Acta*, vol. 30, pp. 1789-1803, 1983.

[Bart80] Bartelt, H.O., Brenner, K.-H., and Lohmann, W., "The Wigner Distribution Function and its Optical Production," *Opt. Commun.*, vol. 32, pp. 32-38, Jan. 1980.

[Bast81b] Bastiaans, M.J., "The Wigner Distribution Function and its Applications to Optics," in Optics in Four Dimensions, ed. L.M. Narducci, American Inst. of Physics, New York, pp. 292-312, 1981.

[Bast83] Bastiaans, M.J., "Signal Description by Means of a Local Frequency Spectrum," Doctoral Dissertation, Technical University Eindhoven, The Netherlands, 1983.

[Bast86] Bastiaans, M.J., "Application of the Wigner Distribution to Partially Coherent Light," *J. Opt. Soc. Am.*, vol. 3, pp. 1227-1238, 1986.

[Bast92] Bastiaans, M.J., "Application of the Wigner Distribution Function in Optics," in The Wigner Distribution - Theory and Applications in Signal Processing, W.F.G. Mecklenbräuker, ed., North Holland Elsevier Science Publishers, 1992.

[Berr77] Berry, M.V., "Semiclassical Mechanics in Phase Space: A Study of Wigner's Function," *Phil. Trans. Roy. Soc.*, vol. A.287, pp. 237-271, 1977.

[Boa86a] Boashash, B. and Abeysekera, R.M.S.S., "Two Dimensional Processing of Speech and ECG Signals Using the Wigner Ville Distribution," *Proc. of SPIE*, vol. 697, 1986.

[Boa86b] Boashash, B., White, L., and Imberger, J., "Wigner-Ville Analysis of Non-Stationary Random Signals - with Application to Turbulent Microstructure Signals," *IEEE Int. Conf. Acoust., Speech, Sig. Proc.*, pp. 2323-2326, Tokyo, Japan, 1986.

[Boa86c] Boashash, B. and Whitehouse, H.J., "Seismic Applications of the Wigner-Ville Distribution," *IEEE Int. Symp. on Ckts and Syst.*, San Jose, CA, pp. 34-37, 1986.

[Boa87a] Boashash, B., Lovell, B., and White, H.J., "Time-Frequency Analysis and Pattern Recognition Using Singular Value Decomposition of the Wigner-Ville Distribution," *Proc. SPIE Conf.*, vol. 826, pp. 104-114, San Diego, CA, Aug. 18-19, 1987.

[Boa87b] Boashash, B. and Black, P.J., "An Efficient Real-Time Implementation of the Wigner-Ville Distribution," *IEEE Trans. Acoust., Speech, Sig. Proc.*, vol. 35, pp. 1611-1618, 1987.

[Boa88a] Boashash, B. and O'Shea, P., "Time-Frequency Analysis Applied to Signaturing of Underwater Acoustic Signals," *IEEE Int. Conf. Acoust., Speech, Sig. Proc.*, New York, N.Y., pp. 2817-2820, Apr. 11-14, 1988.

[Boa88b] Boashash, B. and O'Shea, P., "Application of the Wigner-Ville Distribution to the Identification of Machine Noise," *Proc. SPIE Conf. Adv. Alg. and Arch. for Sig. Proc. III*, vol. 975, San Diego, CA, Aug. 15-17, 1988.

[Boa89] Boashash, B., Lovell, B. and Kootsookos, P.J., "Time-Frequency Signal Analysis and Instantaneous Frequency Estimation: Their Inter-Relationship and Applications," *IEEE Int. Conf. Ckts and Syst.*, Portland, Oregon, pp. 1237-1242, Apr. 1989.

[Boa90a] Boashash, B., "Time-Frequency Signal Analysis," chapter in Advances in Spectrum Estimation, ed. S. Haykin, Prentice-Hall, 1990.

[Boa90b] Boashash, B. and O'Shea, P., "A Methodology for Detection and Classification of Underwater Acoustic Signals Using Time-Frequency Analysis Techniques," *IEEE Trans. Acoust., Speech, Sig. Proc.*, vol. 38, no. 11, pp. 1829-1841, Nov. 1990.

[Boa91a] Boashash, B. and Ristic, B., "Time Varying Higher Order Spectra," *Asilomar Conf. on Sig., Syst., and Comp.*, pp. 393-397, Pacific Grove, CA, Nov. 1991.

[Boa91b] Boashash, B., ed., Time-Frequency Signal Analysis - Methods and Applications, Longman-Cheshire, Melbourne, Australia, 1991.

[Bole87] Boles, P. and Boashash, B., "Use of the Wigner-Ville Distribution to Separate Seismic Events and to Analyse

Reflected Vibroseis Signals in the Time-Frequency Plane," *Int. Symp. Sig. Proc. Alg. 87*, Brisbane, Australia, Aug. 24-28, 1987.

[Boua83] Bouachache, B., "Wigner-Ville Analysis of Time-Varying Signals: An Application in Seismic Prospecting," *EUSIPCO-83: Second European Sig. Proc. Conf.*, Erlangen, W. Germany, Sept. 12-16, 1983.

[Boua84] Bouachache, B. and Rodriguez, F., "Recognition of Time-Varying Signals in the Time-Frequency Domain by Means of the Wigner Distribution," *IEEE Int. Conf. Acoust., Speech, Sig. Proc.*, pp. 22.5.1-22.5.4, Mar. 19-21, 1984.

[Boud83] Boudreaux-Bartels, G.F., "Time-Frequency Signal Processing Algorithms: Analysis and Synthesis Using Wigner Distributions," PhD Dissertation, Rice University, Houston, TX, Dec. 1983.

[Boud86] Boudreaux-Bartels, G.F. and Parks, T.W., "Time-Varying Filtering and Signal Estimation Using Wigner Distribution Synthesis Techniques," *IEEE Trans. Acoust., Speech, Sig. Proc.*, vol. ASSP-34, pp. 442-451, June 1986.

[Boud87] Boudreaux-Bartels, G.F. and Wiseman, P.J., "Wigner Distribution Analysis of Acoustic Well Logs," *IEEE Int. Conf. Acoust., Speech, Sig. Proc.*, Dallas, TX, pp. 2237-2440, Apr. 6-9, 1987.

[Boud92a] Boudreaux-Bartels, G.F., "Time-Varying Signal Processing Using Wigner Distribution Synthesis Algorithms," in The Wigner Distribution - Theory and Applications in Signal Processing, W.F.G. Mecklenbräuker, ed., North Holland Elsevier Science Publishers, 1992.

[Bre82] Brenner, K.-H. and Wodkiewica, K., "The Time-Dependent Physical Spectrum of Light and the Wigner Distribution Function," *Opt. Commun.*, vol. 43, pp. 103-106, 1982.

[Bre83] Brenner, K.-H., "A Discrete Version of the Wigner Distribution Function," *EUSIPCO-83, Second Euro. Sig. Proc. Conf.*, Erlangen, Germany, Sept. 12-16, 1983.

[Cha82] Chan, D.S.K., "A Non-Aliased Discrete-time Wigner Distribution for Time-Frequency Signal Analysis," *IEEE Int. Conf. Acoust., Speech, Sig. Proc.*, pp. 1333-1336, Paris, France, May 1982.

[Che83] Chester, D., Taylor, F.J., and Doyle, M., "Application of the Wigner Distribution to Speech Processing," *IEEE ASSP Spect. Est. Workshop II*, pp. 98-102, Tampa, FL, Nov. 10-11, 1983.

[Chi87] Chioliaz, M., Flandrin, P., and Gache, N., "Utilisation de la Représentation de Wigner-Ville Comme Outil de Diagnostic des Défauts de Fonctionnement De Moteurs Thermiques," *11ème Conf. GRETSI*, Nice, France, June 1-5, 1987.

[Cla80a] Claasen, T.A.C.M. and Mecklenbräuker, W.F.G., "The Wigner Distribution - A Tool for Time-Frequency Signal Analysis - Part I: Continuous-time Signals," *Philips J. Res.*, vol. 35, pp. 217-250, 1980.

[Cla80b] Claasen, T.A.C.M. and Mecklenbräuker, W.F.G., "The Wigner Distribution - A Tool for Time-frequency Signal Analysis - Part II: Discrete-Time Signals," *Philips J. Res.*, vol. 35, no. 4/5, pp. 276-300, 1980.

[Cla80c] Claasen, T.A.C.M. and Mecklenbräuker, W.F.G., "The Wigner Distribution - A Tool for Time-Frequency Signal Analysis - Part III: Relations with Other Time-Frequency Signal Transformations," *Philips J. Res.*, vol. 35, no. 6, pp. 372-389, 1980.

[Cla83] Claasen, T.A.C.M. and Mecklenbräuker, W.F.G., "The Aliasing Problem in Discrete-Time Wigner Distributions," *IEEE Trans. Acoust., Speech, Sig. Proc.*, pp. 1067-1072, Oct., 1983.

[CohF88] Cohen, F., Kadambe, S. and Boudreaux-Bartels, G.F., "Automated Tracking of Chirp Signals Using Unsupervised Clustering," *IEEE Int. Conf. Acoust., Speech, Sig. Proc.*, New York, NY, pp. 2180-2183, Apr. 1988.

[Con85] Conner, M. and Yao, L., "Optical Generation of the Wigner Distribution of 2-D Real Signals," *Appl. Opt.*, vol. 24, pp. 3825-3829, 1985.

[Cri89] Cristobal, G., Bescos, J., and Santamaria, J., "Image Analysis through the Wigner Distribution Function," *Appl. Opt.*, vol. 28, no. 2, pp. 262-271, Jan. 15, 1989.

[Day88] Day, D.D., "The Modified Wigner Distribution with Application to Acoustic Well Logging," *IEEE Int. Conf. Acoust., Speech, Sig. Proc.*, pp. 2713-2717, New York, NY, Apr. 1988.

[DeBr67] DeBruijn, N.G., "Uncertainty Principles in Fourier Analysis," in Inequalities, O. Shisha, ed., Academic Press, New York, 1967.

[DeBr73] DeBruijn, N.G., " A Theory of Generalized Functions with Applications to Wigner Distribution and Weyl Correspondence," *Nieuw Arch. Wiskunde*, vol. 21, pp. 205-280, 1973.

[Eas84] Easton, R.L., Ticknor, A.J., and Barret, H.H., "Application of the Radon Transform to Optical Production of the Wigner Distribution Function," *Opt. Eng.*, vol. 23, pp. 738, 1984.

[FlaP83a] Flandrin, P. and Martin, W., "Sur les Conditions Physiques Assurant L'Unicité de la Représentation de Wigner-Ville Comme Représentation Temps-Fréquence," *Neuvième Colloque sur le Traitement du Signal et ses Appl., GRETSI*, pp. 43-49, May 1983.

[FlaP83b] Flandrin, P. and Martin, W., "Pseudo-Wigner Estimators for the Analysis of Non-stationary Processes," *IEEE ASSP Spectrum Est. Workshop II*, pp.181-185, Tampa, FL, Nov. 10-11, 1983.

[FlaP84a] Flandrin, P., Martin, W., and Zakharia, M., "On a Hardware Implementation of the Wigner-Ville Transform," in Digital Signal Processing-84, V. Cappellini and A.G. Constantinides, eds., North-Holland, Amsterdam, pp. 262-266, 1984.

[FlaP84b] Flandrin, P. and Escudié, B., "An Interpretation of the Pseudo-Wigner-Ville Distribution," *Sig. Proc.*, vol. 6, pp. 27-36, 1984.

[FlaP86] Flandrin, P., "Time-Frequency Processing of Bat Sonar Signals," *Animal Sonar Systems Symposium*, Helsinger (DK), Sept. 10-19, 1986, also in Animal Sonar - Processes and Performance, P. E. Nachtigall and P.W.B. Moore, eds., pp. 797-802, New York: Plenum Press, 1988.

[FlaP87a] Flandrin, P. and Hlawatsch, F., "Signal Representation Geometry and Catastrophes in the Time-Frequency Plane," in Mathematics in Signal Processing, T.S. Durrani, J. Abbiss, J. Hudson, R. Madan, J. Mcwhirter, and T. Moore, eds., pp. 3-14, Clarendon Press, Oxford, 1987.

[FlaP88] Flandrin, P., "A Time-Frequency Formulation of Optimum Detection," *IEEE Trans. Acoust., Speech, Sig. Proc.*, vol. 36, no. 9, pp. 1377-1384, Sept. 1988.

[FlaP90b] Flandrin, P. and Rioul, O., "Affine Smoothing of the Wigner-Ville Distribution," *IEEE Int. Conf. Acoust., Speech, Sig. Proc.*, pp. 2455-2458, Albuquerque, NM, April 3-6, 1990.

[FlaP90c] Flandrin, P. and Sessarego, J.P., "Méthodes Temps-Fréquence en Acoustique," in *Coll. de Phys. C2, Suppl. J. Phys.*, T.51.N.2, pp. 707-716, 1990.

[FlaP91b] Flandrin, P., "Sur une Classe Générale d'Extensions Affines de la Distribution de Wigner-Ville," *Treizième Colloque GRETSI*, Juan-les-Pins, France, Sept. 16-20, 1991.

[FlaP92b] Flandrin, P., "The Wigner-Ville Spectrum of Non-Stationary Random Signals," in The Wigner Distribution - Theory and Applications in Signal Processing, W.F.G. Mecklenbräuker, ed., North Holland Elsevier Science Publishers, 1992.

[Fon91a] Fonollosa, J.R. and Nikias, C.L., "Wigner Polyspectra: Higer-Order Spectra in Time Varying Signal Processing," *IEEE Int. Conf. Acoust., Speech, Sig. Proc.*, Toronto, Canada, May 14-17, 1991.

[Fon91b] Fonollosa, J.R. and Nikias, C.L., "General Class of Time-frequency Higher-order Spectra: Definition, Properties, Computation and Application to Transient Signal Analysis," *Int. Sig. Proc. Workshop on Higher Order Spectra*, Chamrouse, France, July 1991.

[For89] Forrester, B.D., "Use of the Wigner-Ville Distribution in Helicopter Fault Detection," *Proc. Int. Symp. Sig. Proc. Alg. 89*, pp. 78-82, 1989.

[Gar87] Garudadri, H., Gilbert, J.H.V., Benguerel, A-P., and Beddoes, M.P., " Invariant Acoustic Cues in Stop Consonants: A Cross-Language Study Using the Wigner Distribution," *J.*

Acoust. Soc. Am. Suppl. 1, vol. 82, S55, 1987.

[Gerr88] Gerr, N.L., "Introducing a Third-Order Wigner Distribution," *Proc. IEEE*, vol. 76, no. 3, pp. 290-292, Mar. 1988.

[Gup86] Gupta, A.K. and Askura, T., "New Optical System for the Efficient Display of Wigner Distribution Functions Using a Single Object Transparency," *Opt. Commun.*, vol. 60, pp. 265-268, 1986.

[Ham85] Hammond, J.K. and Harrison, R.F., "Wigner-Ville and Evolutionary Spectra for Covariance Equivalent Non-Stationary Random Process," *IEEE Int. Conf. Acoust., Speech, Sig. Proc.*, pp. 1025-1027, 1985.

[Har89] Harris, F.J. and Salem, H.A., "Performance Comparison of Wigner-Ville Based Techniques to Standard FM-Discrimination for Estimating Instantaneous Frequency of a Rapidly Slewing FM Sinusoid in the Presense of Noise," in *Adv. Alg. and Arch. for Sig. Proc. III*, F.T. Luk, ed., Proc. SPIE, vol. 975, pp. 232-244, San Diego, CA, 1989.

[Hla84] Hlawatsch, F., "Interference Terms in the Wigner Distribution," *Proc. Int. Conf. on Dig. Sig. Proc.*, pp. 363-367, Florence, Italy, Sept. 5-8, 1984.

[Hla89] Hlawatsch, F. and Krattenthaler, W., "A New Approach to Time-Frequency Signal Decomposition," *Proc. IEEE Int. Symp. Ckts and Syst.*, Portland, Oregon, pp. 1248-1251, May 1989.

[Hla91a] Hlawatsch, F. and Kozek, W., "Time-Frequency Analysis of Linear Signal Spaces," *IEEE Int. Conf. Acoust., Speech, Sig. Proc.*, pp. 2045-2048, Toronto, Canada, May 1991.

[Hla91b] Hlawatsch, F. and Kozek, W., "Time-Frequency Synthesis of Nonstationary Stochastic Processes," submitted to *IEEE Trans. Info. Th.*

[Hla92a] Hlawatsch, F. and Flandrin, P., "The Interference Structure of the Wigner Distribution and Related Time-Frequency Signal Representations," in The Wigner Distribution - Theory and Applications in Signal Processing, W. Mecklenbräuker, ed., North Holland Elsevier Science Publishers, 1992.

[Hla92b] Hlawatsch, F. and Krattenthaler, W., "Signal Synthesis Algorithms for Bilinear Time-Frequency Signal Representations," in The Wigner Distribution - Theory and Applications in Signal Processing, W. Mecklenbräuker, ed., North Holland Elsevier Science Publishers, 1992.

[Hla92c] Hlawatsch, F. and Kozek, W., "Time-Frequency Weighting and Displacement Effects in Linear, Time-Varying Systems," to appear *IEEE Int. Symp. Ckts and Syst.*, San Diego, CA, May 1992.

[Hla92d] Hlawatsch, F., "Wigner Distribution Analysis of Linear Time-Varying Systems," to appear *IEEE Int. Symp. Ckts and Syst.*, San Diego, CA, May 1992.

[Hud74] Hudson, R.I., "When is the Wigner Quasi-Probability Density Non-negative?," *Rep. Math. Phys.*, Vol. 6, pp. 249-252, 1974.

[Imb86] Imberger, J. and Boashash, B., "Application of the Wigner-Ville Distribution to Temperature Gradient Microstructure: A New Technique to Study Small-Scale Variations," *J. of Physical Oceanography*, vol. 16, pp. 1997-2012, Dec. 1986.

[Iwa86] Iwai, T., Gupta, A.K., and Asakura, T., "Simultaneous Optical Production of the Sectional Wigner Distribution Function for Two-dimensional Object," *Opt. Commun.*, vol. 58, pp. 15-19, 1986.

[Jac82] Jacobson, L. and Wechsler, H., "The Wigner Distribution as a Tool for Deriving an Invariant Representation of 2-D Images," *Proc. IEEE Conf. Pattern Recog. and Image Proc.*, pp. 218-220, Las Vegas, Nevada, 1982.

[Jac83] Jacobson, L. and Wechsler, H., "The Composite Pseudo Wigner Distribution (CPWD): a Computable and Versatile Approximation to the Wigner Distribution (WD)," *IEEE Int. Conf. Acoust., Speech, Sig. Proc.*, pp. 254-256, Boston, MA, Apr. 1983.

[Jac88] Jacobson, L. and Wechsler, H. "Joint Spatial/Spatial-Frequency Representation," *Sig. Proc.*, vol. 14, pp. 37-68, 1988.

[JanC83] Janse, C.P. and Kaizer, A.J.M., "Time-Frequency Distributions of Loudspeakers: The Application of the Wigner Distribution," *J. Audio Eng. Soc.*, vol. 31, pp. 198-223, 1983.

[JanA79] Janssen, A.J.E.M., "Application of the Wigner Distribution to Harmonic Analysis of Generalised Stochastic Processes," PhD dissertation, University of Eindhoven, Amsterdam, 1979, also *MC-tract 114, Mathematisch-Centrum*, Amsterdam, The Netherlands, 1979.

[JanA82] Janssen, A.J.E.M., "On the Locus and Spread of Pseudo-Density Functions in the Time-Frequency Plane," *Philips J. Res.*, vol. 37, pp. 79-110, 1982.

[Jeo90b] Jeong, J. and Williams, W.J., "Time-Varying Filtering and Signal Synthesis Using the Extended Discrete-Time Wigner Distribution," in *ISSPA 90, Sig. Proc., Theories, Impl. and Appl.*, B. Boashash and P. Boles, eds., pp. 895-898, Gold Coast, Australia, Aug. 1990.

[Jeo91] Jeong, J. and Williams, W.J., "Time-Varying Filtering and Signal Synthesis," in Time-Frequency Signal Analysis - Methods and Applications, B. Boashash, ed., Longman and Cheshire, Melbourne, Australia, 1991.

[Jia84] Jiao, J.-Z., Wang, B., and Hong, L., "Wigner Distribution Function and Optical Geometrical Transformation," *Appl. Opt.*, vol. 23, pp. 1249-1254, 1984.

[JonG90] Jones, G. and Boashash, B., "Instantaneous Frequency, Instantaneous Bandwidth and the Analysis of Multi-Component Signals," *IEEE Int. Conf. Acoust., Speech, Sig. Proc.*, pp. 2467-2470, 1990.

[Kad89] Kadambe, S., Boudreaux-Bartels, G.F., and Duvaut, P., "Window Length Selection for Smoothing Wigner Distribution by Applying an Adaptive Filter," *IEEE Int. Conf. Acoust., Speech, Sig. Proc.*, pp. 2226-2229, Glasgow, Scotland, May 1989.

[Kay85] Kay, S. and Boudreaux-Bartels, G.F., "On the Optimality of the Wigner Distribution for Detection," *IEEE Int. Conf. Acoust., Speech, Sig. Proc.*, pp. 1017-1020, Tampa, FL, Mar. 1985.

[KenO88] Kenny, O. and Boashash, B., "An Optical Signal Processor for Time-frequency Signal Analysis Using the Wigner-Ville Distribution," *J. Elec. Electron. Eng.*, (Australia), pp. 152-158, 1988.

[Kit87] Kitney, R.I. and Giddens, D.P., "Doppler Ultrasound Measurement of Arterial Blood Velocity Using Linear Estimation and the Zoom Wigner Distribution," *Proc. 9th Annual Conf. of IEEE Eng. in Medicine and Biology*, Boston, MA, Nov. 13-16, 1987.

[Kob86] Kobayashi, F. and Miura, N., "Wigner Distribution and MEM in the Analysis of Time-Varying Signals," *Trans. Soc. Instrum. Control Eng. Japan*, vol. 22, pp. 1228-1230 (in Japanese), 1986.

[Koc90] Koczwara, T.E. and Jones, D.L., "On Mask Selection for Time-Varying Filtering Using the Wigner Distribution," *IEEE Int. Conf. Acoust., Speech, Sig. Proc.*, Albuquerque, NM, pp. 2487-2490, Apr. 3-6, 1990.

[Koz91] Kozek, W. and Hlawatsch, F., "Time-Frequency Filter Banks with Perfect Reconstruction," *IEEE Int. Conf. Acoust., Speech, Sig. Proc.*, pp. 2049-2052, Toronto, Canada, May 1991.

[Kra88] Krattenthaler, W. and Hlawatsch, F., "Two Signal Synthesis Algorithms for Pseudo Wigner Distribution," *IEEE Int. Conf. Acoust., Speech, Sig. Proc.*, New York, NY, pp. 1550-1553, Apr. 1988.

[Kra90] Krattenhaler, W. and Hlawatsch, F., "General Signal Synthesis Algorithms for Smoothed Versions of Wigner Distribution," *IEEE Int. Conf. Acoust., Speech, Sig. Proc.*, Albuquerque, NM, pp. 1611-1614, Apr. 1990.

[Kra93] Krattenthaler, W. and Hlawatsch, F., "Time-Frequency Design and Processing of Signals via Smoothed Wigner Distributions," to appear in *IEEE Trans. Sig. Proc.*, Feb. 1993.

[Kru76] Kruger, J.G. and Poffyn, A., "Quantum Mechanics in Phase Space, I. Unicity of the Wigner Distribution Function," *Physica*, vol. 85A, pp. 84-100, 1976.

[Kum84a] Kumar, B.V.K.V. and Carroll, C.W., "Performance of Wigner Distribution Function Based Detection Methods," *Opt.*

Eng., vol. 23, no. 6, pp. 732-737, Nov./Dec. 1984.

[Kum84b] Kumar, B.V.K.V., "Role of Wigner Distribution Function in Pattern Recognition," *Conf. on Intelligent Robots and Comp. Vision*, Cambridge, MA, Nov. 1984.

[Kum86] Kumar, B.V.K.V., Neuman, C.P., and DeVos, K.J., "Discrete Wigner Synthesis," *Sig. Proc.*, vol. 11, pp. 277-304, 1986.

[Kum87] Kumar, B.V.K.V. and deVos, K.J., "Linear System Description using Wigner Distribution Functions," *Adv. Alg. and Arch. for Sig. Proc. II*, Proc. SPIE, vol. 826, pp. 115-124, 1987.

[MarN84] Marinovic, N.M. and Eichmann, G., "Feature Extraction and Pattern Classification in Spatial Frequency Domain," *Proc. Conf. Intell. Robots and Comp. Vision*, Proc. SPIE, vol. 579, pp. 15-20, 1985.

[MarN86a] Marinovic, N.M. and Smith, W.A., "Application of Joint Time-Frequency Distributions to Ultrasonic Transducers," *ISCAS-86*, pp. 50-54, 1986.

[MarN86b] Marinovic, N.M, "The Wigner Distribution and the Ambiguity Function: Generalizations, Enhancement, Compression and Some Applications," PhD Dissertation, The City University of New York, 1986.

[MarN88] Marinovic, N.M., Oklobdzija, V.G., et al., "VLSI Architecture of a Real-time Wigner Distribution Processor for Acoustic Signals," *IEEE Int. Conf. Acoust., Speech, Sig. Proc.*, pp. 2112-2115, 1988.

[Mart85a] Martin, W. and Flandrin, P., "Wigner-Ville Spectral Analysis of Nonstationary Processes," *IEEE Trans. Acoust., Speech, Sig. Proc.*, vol. 33, no. 6, pp. 1461-1470, Dec. 1985.

[Mart85b] Martin, W. and Flandrin, P., "Detection of Changes of Signal Structure by Using the Wigner-Ville Spectrum," *Sig. Proc.*, vol. 8, p. 215, 1985.

[Mart86] Martin, W. and Krüger-Alef, K., "Application of Wigner Ville Spectrum to the Spectral Analysis of a Class of Bio-Acoustical Signals Blurred by Noise," *Acustica*, vol. 61, no. 3, pp. 176-183, Sept. 1986.

[Mat86] Mateeva, T. and Sharlandjiev, P., "The Generation of a Wigner Distribution Function of Complex Signals by Spatial Filtering," *Opt. Commun.*, vol. 57, p. 153, 1986.

[McH89] McHale, T.J., "Time-Varying Multicomponent Signal Analysis using a Weighted Wigner Distribution Synthesis Algorithm," Master's Thesis, University of Rhode Island, Kingston, RI, Aug.1989.

[Mec92] Mecklenbräuker, W.F.G., ed., The Wigner Distribution - Theory and Applications in Signal Processing, Elsevier Science Publishers, in press, 1992.

[Morg86] Morgan, N.H. and Gevins, A.S., "Wigner Distribution of Human Event-Related Brain Potentials," *IEEE Trans. Biomedical Engg.*, vol. BME 33, no. 1, Jan. 1986.

[Mou85] Mourgues, G., Feix, M.R., Andrieux, J.C., and Bertrand, P., "Not Necessary but Sufficient Conditions for the Positivity of Generalized Wigner Functions," *J. Math. Phys.*, vol. 26, pp. 2554-2555, 1985.

[Moy49] Moyal, J.E., "Quantum Mechanics as a Statistical Theory," *Proc. Cambridge Phil. Soc.*, vol. 45, pp. 99-124, 1949.

[Mul88] Mullick, S.K. and Topkar, V.A., "A Wigner Distribution Based Receiver," *Signal Proc.*, vol. 14, pp. 185-196, 1988.

[Nut88a] Nutall, A.H., "Wigner Distribution Function: Relation to Short-Term Spectral Estimation, Smoothing and Performance in Noise," Naval Underwater Systems Center Technical Report 8225, New London, CT, Feb. 16, 1988.

[Nut88b] Nutall, A.H., "The Wigner Distribution Function with Minimum Spread," Naval Underwater Systems Center Technical Report 8317, New London, CT, June 1988.

[Nut89] Nutall, A.H., "Alias-free Discrete-time Wigner Distribution Function and Complex Ambiguity Function," Naval Underwater Systems Center, NUSC Tech. Rep. 8533, Apr. 14, 1989.

[Oco83] O'Connell, R.F., "The Wigner Distribution Function - 50th Birthday," *Found. Phys.*, vol. 13, no. 1, pp. 83-92, 1983.

[Oje84] Ojeda-Castaneda, J. and Sicre, E.E., "Bilinear Optical Systems, Wigner Distribution Function and Ambiguty Function Representations," *Opt. Acta*, vol. 31, pp. 255-260, 1984.

[Pei88] Pei, S.C. and Wang, T.Y., "The Wigner Distribution of Linear Time-Variant Systems," *IEEE Trans. Acoust., Speech, Sig. Proc.*, vol. 36, pp. 1681-1684, 1988.

[Pey85] Peyrin, F., Vray, D., Gimenez, G., and Person, R., "Application of the Wigner Ville Transform to Fish Echo-Sounder Signals," 1985 *Proc. of Malecon - Mediterranean Electro-chemical Conf.*, vol. 2, Madrid, Spain, Oct. 9-10, 1985.

[Pey86] Peyrin, F. and Prost, R., "A Unified Definition for the Discrete-Time, Discrete-Frequency and Discrete-Time/Frequency Wigner Distributions," *IEEE Trans. Acoust., Speech, Sig. Proc.*, pp. 858-867, Aug. 1986.

[Prei82] Preis, D., "Phase Distortion and Phase Equalization in Audio Signal Processing - A Tutorial Review," *J. Audio Eng. Soc.*, vol. 30, pp. 774-794, Nov. 1982.

[Prei87] Preis, D., Hlawatsch, F., Bloom, P.J., and Deer, J.A., "Wigner Distribution Analysis of Filters with Perceptible Phase Distortion," *J. Audio Eng. Soc.*, pp. 1004-1012, Dec. 1987.

[Pres83] Press, W., "Wigner Distribution Function as a Speech Spectrogram with Unlimited Resolution Simultaneously in Time and Frequency," r83-106-01, The Mitre Corp., July 1983.

[Ram87] Ramamoorthy, P.A., Iyer, V.K., and Ploysongsang, Y., "Autoregressive Modeling of the Wigner Spectrum," *IEEE Int. Conf. Acoust., Speech, Sig. Proc.*, Dallas, TX, pp. 1509-1512, Apr. 1987.

[Rao90] Rao, P. and Taylor, F.J., "Estimation of Instantaneous Frequency Using the Wigner Distribution," *Electronics Let.*, vol. 26, no. 4, pp. 246-248, Feb. 1990.

[Rao91] Rao, P. and Taylor, F.J., "Detection and Localization of Narrow-Band Transient Signals Using the Wigner Distribution," *J. Acoust. Soc. Am.*, vol. 90, pp.1423-1433, Sept. 1991.

[Raz90] Raz, S., "Synthesis of Signals from Wigner Distributions: Representations on Biorthogonal Bases," *Sig. Proc.*, vol. 20, pp. 303-314, 1990.

[Sah90] Sahiner, B. and Yagle, A.E., "Application of Time-Frequency Distributions to Magnetic Resonance Imaging of Non-Constant Flow," *IEEE Int. Conf. Acoust., Speech, Sig. Proc.*, pp. 1865-1868, Apr. 1990.

[Sal85] Saleh, B.E.A. and Subotic, N.S., "Time-Variant Filtering of Signals in the Mixed Time-Frequency Domain," *IEEE Trans. Acoust., Speech, Sig. Proc.*, vol. 33, pp. 1479-1485, 1985.

[Ses89] Sessarego, J.P., Sageloli, J., Flandrin, P., and Zakharia, M., "Time-Frequency Wigner-Ville Analysis of Echoes Scattered by a Spherical Shell," in [Com89], pp. 147-153, 1989.

[Ste82] Stein, S. and Szu, H.H., "Two Dimensional Optical Processing of One-Dimensional Acoustic Data," *Opt. Eng.*, vol. 21, pp. 804-813, 1982.

[Sub84] Subotic, N. and Saleh, B.E.A., "Generation of the Wigner Distribution of Two-Dimensional Signals by a Parallel Optical Processor," *Opt. Lett.*, vol. 9, pp. 471, 1984.

[SwaA91] Swami, A., "Third-Order Wigner Distributions: Definitions and Properties," *IEEE Int. Conf. Acoust., Speech, Sig. Proc.*, Toronto, Canada, May 14-17, 1991.

[Szu81] Szu, H.H. and Blodgett, J.A., "Wigner Distribution and Ambiguity Function," in Optics in Four Dimensions, ed. L.M. Narducci, American Institute of Physics, New York, pp. 355-381, 1981.

[Szu86] Szu, H.H., "Applications of Wigner and Ambiguity Functions to Optics," *IEEE Int. Symp. Ckts. and Syst.-86*, San Jose, CA, pp. 46-49, 1986.

[Vel89a] Velez, E.F. and Absher, R.G., "Transient Analysis of Speech Signals Using The Wigner Time-Frequency Representation," *IEEE Int. Conf. Acoust., Speech, Sig. Proc.*, pp. 2242-2245, Glasgow, Scotland, May 23-26, 1989.

[Vel89b] Velez, E.F. and Absher, R.G., "Smoothed Wigner-Ville Parametric Modeling for the Analysis of Nonstationary Signals," *IEEE Int. Symp. Ckts and Syst.*, Portland, Oregon, May 9-11, 1989.

[Vel90] Velez, E.F. and Absher, G., "Spectral Estimation Based

on the Wigner-Ville Representation," *Sig. Proc.*, vol. 20, no. 4, pp. 325-346, Aug. 1990.

[Verr89] Verrault, E., "Détection et Caractérisation des Râles Crépitants," Doctoral Dissertation, Université Laval, Quebec, Canada, Nov. 1989.

[Vers88] Verschuur, D.J., Kaizer, A.J.M., Druyvesteer, W.F., and DeVries, D., "Wigner Representation of Loudspeaker Responses in a Living Room," *J. Audio Eng. Soc.*, vol. 36, pp. 203-212, Apr. 1988.

[Vil48] Ville, J., "Théorie et Applications de la Notion de Signal Analytique," *Câbles et Transmission*, vol. 2 A, pp. 61-74, 1948, translated into English by I. Selin, RAND Corp. Report T-92, Santa Monica, CA, Aug. 1958.

[Whi87] White, L.B. and Boashash, B., "Time-Frequency Coherence - A Theoretical Basis for Cross Spectral Analysis of Non-Stationary Signals," *Proc. IASTED Int. Symp. on Sig. Proc. and its Appl.*, ed. B. Boashash, vol. 1, Brisbane, Australia, pp. 18-23, Aug. 24-28, 1987.

[Whi88] White, L.B. and Boashash, B., "Estimating the Instantaneous Frequency of a Gaussian Random Process," *IEEE Trans. Acoust., Speech, Sig. Proc.*, vol. 36, no. 3, pp. 417-420, Mar. 1988.

[Whi89] White, L.B., "Some Aspects of the Time-frequency Analysis of Random Processes," Thesis, University of Queensland, Australia, 1989.

[Whi90a] White, L.B., Qiu, L., and Boashash, B., "Instantaneous Frequency Estimation: Statistical Properties; Application to Time-Varying Filtering," *IEEE Int. Conf. Acoust., Speech, Sig. Proc.*, Albuquerque, NM pp. 1221-1224, 1990.

[Whi90b] White, L.B. and Boashash, B., "Cross Analysis of Non-Stationary Random Processes," *IEEE Trans. Info. Th.*, July 1990.

[Wig32] Wigner, E.P., "On the Quantum Correction for Thermo-Dynamic Equilibrium," *Physics Review*, vol. 40, pp. 749-759, 1932.

[Wig71] Wigner, E.P., "Quantum-mechanical Distribution Functions Revisited," in Perspectives in Quantum Theory, W. Yourgrau and A. van der Merwe, eds., New York: Dover Publ., 1971.

[Wok87] Wokurek,W., Hlawatsch, F., and Kubin, G., "Wigner Distribution Analysis of Speech Signals," *Int. Conf. on Dig. Signal Proc.*, pp. 294-298, Florence, Italy, Sept. 7-10, 1987.

[Won90] Wong, K.M. and Jin, Q., "Estimation of the Time-Varying Frequency of a Signal - the Cramér-Rao Bound and the Application of the Wigner Distribution," *IEEE Trans. Acoust., Speech, Sig. Proc.*, vol. 38, no. 3, pp. 519-536, Mar. 1990.

[Yen87] Yen, N., "Time and Frequency Representation of Acoustic Signals by Means of the Wigner Distribution Function: Implementation and Interpretation," *J. Acoust. Soc. Am.*, vol. 81, no. 6, pp. 1841-1850, June 1987.

[Yu87] Yu, K.-B and Cheng, S., "Signal Synthesis from Pseudo-Wigner Distributions and Applications," *IEEE Trans. Acoust., Speech, Sig. Proc.*, vol. 35, pp. 1289-1302, 1987.

[Zhu90] Zhu, Y.M., Peix, G., and Babot, D., "Detection of Defects in Wave Composites by Applying the Wigner Distribution to Radioscopic Images Obtained with a Linear Solid State Array," *NDT International*, vol. 23, pp. 75-82, 1990.

Ambiguity Function References (see also [Boud83, Boud92b, CohL66, CohL86, Hla91c, Hla92a, Hla92e, Levi67, MarN86b, Mec87, Mon67, Nut89, Oje84, Papo77, Rih68b, Szu81, Szu86])

[Alt70] Altes, R.A. and Titlebaum, E.L., "Bat Signals as Optimally Doppler Tolerant Waveforms," *J. Acoust. Soc. Am.*, vol. 48, no. 2 (part 2), pp. 1014-1020, Oct. 1970.

[Aus85] Auslander, L. and Tolimieri, R., "Radar Ambiguity Function and Group Theory, " *SIAM J. Math. Anal.*, vol. 165, no. 3, pp 577-601, 1985.

[Aus88] Auslander, L. and Tolimieri, R., "Computing Decimated Cross-Ambiguity Functions," *IEEE Trans. Acoust., Speech, Sig. Proc.*, vol. 36, no. 3, pp. 359-364, 1988.

[Aus91b] Auslander, L. and Gertner, I., "Computing the Ambiguity Function on Various Domains," submitted for publication, 1991.

[Bel91] Bellegarda, J.R. and Titlebaum, E.L., "The Hit Array: An Analysis Formalism for Multiple Access Frequency Hop Coding," *IEEE Trans. Aerospace, Elect. Syst.*, vol. 27, no.1, pp. 30-39, Jan. 1991.

[Bla67] Blau, W., "Synthesis of Ambiguity Function for Prescribed Responses," *IEEE Trans. AER EL*, vol. AES-3, pp. 656-663, 1967.

[Cos84] Costas, J.P., "A Study of a Class of Detection Waveforms Having Nearly Ideal Range-Doppler Ambiguity Properties," *Proc. IEEE*, vol. 72, no. 8, pp. 996-1009, Aug. 1984.

[Debu70] Debuda, R., "Signals that Can be Calculated from Their Ambiguity Function," *IEEE Trans. Info. Theory*, vol. IT-16, pp. 195-202, Mar. 1970.

[DeL67] DeLong, Jr., D.F. and Hofstetter, E.M., "On the Design of Optimum Radar Waveforms for Clutter Rejection," *IEEE Trans. Info. Theory*, vol. IT-13, pp. 454-463, July 1967.

[Dru91] Drumheller, D.M and Titlebaum, E.L., "Cross-Correlation Properties of Algebraically Constructed Costas Arrays," *IEEE Trans. Aerospace and Elect. Syst.*, vol. 27, no. 1, pp. 2-10, Jan. 1991.

[Gaa68] Gaarder, N.T., "Scattering Function Estimation," *IEEE Trans. Info. Theory*, vol. IT-14, pp. 684-693, September, 1968.

[Gers63] Gersho, A., "Characterization of Time-Varying Linear Systems," *Proc. IEEE*, p. 238, January, 1963.

[Gol68] Goldman, J., "Estimation of a Random Time-Varying Transfer Function," *IEEE Trans. Info. Th.*, vol. IT-14, pp. 598-599, July 1968.

[Gui78] Guigay, J.-P., "The Ambiguity Function in Diffraction and Isoplanatic Imaging by Partially Coherent Beams," *Opt. Commun.*, vol. 26, pp. 136-138, 1978.

[Hol67] Hollis, E.E., "Comparison of Combined Barker Codes for Coded Radar Use," *IEEE Trans. Aerospace Electr. Syst.*, vol. AES-3, pp. 141-143, 1967.

[Jou77] Jourdain, G., "Synthèse de Signaux Certains dont on Connaît la Fonction d'Ambiguïté de Type Woodward ou de Type en Compression," *Ann. Télécomm.*, vol. 32, pp. 19-34, 1977.

[Kai63] Kailath, T., "Time-Variant Communication Channels," *IEEE Trans. Info. Theory*, vol. IT-9, pp. 233-237, Oct. 1963.

[KenR69] Kennedy, R.S., Fading Dispersive Communications Channels, Wiley Publ., 1969.

[Kla60a] Klauder, J.R., Price, A.C., Darlington, S., and Albersheim, W.J., "The Theory and Design of Chirp Radars," *Bell System Tech. J.*, vol. 39, pp. 745-808, July 1960.

[Kla60b] Klauder, J.R., "The Design of Radar Signals Having Both High Range Resolution and High Velocity Resolution," *Bell System Tech. J.*, vol. 39, pp. 809-820, July 1960.

[Ler58] Lerner, R.M., "Signals with Uniform Ambiguity Functions," *1958 IRE National Convention Record, Pt. 4*, pp. 27-36, 1958.

[Ler63] Lerner, R.M., "Communications and Radar - Section B - Radar Waveform Selection," *IEEE Trans. Info. Th.*, vol. IT-9, pp. 246-248, Oct. 1963.

[Lieb90] Lieb, E.H., "Integral Bounds for Radar Ambiguity Functions and Wigner Distributions," *J. Math. Phys.*, vol. 31, no. 3, pp. 594-599, Mar. 1990.

[MarS90] Maric', S.V., and Titlebaum, E.L., "Frequency Hop Multiple Access Codes Based Upon the Theory of Cubic Congruences," *IEEE Trans. Aerospace, Elect. Syst.*, vol. 26, no. 6, pp. 1035-1039, Nov. 1990.

[MarN91] Marinovic, N. and Oklobdzija, V.G., "VSLI Chip Architectures for Real-Time Ambiguity Function Computation," *1991 Asilomar Conf. Sig., Syst., and Comp.*, pp. 74-78, Pacific Grove, CA, Nov. 4-6, 1991.

[Miz75] Mizumach, M. and Sakai, Y., "Radar Signal-Design for

Estimation of 2 Closely Spaced Targets," *Electr. Co. J.*, vol. 58, 1975.

[Papo74] Papoulis, A., "Ambiguity Function in Fourier Optics," *J. Opt. Soc. Am.*, vol. 64, pp. 779-788, 1974.

[Pri65] Price, R. and Hofstetter, E.M., "Bounds in the Volume and Height Distribution of the Ambiguity Function," *IEEE Trans. Info. Theory*, vol. IT-11, pp. 207-214, 1965.

[Rih68a] Rihaczek, A.W., "Design of Zigzag FM Signals," *IEEE Trans. AER EL*, vol.AES-4, 1968.

[Rih69] Rihaczek, A.W., Principles of High-resolution Radar, McGraw Hill, New York, 1969.

[Rih71] Rihaczek, A.W., "Radar Waveform Selection - A Simplified Approach," *IEEE Trans. AER EL*, vol. AES-7, pp. 1078-1086, Nov. 1971.

[Sed70] Sedletskiy, R.M., "Numerical Synthesis of Signals from Modulus of Ambiguity Functions," *Radio Eng. R*, vol. 15, pp. 702-704, Apr. 1970.

[Sie56] Siebert, W.M., "A Radar Detection Philosophy," *Trans. IRE PGIT*, vol. IT-2, pp. 204-221, Sept. 1956.

[Sie58] Siebert, W.M., "Studies of Woodward's Uncertainty Function," *Quart. Progress Rep.*, pp. 90-94, Res. Lab. of Electronics, MIT, Apr. 1958.

[Siv82] Sivaswamy, R., "Self-Clutter Cancellation and Ambiguity Properties of Sub-Complementary Signals," *IEEE Trans. AER EL*, vol. AES-18, pp. 163-181, Mar. 1982.

[Sko62] Skolnik, M.I., Introduction to Radar Systems, McGraw Hill, NY, 1962.

[Ste81] Stein, S., "Algorithms for Ambiguity Function Processing," *IEEE Trans. Acoust., Speech, Sig. Proc.*, vol. ASSP-29, pp. 588-599, 1981.

[Stu64] Stutt, C.A., "Some Results on Real-Part/Imaginary-Part and Magnitude-Phase Relations in Ambiguity Functions," *IEEE Trans. Info. Th.*, pp. 321-327, Oct. 1964.

[Stu68] Stutt, C.A. and Spafford, L.J., "A 'Best' Mismatched Filter Response for Radar Clutter Discrimination," *IEEE Trans. Info. Th.*, vol. IT-14, pp. 280-287, Mar. 1968.

[Sus62] Sussman, S.M., "Least-Squares Synthesis of Radar Ambiguity Functions," *Trans. IRE*, vol. IT-8, pp. 246-254, Apr. 1962.

[Tit66] Titlebaum, E.L. and DeClaris, N., "Linear Transformations of the Ambiguity Function," *IEEE Trans. Info. Th.*, vol. 12, no. 2, pp. 120-125, Apr. 1966.

[Tit91a] Titlebaum, E.L., Bellegards, J.R., and Maric', S.V., "Ambiguity Properties of Quadratic Congruential Coding," *IEEE Trans. Aerospace, Elect. Syst.*, vol. 27, no. 1, pp. 18-29, Jan. 1991.

[Tit91b] Titlebaum, E.L. and Bellegarda, J.R., "Bounds on Auto- and Cross-Ambiguity Functions for Costas Arrays," submitted to *Proc. IEEE*, 1991.

[Tol85] Tolimieri, R. and Winograd, S., "Computing the Ambiguity Surface," *IEEE Trans. Acoust., Speech, Sig. Proc.*, vol. 33, no. 4, pp. 1239-1245, Oct. 1985.

[Turi57] Turin, G.L., "A Review of Correlation, Matched-Filter, and Signal Coding Techniques, with Emphasis on Radar Applications," *Tech. Memo 559*, vol. 1, Systems Development Labs, Hughes Aircraft, Co., Culver City, Apr. 1957.

[Tury63] Turyn, R.J., "Ambiguity Functions of Complementary Sequences," *IEEE Trans. Info. Theory*, vol. IT-9, pp. 46-47, Jan. 1963.

[Vak67a] Vakman, D.Y., "Feasibility of Synthesis of Phase-manipulated Signals," *Radio Eng. R*, vol. 12, pp. 894-902, June 1967.

[Vak67b] Vakman, D.Y., "Optimum Signals Which Maximize Partial Volume under an Ambiguity Surface," *Radio Eng. R*, vol. 12, pp. 1260-1268, Aug. 1967.

[Vak68] Vakman, D.Y., Sophisticated Signals and the Uncertainty Principle in Radar, translated from Russian by K.N. Trirogoff, New York: Springer-Verlag, 1968.

[Vak76] Vakman, D.Y., A Regular Method of Synthesis of Phase-Manipulated Signals, Sovetskoye Radio, 1976.

[Van71] Van Trees, H.L., Detection, Estimation and Modulation Theory, Part III, J. Wiley & Sons Publ., New York, 1971.

[Widn61] Widnall, W.S., "A Critique of Wilcox's Method of Ambiguity Function Synthesis," Report # 34G-1, ASTIA Doc. No. AD 267 537, MIT Lincoln Labs, Lexington, MA, Nov. 18, 1961.

[Wilc60] Wilcox, C.H., "The Synthesis Problem for Radar Ambiguity Functions," MRC Tech. Summary Rep. No. 157, Univ. of Wisc., Madison, Wisc., Apr. 1960.

[Wolf69] Wolf, J.D., Lee, G.M., and Suyo, C.E., "Radar Waveform Synthesis by Mean-Square Optimization Techniques," *IEEE Trans. AER EL*, Vol. AES-5, pp. 611-619, 1969.

[Woo53] Woodward, P.M., Probability and Information Theory with Application to Radar, Pergamon Press, London, 1953.

General / Other Time-Frequency References (see also [Alt90, Bast83, Boa90a, Boa91a, Boa91b, Boud83, Cla80c, FlaP83a, FlaP83b, FlaP87a, FlaP88, FlaP90b, FlaP91b, Fon91b, Fow91, Ham85, Hla91a, Hla92a, Hla92b, JanC83, JanA82, Kra90, Kru76, MarN86b, Mec92, Mou85, Rio92, Wig71])

[Ack70] Ackroyd, M.H., "Short-time Spectra and Time-Frequency Energy Distributions," *J. Acoust. Soc. Amer.*, vol. 50, pp. 1229-1231, 1970.

[Bara91] Baraniuk, R.G. and Jones, D.L., "A Radially Gaussian, Signal Dependent Time-Frequency Representation," *IEEE Int. Conf. Acoust., Speech, Sig. Proc.*, Toronto, Canada, pp. 3181-3184, May 1991.

[Bert88] Bertrand, J. and Bertrand, P., "Time-Frequency Representations of Broad-Band Signals," *IEEE Int. Conf. Acoust., Speech, Sig. Proc.*, pp. 2196-2199, New York, NY, Apr. 11-14, 1988, also in [Com89], pp. 164-171, also in The Physics of Phase Space, Y.S. Kim and W.W. Zachary, eds., New York, Springer, pp. 250-252, 1987.

[Bert91] Bertrand, J. and Bertrand, P., "Affine Time Frequency Distributions," in Time-Frequency Signal Analysis - Methods and Applications, ed. B. Boashash, Longman-Chesire, Melbourne, Australia, 1991, also in *Proc. Int. Symp. Sig. Proc. and Appl.*, Gold Coast, Australia, 1990.

[Boud91b] Boudreaux-Bartels, G.F. and Papandreou, A., "On a Generalization of the Choi-Williams Exponential Distribution," *Asilomar Conf. Sig., Syst., Comp.*, pp. 364-369, Pacific Grove, CA, Nov. 1991.

[Boud92b] Boudreaux-Bartels, G.F. and Hlawatsch, F., "References for the Short-time Fourier Transform, Gabor Expansion, Wavelet Transform, Wigner Distribution, Ambiguity Function, and Other Time-Frequency and Time-Scale Signal Representations," Technical Report No. 0492-0001, University of Rhode Island, Electrical Engineering Department, Kingston, RI, Apr. 1992.

[Choi89] Choi, H.I. and Williams, W.J., "Improved Time-Frequency Representation of Multicomponent Signals Using Exponential Kernels," *IEEE Trans. Acoust., Speech, Sig. Proc.*, Vol. ASSP-37, no. 6, pp. 862-871, 1989.

[Cla84] Claasen, T.A.C.M. and Mecklenbräuker, W.F.G., "On the Time-Frequency Discrimination of Energy Distributions - Can They Look Sharper than Heisenberg?" *IEEE Int. Conf. Acoust., Speech, Sig. Proc.*, pp. 41B7.1-41B7.4, San Diego, CA, 1984.

[CohL66] Cohen, L., "Generalized Phase-Space Distribution Functions," *J. of Math. Phys.*, vol. 7, pp. 781-786, 1966.

[CohL85] Cohen, L. and Posch, T., "Positive Time-Frequency Distribution Functions," *IEEE Trans. Acoust., Speech, Sig. Proc.*, vol. 33, no. 1, pp. 31-37, Feb. 1985.

[CohL86] Cohen, L. and Posch, T.E., "Generalized Ambiguity Functions," *IEEE Int. Conf. Acoust., Speech, Sig. Proc.*, pp. 27.6.1-27.6.4, Tampa, FL, Mar. 1985.

[CohL89] Cohen, L., "Time-Frequency Distributions - A Review," *Proc. IEEE*, vol. 77, no. 7, pp. 941-981, July 1989.

[CohL91] Cohen, L., "Time-Frequency Distribution and Instantaneous Frequency," *Adv. Sig. Proc. Alg., Arch. and Impl. II*, Proc. SPIE Conf., vol. 1566, July 1991.

[Esc79] Escudié, B., Flandrin, P., and Gréa, J., "Positivité des Représentations en Temps et Fréquence des Signaux d'Energie Finie, Représentation Hilbertienne et Conditions à Observation des Signaux," *Septième Colloque GRETSI sur le Traitment du Signal et Applications*, pp. 28/5-2/6/79, Nice, France, 1979.

[FlaP80] Flandrin, P. and Escudié, B., "Time and Frequency Representation of Finite Energy Signals: A Physical Property as a Result of a Hilbertian Condition," *Sig. Proc.*, vol. 2, pp. 93-100, 1980.

[FlaP84c] Flandrin, P., "Some Features of Time-Frequency Representations of Multi-component Signals," *IEEE Int. Conf. Acoust., Speech, Sig. Proc.*, pp. 41.B.4.1-4, San Diego, CA, 1984.

[FlaP87b] Flandrin, P., "Time-Dependent Spectra of Non-Stationary Stochastic Processes," Lecture given at the CISM Advanced School "Time and Frequency Representation of Signals and Systems," Udine, Italy, Sept. 21-25, 1987.

[FlaP87c] Flandrin, P., "Représentations Temps-fréquence des Signaux Non-stationnaires," Thèse Doct. Etat, Institut National Polytechnique de Grenoble, France, 1987.

[FlaP89] Flandrin, P., "Some Aspects of Non-Stationary Signal Processing With Emphasis on Time-Frequency and Time-Scale Methods," in [Com89], pp.68-98.

[Grac81] Grace, O.D., "Instantaneous Power Spectra," *J. Acoust. Soc. Am.*, vol. 69, pp. 191-198, 1981.

[Hea91] Hearon, S. and Amin, M., "Statistical Trade Offs in Modern Time-Frequency Kernel Design," *Asilomar Conf. on Sig., Syst., Comp.*, pp. 359-363, Pacific Grove, CA, Nov. 1991.

[Hla88] Hlawatsch, F., "A Study of Bilinear Time-frequency Signal Representations with Applications to Time-frequency Signal Synthesis," Doctoral Dissertation, Technische Universität Wien, Vienna, Austria, 1988.

[Hla91c] Hlawatsch, F., "Duality and Classification of Bilinear Time-Frequency Signal Representations," *IEEE Trans. Sig. Proc.*, vol.39, no. 7, pp. 1564-1574, July 1991.

[Hla91d] Hlawatsch, F., "Time-Frequency Methods for Signal Processing," Technical Report No. 1291-0001, University of Rhode Island, Electrical Engineering Dept., Kingston, RI, Dec. 1991.

[Hla92e] Hlawatsch, F. and Krattenthaler, W., "Bilinear Signal Synthesis," *IEEE Trans. Sig. Proc.*, pp. 352-363, Feb. 1992.

[Hla92f] Hlawatsch, F., "Regularity and Unitarity of Bilinear Time-frequency Signal Representations," *IEEE Trans. Info. Th.*, pp. 82-94, Jan. 1992.

[JanA85] Janssen, A.J.E.M. and Claasen, T.A.C.M., "On Positivity of Time-Frequency Distributions," *IEEE Trans. Acoust., Speech, Sig. Proc.*, vol.33, no. 4, pp. 1029-1032, Aug. 1985.

[JanA87] Janssen, A.J.E.M.,"A Note on 'Positive Time-frequency Distributions'," *IEEE Trans. Acoust., Speech, Sig. Proc.*, vol. 35, pp. 701-703, May 1987.

[JanA92] Janssen, A.J.E.M., "Positivity and Spread of Bilinear Time-Frequency Distributions," in The Wigner Distribution - Theory and Applications in Signal Processing, W.F.G. Mecklenbräuker, ed., Elsevier Science Publishers, 1992.

[Jeo92a] Jeong, J. and Williams, W.J., "Kernel Design for Reduced Interference Distributions," *IEEE Trans. Sig. Proc.*, vol. 40, no. 2, pp. 402-412, Feb. 1992.

[Jeo92b] Jeong, J. and Williams, W.J., "Alias-Free Generalized Discrete-time Time-frequency Distributions," to appear in *IEEE Trans. Sig. Proc.*

[JonD90] Jones, D.L. and Parks, T.W., "A High Resolution Data-Adaptive Time-Frequency Representation," *IEEE Trans. Acoust., Speech, Sig. Proc.*, vol. 38, pp. 2127-2135, 1990.

[JonD92] Jones, D.L. and Parks, T.W., "A Resolution Comparison of Several Time-Frequency Representations," *IEEE Trans. Sig. Proc.*, vol. 40, no. 2, pp. 413-420, Feb. 1992.

[Levi67] Levin, M.J., "Instantaneous Spectra and Ambiguity Functions," *IEEE Trans. Info. Th.*, vol. IT-13, pp. 95-97, 1967.

[McA90] McAulay, R.J. and Quatieri, T.F., "Pitch Estimation and Voicing Detection Based on a Sinusoidal Model," *Proc. Int. Conf. Acoust. Speech, Sig. Proc.*, Albuquerque, NM, pp. 249-252, 1990.

[McA92] McAulay, R.J. and Quatieri, T.F., "Low-rate Speech Coding Based on the Sinusoidal Model," in Advances in Speech Signal Processing, S. Furui and M.M. Sondhi, eds., New York: Mercel Dekker Publ., 1992.

[Mec87] Mecklenbräuker, W.F.G., "A Tutorial on Non-Parametric Bilinear Time-Frequency Signal Representations," Les Houches, Session XLV, 1985, Signal Processing, eds. J.L. Lacoume, T.S. Durrani, and R. Stora, pp. 277-336, 1987.

[Pag52] Page, C.H., "Instantaneous Power Spectra," *J. Appl. Phys.*, vol. 23, pp. 103-106, 1952.

[Papa91] Papandreou, A. and Boudreaux-Bartels, G.F., "Generalization of the Choi-Williams Distribution and the Butterworth Distribution for Time-Frequency Analysis," submitted to *IEEE Trans. Sig. Proc.*

[Papa92] Papandreou, A. and Boudreaux-Bartels, G.F., "Distributions for Time-Frequency Analysis: A Generalization of Choi-Williams and the Butterworth Distribution," *IEEE Int. Conf. Acoust., Speech, Sig. Proc.*, San Diego, CA, Mar. 1992.

[Papo77] Papoulis, A., Signal Analysis, McGraw-Hill Book Co., New York, 1977.

[Rih68b] Rihaczek, A.W., "Signal Energy Distribution in Time and Frequency," *IEEE Trans. Info. Th.*, vol. IT-14, no. 3, pp. 369-374, 1968.

[Ril89] Riley, M.D., Speech Time-Frequency Representations, Kluwer Academic Publ., 1989.

[Urb90] Urbanke, R., "Zeit Frequenz-Signalanalyse mit der Exponentialverteilung und den 'Reduced-Interference' - Verteilungen: Interferenzgeometrie und zeitdiskrete Implementierung," Diploma Thesis, Technische Universität Wien, Vienna, Austria, Aug. 1990.

[Widm92] Widmalm, S.E., Williams, W.J., and Zheng, C.S., "Time-Frequency Distributions of TMJ Sounds," *J. Oral Rehabilitation*, in press.

[Will91] Williams, W.J. and Jeong, J., "Reduced Interference Time-Frequency Distributions," in Time-Frequency Signal Analysis - Methods and Applications, B. Boashash, ed., Longman-Cheshire, Melbourne, Australia, 1991, also in *Int. Symp. Sig. Proc. Alg: Sig. Proc., Theories, Impl. and Appl.*, pp. 878-881, Aug. 1990.

[Zhao90] Zhao, Y., Atlas, L.E., and Marks, R.J., "The Use of Cone-Shaped Kernels for Generalized Time-Frequency Representations of Nonstationary Signals," *IEEE Trans. Acoust., Speech, Sig. Proc.*, vol. ASSP-38, no. 7, pp. 1084-1091, July 1990.

[Zhe89] Zheng, C., Widmalm, S.E. and Williams, W.J., "New Time-Frequency Analysis of EMG and TMJ Sound Signals," *Proc. of IEEE Int. Conf. on Engineering in Medicine and Biology*, vol. 6, pp. 741-742, Nov. 1989.